2018

Establishing relationships among environmental stressors, host immune status, and wasting disease susceptibility in the dominant seagrass species Thalassia testudinum

Paige Joy Duffin
University of North Florida, n00722147@ospreys.unf.edu

ESTABLISHING RELATIONSHIPS AMONG ENVIRONMENTAL STRESSORS, HOST IMMUNE STATUS, AND WASTING DISEASE SUSCEPTIBILITY IN THE DOMINANT SEAGRASS SPECIES *THALASSIA TESTUDINUM*

by

Paige Joy Duffin

A thesis submitted to the Department of Biology

in partial fulfillment of the requirements for the degree of

Master of Science in Biology

UNIVERSITY OF NORTH FLORIDA

COLLEGE OF ARTS AND SCIENCES

August, 2018

CERTIFICATE OF APPROVAL

Establishing relationships among environmental stressors, host immune status, and wasting disease susceptibility in the dominant seagrass species *Thalassia testudinum*

The thesis of Paige J. Duffin is approved: Date

_____ _____
Dr. Cliff Ross
Committee Chairperson

_____ _____
Dr. Matthew Gilg

_____ _____
Dr. Eric Bricker

Accepted for the Department of Biology:

_____ _____
Dr. Cliff Ross
Chairperson

Accepted for the College of Arts and Sciences:

_____ _____
Dr. George Rainbolt
Dean

Accepted for the University:

_____ _____
Dr. John Kantner
Dean of Graduate School

ACKNOWLEDGEMENTS

I would like to express gratitude and thankfulness to all those who have assisted me during the various stages of my thesis project. Specifically, I would like to thank my primary advisor, Dr. Cliff Ross, for his support, advice, and guidance over the past few years, as well as the other members of my committee, Dr. Matt Gilg and Dr. Eric Bricker. I would also like to extend special regards to Dan Martin for his expertise on *Labyrinthula* as well as his willingness to endure months of trial-and-error alongside me in the generation of the qPCR assay. This project would not have been possible without your invaluable contributions. Special thanks to Dr. Katrina Lohan, who also assisted heavily in this aspect of the project. Additionally, I want to acknowledge and give sincere thanks to Dr. Brad Furman for lending his statistical experience to the task of metadata analyses that were necessary for the field study in Florida Bay (Chapter 3). It was an honor to work with, and learn from, such knowledgeable scientists. I also received a great deal of assistance from two undergraduates, Lina Borges and Amanda Schaaf; thank you for your meaningful contributions and the positive energy you brought to the lab bench. A distinct recognition to the Coastal Conservation Association of Florida and the University of North Florida for providing financial support for this project.

On a personal note, I would like to extend my deepest gratitude to my friends and family for their endless supply of love and support; in particular, I am indebted to my roommate and best friend of seven years, Alexandra Linton, my inspiring and kind sister, Julia Duffin, and my driven and loving significant other, David Reynolds. Finally, I wish to express my appreciation towards -and dedicate this body of work to- my parents, Kari and Eric Duffin, whose love and support assumes countless forms. My success stems directly from your hard work, generosity, and selflessness. Thank you.

TABLE OF CONTENTS

LIST OF FIGURES

LIST OF TABLES

ABSTRACT

A growing body of evidence supports the observation that marine disease outbreaks, especially those caused by opportunistic pathogens, are increasing in frequency and severity. One genus of such pathogens, *Labyrinthula*, has been identified as the causative agent of seagrass wasting disease, an epidemic that has historically plagued seagrass beds around the world. It is suspected that pathogenicity is intimately linked to the ability of the host to initiate defense responses, but a lack of compelling evidence prevents any meaningful application of preliminary observations. This body of work investigated the roles of host genotype, host immune status, and environmental stressors in dictating the susceptibility of *Thalassia testudinum* (turtlegrass) to seagrass wasting disease, through two investigational studies. The first, a lab-based study, addressed the deficit in empirical methods through the development of techniques that measured: [1)] *Labyrinthula* loading in host tissue through a novel qPCR-based assay and [2)] immune status in the seagrass host via four immune biomarker assays, measuring peroxidase (POX), exochitinase (EXOC), polyphenol oxidase (PPO), and lysozyme (LYS) activity. These methods were used to analyze turtlegrass individuals exposed to [1)] abiotic stressors alone or [2)] abiotic stressors followed by pathogen-challenge, in a controlled laboratory setting. The qPCR assay successfully quantified pathogen loading in seagrass tissue with high specificity. All four biomarkers were constitutively active in host tissue, but expression was largely unaffected by the chosen abiotic stressors. There were significant positive relationships between pathogen loading and two of the four biomarkers (POX and EXOC), regardless of abiotic stress treatment. Finally, despite the widely variable response among individuals, regardless of treatment, we identify a potential trade-off mediated immune response in *T. testudinum*, when faced with pathogen invasion. The second investigation

was a field study conducted in Florida Bay, a shallow, subtropical estuary characterized by many spatiotemporally unique basins, where *T. testudinum* dominates. Samples collected from 15 representative sites were analyzed using the methods developed in the first study as well as historical monitoring databases, in an effort to identify ecologically significant trends that existed in patterns between: [1)] pathogen loading and immune status; [2)] pathogen loading and geographic site; [3)] pathogen loading and morphometric characteristics; [4)] pathogen loading and water quality data; [5)] immune status and geographic site; [6)] immune status and morphometric characteristics; and [7)] immune status and water quality data. The results revealed that both pathogen loading and immune status varied as a function of location in Florida Bay. Furthermore, based on the trends observed among and between sites with regards to pathogen loading, immune status, leaf morphology and water quality, a mechanism in which all four of these parameter sets interact is proposed as a potential explanation for the differences observed in *Labyrinthula* prevalence and severity within the bay. The results of both investigations address whether wasting disease susceptibility is driven primarily by variability in the environment or in the host species, and provide valuable insight regarding the extent to which seagrasses possess the capacity for resilience against marine pathogens.

CHAPTER 1: BACKGROUND ON SEAGRASSES AND WASTING DISEASE

1.1 Introduction to Plant Pathosystems

A growing body of evidence supports the observation that marine disease outbreaks are increasing in frequency and severity. Many of these diseases are caused by opportunistic pathogens, which co-exist with their host in the aquatic community but only infect when the host species' immunity becomes compromised or suppressed (Burge et al. 2014). Opportunistic parasitism is best described using a generalized disease ecology concept known as the pathosystem model, which predicts that system equilibrium is maintained by factors which control three primary components: the parasite, the host, and surrounding environmental factors (Robinson 1976, Sullivan et al. 2013) (figure 1-1). Events that disturb the equilibrium of these three pathosystem components (figure 1-1), such as a shift in environmental conditions to favor the parasite or a beneficial mutation which gives the parasite a temporary evolutionary advantage in the host-pathogen arms race (i.e., coevolution), may cause a dynamic change in the interaction outcome, such as an outbreak of disease (figure 1-1). This thesis revolves around seagrass wasting disease, a pathosystem in which the host, seagrass, represents an integral part of marine ecosystems around the globe. In particular, the studies presented herein focus on the host species *Thalassia testudinum*, commonly known as turtlegrass, through lab and field-based investigations which seek to elucidate both how the state of the host affects its susceptibility to seagrass wasting disease as well as how the host is affected upon infection by the etiological agent. Thus, it is the aim of this introduction to [1)] highlight the importance of the host in aquatic ecosystems through a brief overview of the basic biology and ecology of seagrasses, and [2)]

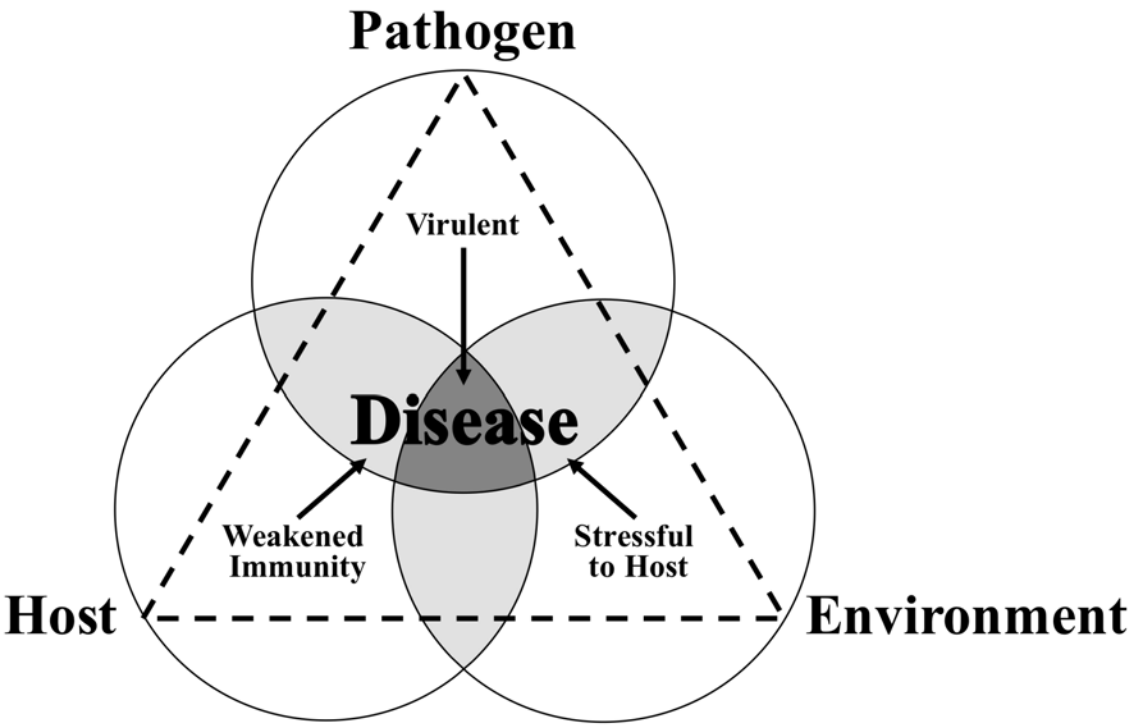

Figure 1-1. Plant pathosystem model depicting the complex interplay between an opportunistic pathogen, its host, and the surrounding environment, in the context of disease prevalence. This diagram is adapted from Sullivan et al. (2013), originally based on a concept synthesized by Robinson (1976).

describe pertinent background information and outline the major questions that were addressed in this thesis.

1.2 Highlights in Seagrass Biology and Ecology

Seagrass meadows form the basis of some of the most highly productive and ecologically diverse communities in the aquatic realm (Robblee et al. 1991, Zieman et al. 1999, Orth et al. 2006, Hemminga & Duarte 2008). As autogenic engineers, seagrasses form the basis of the three-dimensional structure and habitat space in the subtropical and temperate coastal systems where they dominate (Orth et al. 1984, Orth et al. 2006). They provide additional vital ecosystem services to shallow-water communities around the globe, including sediment stabilization, wave attenuation, carbon sequestration, oxygen production, and nutrient cycling (Short et al. 2000, Duarte 2002, Dawes et al. 2004, Orth et al. 2006). Seagrasses exert significant ecological control as habitat modifiers; estimates of faunal diversity and species richness are substantially greater in seagrass beds when contrasted with nearby areas lacking vegetation (Sheridan 1997, Kenworthy et al. 2006). Many economically and biologically important species spend at least a portion of their lives within the refuge of seagrass 'safe havens' (Orth et al. 1984, Kenworthy et al. 2006, Hemminga & Duarte 2008), but the facilitative role of these marine plants extends well beyond the limits of the bed itself. Seagrass biomes regularly subsidize nearby mangrove, coral, continental shelf, deep sea, salt marsh, and even terrestrial food webs, meaning an even broader suite of organisms are connected to and rely on adjacent seagrass meadows as sources of primary and secondary productivity 'spillover' (Heck et al. 2008). Costanza et al. (1997) estimated that the value of ecosystem services provided by seagrass (and algal) beds is double the net worth of

mangrove/marsh communities, and exceeds the value coral reef habitats by over a factor of three (seagrasses/algae beds ≈ $18,500; mangrove/marsh ≈ $9,000; coral reef ≈ $5,000, in dollars per hectare per year). With this statistic in mind, it is troubling to note that seagrasses receive 3 to 50 times less media, research, and journal attention than mangrove/marsh and coral reef ecosystems (Orth et al. 2006).

Seagrasses are submerged angiosperms with surprisingly elusive and complicated life histories (Waycott et al. 2006). They comprise a functional and ecological group, not a taxonomic group; they evolved from terrestrial angiosperms at least three to five times independently and migrated into aquatic systems around 70 to 100 million years ago (den Hartog & Kuo 2006, Papenbrock 2012). Due to their complex (and often disputed) origins, seagrasses are not conventionally distinguished from other organisms by their phylogenetic traits, but by those characteristics and adaptations which make them unique as an ecological group (den Hartog & Kuo 2006). These features include, but are not limited to: their ability to live and grow while permanently submerged in marine or highly saline water, the existence of an anchoring system consisting of rhizome and root structures, the means to undergo hydrophilous (underwater) pollination and produce seeds capable of underwater dispersal, and the presence of specialized leaves featuring a reduced cuticle, elevated photosynthetic abilities in the epidermis, and the absence of epidermal stomata (Les et al. 1997, Orth et al. 2006, Hemminga & Duarte 2008, Papenbrock 2012). Despite their polyphyletic origins, taxonomic diversity is low among aquatic angiosperms, with only about 60 species defined as true seagrasses (reviewed in den Hartog & Kuo 2006).

Seagrasses have distinctive above and below ground structures that resemble the basic morphology of their terrestrial monocotyledon ancestors. Structures found above-ground generally consist of one or more ramets which bear leaves or blades (Kuo & den Hartog 2006); however, the size and shape of this photosynthetic tissue varies considerably among species, and even among populations of a single species. For example, the long-lived *Thalassia testudinum* possesses a high capacity for phenotypic plasticity (Hackney & Durako 2004). Subterraneous biomass includes roots, which provide a vital anchoring system for the plant body, and rhizomes, which store nutrients and facilitate vegetative growth by lateral expansion, giving rise to runners, or shoots belonging to the same ramet (Kuo & den Hartog 2006). Together these underground structures can form dense mats of tissue that extend meters beneath the surface, securing sediment from mechanical disruption and aerating an otherwise oxygen-deprived medium (Borum et al. 2006).

Life-history strategies vary widely among seagrass genera. Stable environments are dominated by large-bodied, long-lived genera like *Posidonia* and *Thalassia*, known for vegetative expansion, while patchy, disturbed or recovering ecosystems contain smaller, more short-lived genera such as *Halophila, Halodule,* and *Ruppia* (Orth et al. 2006). Seagrass meadows are dynamic ecological systems characterized by rapid change and turnover, especially compared to other autogenic ecosystems such as coral reefs, mangrove forests, and oyster shoals (Duarte et al. 2006). For example, the capacity of seagrasses to undergo clonal, or vegetative, expansion via underground rhizomes adds a compelling element to community dynamics because, while monotypic meadows may appear relatively static and uniform, intraspecific competition for space and resources still exists among clones (Duarte et al. 2006). Other unique

traits such as extreme morphological plasticity (Pérez et al. 1994, Marbà & Duarte 1998, Bricker et al. 2011) and the ability to switch between sexual and asexual persistence strategies (Billingham et al. 2003, Waycott et al. 2006) add layers of complexity to meadow dynamics, but also help explain the mechanism by which seagrasses successfully colonized, and continue to dominate, a wide variety of marine habitats.

1.3 Factors Affecting Seagrass Abundance, Health, and Decline

While seagrasses possess a variety of impressive adaptations to fit their recently acquired marine lifestyle, many of the abiotic limitations they face, in addition to more ubiquitous environmental stressors, can be traced back to their recent transition from terrestrial origins. Perhaps most notably, seagrasses are hindered by their high light requirements (Zimmerman 2006, Ralph et al. 2007). In fact, seagrasses require light levels over an order of magnitude higher than terrestrial angiosperms and other marine primary producers, both of which thrive at very low incident radiation levels (Strickland 1958, Dennison et al. 1993). In addition to the basic physics of light attenuation through the water column (reviewed in Zimmerman & Dekker 2006), this sensitivity of seagrasses to light availability is, to a large extent, considered a consequence of the anoxic sediment in which they reside (Ralph et al. 2007). Generally speaking, marine sediments act as an oxygen sink, whereby plants must maintain a high rate of photosynthesis in order to supply below-ground tissues with enough oxygen to compensate for the constant diffusion of the gas into the surrounding media (Borum et al. 2006). Thus, exceedingly poor sediment conditions, such as extended periods of anoxia and/or sulfide toxicity, represents another factor which deteriorates seagrass health, especially when coupled with insufficient light levels (Borum et al.

2006, Orth et al. 2006) Another abiotic element which often dictates seagrass abundance and productivity is salinity. While salinity tolerance ranges vary across species, many are sensitive to even moderate fluctuations in salinity (van Diggelen et al. 1987, Adams & Bate 1994). For example, photosynthetic rates in *Thalassia testudinum* depreciate quickly when salinities deviate below or above the species' narrow optimal range of 28-30 ppt (Zieman et al. 1999).

In addition to inherent environmental factors which affect seagrass abundance and distributions, anthropogenic, influences represent an increasingly substantial component of meadow dynamics and health. While the presence of robust seagrass communities greatly increases the stability and resilience of our coastlines, their proximity to sea-land margins also renders them especially vulnerable to a spatially and temporally dynamic host of anthropogenic stressors (reviewed in Ralph et al. 2006 and Walker et al. 2006). Harmful pressures directly attributed to human influence are somewhat well-characterized, and range from threats at a local scale (such as habitat destruction and physical damage caused by dredging, boating, etc.), regional stressors (e.g., the introduction of an exotic species, such as an opportunistic herbivore) and global agents of stress (such as global climate change and sea level rise) (Short & Burdick 1996, Short & Wyllie-Echeverria 1996, Orth et al. 2006, Ralph et al. 2006). However, oftentimes the relationship between anthropogenic activity and environmental pressures is less direct, and, thereby, more complicated to identify and manage. One prominent example involves the enrichment of coastal and estuarine waters due to fertilizer runoff from coastal developments; this allows otherwise nutrient-limited phytoplankton to explode in abundance which, in turn, leads to a prolonged reduction in water clarity (Short & Burdick 1996, Ralph et al. 2006). Seagrasses suffer from these turbid conditions, especially when they are already living near or at

the lower threshold limits of their light tolerance. Other well-studied consequences of anthropogenic stressors in coastal marine habitats around the world arrive at a similar conclusion: proximity to human activity results in a cascade of events that exacerbate (or, at the very least, add to) natural stressors acting on seagrass populations (Orth et al. 2006, Hoegh-Guldberg & Bruno 2010, Burge et al. 2014). The most conservative model utilized by Neumann et al. (2015) estimated that human population along the coastal margin will more than double by 2050 (as compared to the baseline year, 2000), and the magnitude of anthropogenic pressure on coastal ecosystems will follow suite. The task of understanding how foundational species in marine ecosystems will respond to a novel assemblage of stressors acting simultaneously and synergistically is one of extreme complexity, but compelling urgency. Thus, one of the most vital considerations when developing effective management strategies is how these drastic shifts affect persistence at the species level. The assessment of a species' potential for resilience amidst volatile change requires identifying and characterizing its adaptive capacity within the context of surrounding biotic and abiotic factors.

Unfortunately, there is evidence to suggest that the unique traits which have allowed seagrasses to thrive and adapt to changes within in these systems may be no match for today's world, as downward trends in global seagrass abundance indicate that the rate of change has already begun to outpace the scale at which evolutionary forces work. In a comprehensive literature review, Waycott et al. (2009) determined that seagrass habitats have experienced a staggering 29% loss in areal coverage between 1879 and 2006. Even more troubling, however, was their observation that the rate of decline is accelerating. Before 1940, the median rate of loss across all sites surveyed was estimated at 0.9% per year; since 1990, this estimate has jumped to

about 7.0% loss per year (Waycott et al. 2009). Thus, despite receiving significantly less attention than other highly productive and ecologically valuable, yet declining, ecosystems, the rate of seagrass habitat loss is comparable to that of tropical rainforests and coral reefs (Orth et al. 2006); the deficit in our understanding of the factors which contribute to this growing loss must be addressed.

1.4 Seagrass Wasting Disease

Emerging evidence supports the observation that marine disease outbreaks, especially those caused by opportunistic pathogens, are increasing in frequency and severity. One genus of such pathogens, *Labyrinthula*, has been identified as the causative agent of a wasting disease (Muehlstein et al. 1988) that has affected both subtropical and temperate host species; it is appropriately referred to as "seagrass wasting disease" (SWD).

History of Die-Off Events

Reports of massive seagrass die-off events began to surface in the early 1930s, as observers became concerned after noting several sequential, acute, and catastrophic mass mortality events in eelgrass (*Zostera marina*) beds in the Atlantic along the eastern border of the United States (Cotton 1933, Renn 1934, Sullivan 2011). Shortly after, on the other side of the Atlantic, temperate European *Z. marina* beds suffered similar casualties (Fischer-Piette et al. 1932). The extent of these initial infection outbreaks was so extreme that eelgrass was virtually eliminated from the North Atlantic until around the 1960s (Short et al. 1987). Investigators searched for the causal etiological agent of the die-offs, and subsequent reports noted that individuals who underwent these "mass-wasting" events displayed disease-like lesions, although older affected

blades so closely resembled naturally senescent tissue that they were deemed indistinguishable from one another (Butcher 1934). Over the next five decades, research conducted on periodic events, reminiscent of the 1930s eelgrass epidemic, detailed the physical symptoms of what was soon referred to as 'seagrass wasting disease,' but failed to produce a definitive culprit behind the losses (Tutin 1938, Moffitt & Cottam 1941, Martin 1954). In the 1980s, another wave of die-offs swept through seagrass meadows, though this time, outbreak reports were more geographically widespread; not only were both Atlantic and Pacific temperate beds affected, but the first accounts of wasting disease in a tropical species, *Thalassia testudinum*, emerged from observations in a shallow estuary at the southern tip of Florida (Robblee et al. 1991, Zieman et al. 1999). This resurgence of outbreaks catalyzed a renewed interest in the subject, and it was during this time that researchers finally indicted a genus of pathogenic protists known as *Labyrinthula* as the definitive causal agent of modern outbreaks (Muehlstein et al. 1988) and, plausibly, the outbreaks which occurred earlier in the 20th century (Robblee et al. 1991, Blakesley et al. 2002, Bull et al. 2011, Sullivan et al. 2013).

Labyrinthula *Biology*

Labyrinthula are a genus of marine slime molds which are found ubiquitously in coastal environments around the globe. It is important to note that not all *Labyrinthula* are parasitic; the ecological function of these microbes may also be saprophytic, mutualistic, mutualistic, or one of commensalism (Raghukumar 2002). They have been historically difficult to classify but current understanding places *Labyrinthula* genus under phylum Heterokontophyta, within supergroup Chromoalveolata (Adl et al. 2012). Labyrinthulomycetes (a class which includes the *Labyrinthula* genus) distinguish themselves from other heterokonts chiefly through their ability

to generate extensive ectoplasmic networks (Tsui et al. 2009). Formed by cytoplasmic extrusions, these networks allow the mononuclear spindle-shaped cells of *Labyrinthula* to aggregate and take on their characteristic form as an amorphous colony, after which individual cells glide freely within the surrounding ectoplasmic membrane (Tsui et al. 2009).

While pathogenic taxa within this heterotrophic genus are often host-specific (Ralph & Short 2002, Martin et al. 2016), the onset of wasting disease generally progresses similarly among affected seagrass species. Spreading from one blade to another through direct contact, the mechanism of infection is thought to begin with unicellular *Labyrinthula* invasion through wounded epidermal tissue (Muehlstein 1992, Burge et al. 2014). Once established through mitotic division and colony formation, the infection site adopts a characteristic brownish-black appearance as the pathogen invades host cells, degrading the cytoplasmic contents and inducing necrosis (Ralph & Short 2002). Lesion spots merge to form bands that spread across the seagrass blade in either direction as the disease progresses (Bull et al. 2011). Whole-leaf mortality may occur even before the necrotic lesions spread throughout because living tissue surrounding the infected region experiences reduced photosynthetic activity and impaired vascular transport (Durako & Kuss 1994, Ralph & Short 2002, Bull et al. 2011). After the majority of blades within the shoot have perished, death of the entire plant (including below-ground rhizomes) follows shortly after (Renn 1934, Sullivan et al. 2013).

1.5 Host-Pathogen Dynamics of SWD

Interestingly, strains of *Labyrinthula* which have been deemed virulent in other contexts (and, thereby referred to as a “pathogenic” strain, or one capable of producing infection) have been

isolated from green seagrass tissue, despite the absence of wasting disease symptoms (Martin et al. 2016). This suggests that the presence of a pathogenic *Labyrinthula* sp. alone is not enough to trigger wasting disease, and that mass mortality events may represent a delicate interplay that involves both host and pathogen dynamics (Sullivan 2011, Martin et al. 2016). In fact, ever since the first recorded outbreaks in the 1930s, researchers have theorized that while healthy seagrass beds are capable of resisting infection, stress imposed on these hosts from the surrounding environment may make them susceptible to a 'secondary opportunistic pathogen' (which we now know as *Labyrinthula*) (Petersen 1934, Renn 1935, Short et al. 1987). More specifically, Tutin (1938) speculated that the stress imposed by light limitations (due to increased regional and localized turbidity) may have weakened the eelgrass defenses against disease and promoting virulence. Two decades later, another paper was published which noted a relationship between variation in precipitation (and, thus, salinity) levels and instances of notable eelgrass loss in northern Atlantic waters of the United States (Martin 1954). Following the second wave of widespread seagrass loss in the 1980s, Blakesley et al. (2002) noted that there appeared to be a relationship between the virulence of pathogenic *Labyrinthula* and surrounding conditions, and proposed a hypothetical model where the combination of high salinity (> 15 ppt), suboptimal host conditions, and high seagrass shoot densities triggered both chronic and rapid die-off events. This prediction fits in with the generalized plant pathosystem model in figure 1-1, which depicts the complex framework between an opportunistic pathogen, its host, and the surrounding environment that underlies disease prevalence. In the context of this thesis the host identity is *Thalassia testudinum*, the pathogen is *Labyrinthula* spp. and the environment is the physical and biological processes existing in a community where both species reside. The circles layered

underneath the generalized equilateral triangle model (figure 1-1) represent the notion that, for example, an interaction between host and pathogen alone does not always confer disease virulence (light gray overlap region; figure 1-1). It is only when specific conditions (such as those found in the white space within the triangle; figure 1-1) associated with all three components align that disease (dark gray centered overlap region; figure 1-1) occurs; in this case, the result might be an outbreak of seagrass wasting disease.

In section 1.3, the general health and state of global seagrass communities was presented through a modern lens by summarizing the temporally and spatially variable catalogue of environmental stressors these vitally important species encounter on a regular basis in today's oceans. In several cases, chronic stress imposed by one or a few abiotic factors has proven to, on its own, be enough to facilitate substantial seagrass loss (Orth et al. 2006, Hoegh-Guldberg & Bruno 2010). However, when the element of disease, and especially disease that may be exacerbated by stressful conditions, is layered on top of what one might consider these 'preexisting' stressors, the picture becomes all the more concerning. Moreover, researchers have hypothesized that, while predicted future environmental changes will presumably affect pathogen and host species alike, the degree of impact will not be shared equally, and the ecology of opportunistic microbial parasites suggests they may have the upper hand over their host counterparts under most scenarios (Andrews & Rouse 1982, Burge et al. 2014).

1.6 Thesis Overview

Despite the body of knowledge that has been presented in this chapter on seagrass wasting disease, there is still much we do not understand about the complex dynamics between the

parasitic microbes of genus *Labyrinthula* and their plant hosts. It is the intent of this thesis to elucidate the roles of environmental stressors and host immunocompetence in wasting disease prevalence and severity in the seagrass *Thalassia testudinum*. Figure 1-2 illustrates two overarching questions which exist in this pathosystem and guided our focus. At the level of the individual, we seek to better understand: what causes pathogenicity? What makes a host susceptible to infection? Population-level questions are equally important, and we aim to grasp: what dictates virulence within and among individuals in a host population (figure 1-2)?

Turtlegrass as the Model Host Species

T. testudinum (turtlegrass) has a broad range that extends throughout the Gulf of Mexico, the Caribbean, and into parts of the Atlantic, and is the dominant seagrass species in almost all regions where it is found (van Tussenbroek et al. 2006). One of the most significant historical wasting disease epidemics was the 1980s Florida Bay die-off, which strictly impacted *T. testudinum* beds (Carlton et al. 1991, Robblee et al. 1991) and, while numerous studies have been published that characterize the interactions between *Zostera marina* (eelgrass) and *Labyrinthula zosterae* (Short et al. 1987, Muehlstein et al. 1991, Ralph & Short 2002, Bergmann et al. 2011), much less is known about *T. testudinum* and the *Labyrinthula* spp. which infect it. The ecological and commercial value of this species throughout subtropical estuary and marine systems mandates a greater understanding of its susceptibility to seagrass wasting disease; for these reasons, it has been chosen as the model organism for the focus of this research.

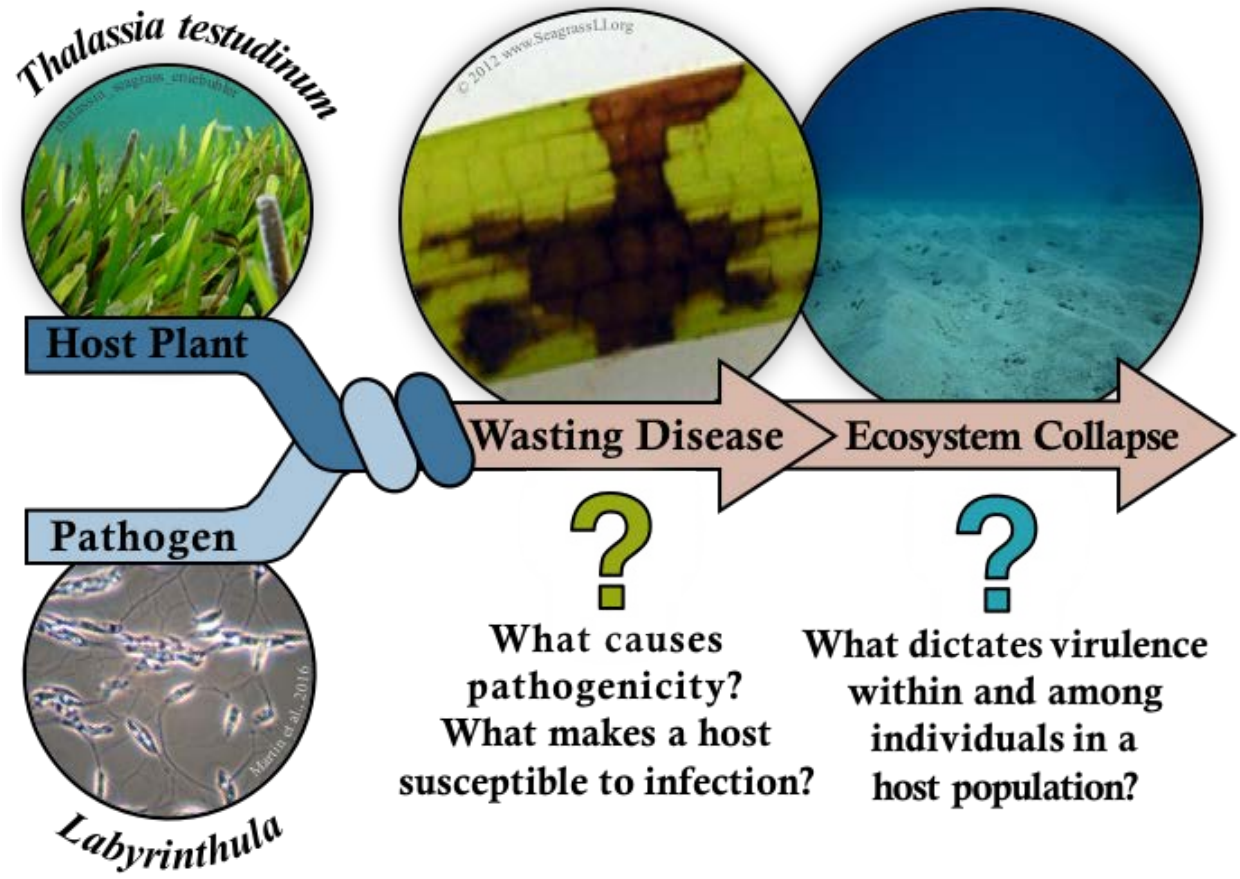

Figure 1-2. Conceptualized diagram representing a simplistic overview of the questions which guided our investigation. It is generally understood that the pathogen (*Labyrinthula*), when actively virulent, interacts with the host plant (*T. testudinum*) and causes wasting disease, which can, in some cases, lead to a collapse in the seagrass population and the ecosystem it supports. However, there are substantial gaps in our knowledge of this system, both on individual and population-level (green and blue question marks, respectively) scales.

Thesis Structure and Guiding Questions

This thesis has been formatted to include a general introduction, followed by two data chapters, which adhere to the basic format of a publishable research article (abstract, introduction, methods, results, and discussion). The fourth chapter summarizes the collective findings, addresses ongoing directions, and recommends future studies based on the information gained through this work. Below, I provide a brief overview of the two data chapters (Chapters 2 and 3), followed by a list of specific questions which guided the work presented in that chapter.

Chapter 2 (Lab-Based Study)

The first data chapter (Chapter 2) is, in essence, a methods paper, containing an emphasis on the methodologies developed as part of this research, including a novel qPCR-based pathogen detection technique and four host immune assays, described within the context of a series of lab-based experiments. More specifically, the following questions were addressed in this chapter:

1. *Part A:* Is it possible to generate a quantitative polymerase chain reaction (qPCR) assay capable of selectively amplifying a broad suite of pathogenic *Labyrinthula* strains that may be used to quantify wasting disease in host tissue?

   Part B: How does the quantification of disease severity in inoculated *T. testudinum* individuals compare between the qPCR-based assay developed in this study and the historical Wasting Index (WI; % lesion coverage)?
2. *Part A:* Are selected immune biomarkers (peroxidase, POX; exochitinase, EXOC; polyphenol oxidase, PPO; lysozyme, LYS) constitutively expressed in seagrass tissue?

Part B: Are the biomarkers differentially expressed in *T. testudinum* individuals following exposure to an abiotic stressor (hypersalinity, hyposalinity, elevated temperature) for one week in a controlled lab setting?

3. *Part A:* Are selected immune biomarkers (POX, EXOC, PPO, LYS) induced in seagrass tissue in response to *Labyrinthula* exposure?

   Part B: Are the biomarkers differentially expressed in *T. testudinum* individuals following exposure to an abiotic stressor (hypersalinity, hyposalinity, elevated temperature) for one week, followed by exposure to the pathogen for one week, in a controlled lab setting?

Chapter 3 (Field-Based Study)

The second data chapter (Chapter 3) aimed to assess the basis of individual susceptibility to *Labyrinthula* infection in a natural *T. testudinum* population by implementing the lab techniques generated in Chapter 2 to assess immune status and wasting disease severity across 15 sites of an environmentally heterogeneous region with historical water quality monitoring data. The following questions guided our efforts:

1. Are there pathogenic *Labyrinthula* isolates present in the samples collected from Florida Bay in 2015?
2. Is there a relationship between the prevalence/severity of seagrass wasting disease and selected biomarkers activity (POX, EXOC, PPO, LYS) across all field collected individuals, pooled together, regardless of site?
3. *Part A:* Is there variation in the prevalence and severity of seagrass wasting disease as a function of location among the 15 different sites surveyed from Florida Bay in 2015?

Part B: Can variation in morphology help explain any patterns observed in pathogen loading across sites?

Part C: Can variation among historical water quality parameters help explain any patterns observed in pathogen loading across sites?

4. *Part A:* Are there differences in immune status as a function of enzyme biomarkers (POX, EXOC, PPO, LYS) among the 15 different sites surveyed from Florida Bay in 2015?

   Part B: Can variation in morphology help explain any patterns observed in immune status at the site-level?

   Part C: Can variation among historical water quality parameters help explain any patterns observed in immune status at the site-level?

CHAPTER 2: INTEGRATING DISEASE LOADING, HOST IMMUNE STATUS AND ENVIRONMENTAL STRESS IN A SEAGRASS PATHOSYSTEM: ASSESSING IMMUNE MARKERS AND A UNIVERSAL QPCR PRIMER SET

2.1 Abstract

Recent trends suggest that marine disease outbreaks caused by opportunistic pathogens, such as seagrass wasting disease, are increasing in frequency and severity. Wasting disease is caused by a genus of slime molds known as *Labyrinthula*, and it is suspected that pathogenicity is intimately linked to the ability of the host to initiate defense responses; however, supportive evidence is lacking. In order to address this deficit, two novel techniques were developed: [1)] a qPCR-based pathogen detection method and [2)] immune profiling via four host immune biomarker assays, measuring peroxidase (POX), exochitinase (EXOC), polyphenol oxidase (PPO), and lysozyme (LYS) activity. These techniques were then used to investigate the roles of environmental stressors in dictating host immunocompetence, and, in turn, how immune status affected susceptibility to *Labyrinthula* infection. This was achieved through a series of controlled experiments which subjected turtlegrass individuals to [1)] abiotic stressors alone and [2)] abiotic stressors followed by pathogen-challenge. The qPCR assay was successful in quantifying *Labyrinthula* load in both culture and seagrass tissue across a broad range of predominately pathogenic strains, with a detection limit of less than one *Labyrinthula* cell. Immune assays revealed that all four biomarkers were constitutively active in turtlegrass individuals, but expression was largely unaffected by the chosen abiotic stressors. Furthermore, we identified positive correlations between pathogen loading and two of the four biomarkers (POX and EXOC), regardless of abiotic stress treatment. Finally, a potential trade-off mediated immune response is proposed, whereby pathogen invasion facilitates a shift from the host's first line of defense (constitutively expressed proteins, e.g. LYS) to a more

sophisticated and context-dependent attack (via enzymes, like EXOC, induced in response to specific cues).

2.2 Introduction

Marine pathogens can have a profound impact on their hosts, with disease outbreaks leading to sudden population declines in many taxonomic groups. One such example is seagrass wasting disease, which involves complex relationships among marine vascular plants, environmental parameters and protistan Labyrinthulids. *Labyrinthula* comprise the monotypic family Labyrinthulaceae (Stramenopiles, Labyrinthulomycetes; Adl et al. 2012), consisting of some 15-20 presumed terrestrial and marine species (Chitrampalam et al. 2015, Martin et al. 2016, Trevathan-Tackett et al. 2018), though much diversity likely remains unknown. *Labyrinthula* spp. move within a self-produced ectoplasmic network and degrade host cell walls with extracellular enzymes (Muehlstein 1992). Disease signs include splotching and dark (brown to black) streaking and spotting on leaves, which start on the leaf epidermis and eventually penetrate internal tissues, leading to defoliation (Renn 1935). This disease affects seagrasses from local to regional scales (e.g., 90% loss of north Atlantic *Zostera marina;* reviewed in Sullivan et al. 2017). However, whether particular species of these parasites are obligate on seagrasses (meaning they require a seagrass host for survival) or facultative (only parasitic under certain conditions) remains unclear (Martin et al. 2016). Additionally, these parasites vary in their host-specificity, infectivity, and pathogenicity (Martin et al. 2016, Trevathan-Tackett et al. 2018), though the underlying mechanisms remain elusive.

A growing body of research points to links between climatic changes and an increase in transmission, host susceptibility and frequency of marine diseases. However, a better understanding of host-pathogen interactions in the marine environment, the induced responses mediating them, and the role of the environment in altering their outcome is necessary to predict

the timing and spread of outbreaks. The apparent opportunistic nature of *Labyrinthula* implies that pathogenicity involves a delicate interplay between the physiological condition of the both the host and pathogen alike, whereby factors such as environmental stressors can shift the advantage towards one party over the other (Cróquer & Weil 2009, Bishop et al. 2017). Thus, wasting disease is thought to occur when conditions disfavor the seagrass host, resulting in a suppressed or weakened defense system that is susceptible to infection. However, the theory that environmental stressors, such as reduced light availability, hypoxia, and elevated salinity, dictate seagrass immunocompetence (Blakesley et al. 2002, Trevathan-Tackett et al. 2013, Bishop et al. 2017) has not been addressed directly as metrics of immunity have not been established in seagrasses.

Considering seagrasses are descendants of terrestrial plants that evolved into a distinct lineage ~75 million years ago (Jannsen & Bremer 2004), it would be anticipated that components of their innate immunity would have a significant degree of overlap. Plants have evolved a number of immune-related enzymes which may be maintained at constitutive levels or can be induced or activated following pathogen recognition (Osbourn 1996, Engel et al. 2006). Several common enzymes include peroxidase (POX), exochitinase (EXOC), polyphenol oxidase (PPO) and a group of enzymes with lysozyme-like activity (LYS).

POXs are multifunctional redox enzymes with well-documented roles in pathogen defense (Ghosh 2006, Almagro et al. 2008). They regulate biochemical processes such as the cross-linking of cell wall components, the production of secondary metabolites and key reactions in the hypersensitive response (Almagro et al. 2008).

PPOs are responsible for catalyzing the oxidation of monophenols and/or *o*-diphenols to *o*-diquinones. Through secondary reactions, *o*-diquinones can promote quinone toxicity and confer resistance against pathogens (Li & Steffens 2002, Thipyapong et al. 2004). The brown color of quinone adducts that forms as a result of PPO activity may be evident in lesions of infected seagrass tissue (C. Ross pers. obs.).

Chitinolytic enzymes, or chitinases, represent a large family of pathogen-related proteins that are responsible for degrading chitin and are strongly induced upon pathogen pressure (Punja & Zhang 1993). EXOCs represent a subcategory of chitinases that catalyze the progressive cleavage of N-acetylglucosamine residues from the non-reducing end of chitin and are noted to have a role in plant disease resistance (Grover 2012).

LYS refers to a group of enzymes with lysozyme-like activity and are present in many taxa including plants. LYSs function to hydrolytically cleave components of peptidoglycan, effectively breaking down the cell walls of bacteria (Couch et al. 2008). Additionally, Wang et al. (2005) observed that purified LYS proteins from this innate host defense mechanism also exhibited antifungal activity against a broad suite of fungal invaders.

To date, studies assessing seagrass defenses have been limited to phenolic acid production and other associated secondary metabolites (Zapata & McMillan 1979, Trevathan-Tackett et al. 2015). There is a need to expand upon this body of work and establish quantifiable measures of seagrass innate immunity and resistance. Such advances will allow us to address important questions like: is there a link between environmental stressors and immune status? Is there a relationship between environmental stress and disease susceptibility? Are common

immune markers constitutive in nature or do they have the capability of being induced in response to infection?

Current methods in seagrass wasting disease quantification may also impede our ability to accurately resolve the aforementioned questions. More specifically, the degree of *Labyrinthula* infection in plant tissue has been historically measured using the Wasting Index (WI) (Burdick et al. 1993, McKone & Tanner 2009); however, the effectiveness of this indirect method, which relies on the visual observance and measurement of necrotic lesions on seagrass blades, has been questioned on two principles: [1)] the pathogen may be present and inflicting damage within its host before necrotic lesions reach visibly detectable levels (Bergmann et al. 2011) and [2)] necrotic lesions due to *Labyrinthula* infection are often indistinguishable from naturally senescent tissue of the plant (P. Duffin pers. obs.). Bergmann et al. (2011) developed a quantitative real-time polymerase chain reaction (qPCR) approach to quantify loading of *Labyrinthula zosterae*, a relatively well-studied species specific to *Zostera marina* (eelgrass), in host tissue infected with SWD. However, as *Labyrinthula* spp. are thought to co-evolve with their host, this *L. zosterae*-specific detection assay cannot be utilized to assess infection by at least several other virulent *Labyrinthula* strains which have been identified (and others which inevitably exist in the environment but have yet to be identified) (Martin et al. 2016). In order to address important gaps in our understanding of the broader seagrass-*Labyrinthula* pathosystem, studies must expand outside of the *Z. marina/L. zosterae* model. A qPCR-based assay capable of detecting a variety of pathogenic *Labyrinthula* (even if the isolate/species identity is unknown) in host tissue with a high degree of sensitivity (<1 *Labyrinthula* cell) is necessary to facilitate these goals.

The purpose of this study is tri-fold. First, we seek to establish and test a qPCR assay that measures pathogen loading across a multitude of putatively virulent *Labyrinthula* strains, with the ability to quantify cells in diseased seagrass tissue down to a specific cell count. The second goal of this study is to generate integrated measures of seagrass innate immunity and pathogen resistance through the development of assays which measure POX, EXOC, PPO, and LYS biomarker activity. Through the use of these assays one can characterize constitutive (immunity in place whether or not pathogen exposure occurs) and inducible immunity in response to pathogen challenge. We seek to identify what immune responses may represent good indicators of disease resistance and provide the basis for an effective tool in predicting the vulnerability of seagrass populations due to stress. Finally, we investigate the role of common environmental stressors in dictating host immunocompetence in *Thalassia testudinum* and explore the potential link between immune status and susceptibility to *Labyrinthula* infection. Together, the body of knowledge gained and the methods validated through this study will help to understand disease dynamics, and determine appropriate management policies to predict and reduce future seagrass wasting disease outbreaks.

2.3 Methods

Collection and Maintenance of Thalassia testudinum *and* Labyrinthula *Cultures*

Thalassia testudinum: Samples were collected off the Gulf Coast of Florida near Horseshoe Bay (29°20' N, 83°23' W) from a site known to support a robust and healthy population (figure 2-1). Individuals were cleaned of epiphytes and transplanted no more than 24 hours after collection in terra cotta pots filled with a 50:50 mixture of sediment collected from the sampling location and

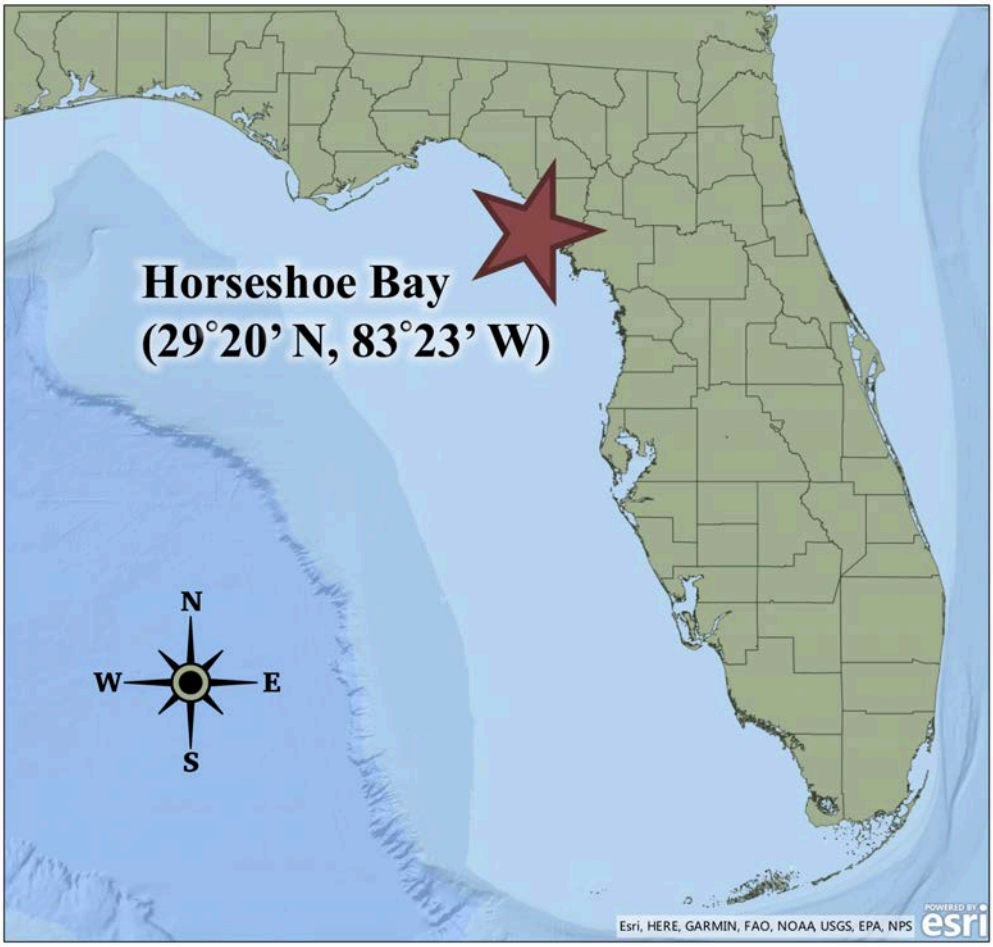

Figure 2-1. Map of Florida detailing the location where *Thalassia testudinum* samples were collected for use in the stress-response experiments. Horseshoe Bay supports a healthy, robust and stable turtlegrass population. Base map obtained using ArcGIS software (ESRI, Version 10.5.1.).

Arag-Alive!™ (CaribSea Inc., Ft. Pierce, FL). The plants were maintained in aquaria at the University of North Florida greenhouse (figure 2-2) in congruence with the methods described in the published master's thesis of N. Bishop (Bishop 2013). At the time of their use in stress-response experiments, the average length and width of the longest blade (3rd or 4th rank) in each *T. testudinum* individual was approximately 12.3 ± 2.8 cm and 0.35 ± 0.05 cm, respectively.

Labyrinthula: The culture used throughout this study to induce seagrass wasting disease in host tissue was a virulent strain known as "8b," which readily infects *T. testudinum* (Trevathan-Tackett 2011, Garcias-Bonet et al. 2011, Martin et al. 2016) and was obtained through D. Martin. The strain was maintained through growth on serum-seawater agar plates (figure 2-3), with subsequent plate transfers occurring every 28-30 days. More details on the maintenance of *Labyrinthula* cultures are accessible in Trevathan (2011) and Bishop (2013).

General Experimental Design

Innate Stress-Response Experiment

In order to determine how the presence of selected abiotic stressors influences constitutive immunity in *T. testudinum*, samples were subjected to environmental stressors under controlled laboratory settings (figure 2-4). Briefly, individuals were randomly assigned to treatment groups (n=5/treatment) and subjected to either ambient, elevated temperature, hypersalinity, or hyposalinity conditions in a microcosm environment for seven days as outlined in figure 2-5. Microcosms were created using 3.8-liter polyethylene terephathalate containers (Rubbermaid©, Whinchester, VA, US). Each container was equipped with a Hydor© Pico Evolution Mini Pump (Hydor©, Sacramento, CA, US) to promote circulation and elevated temperature treatments were heated using Hydor© Submersible Aquarium Heaters

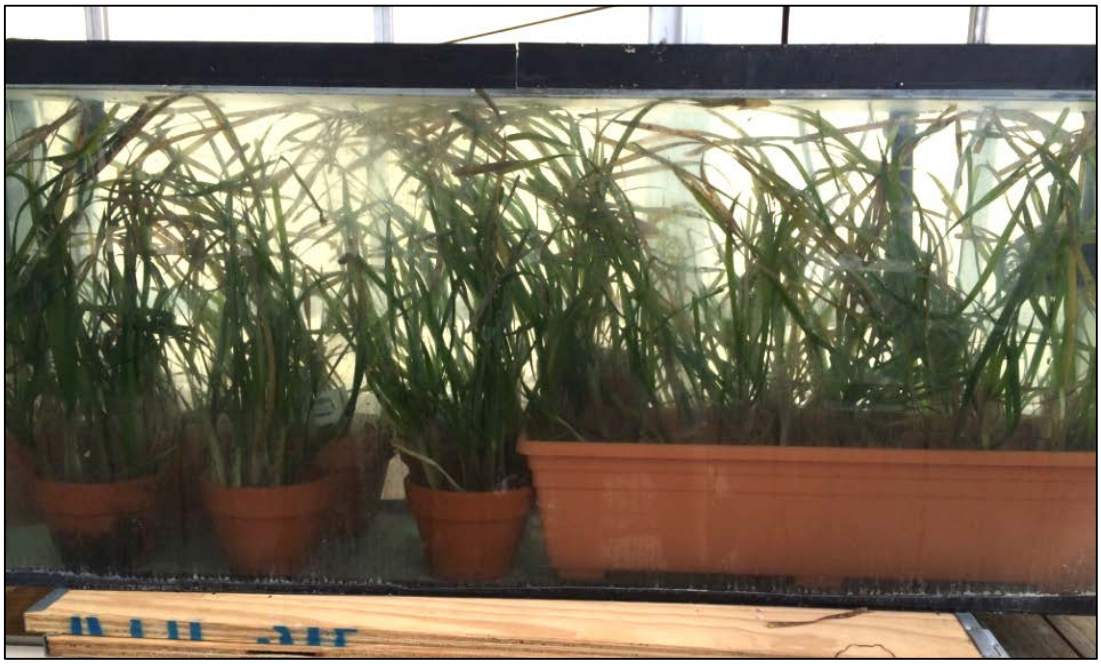

Figure 2-2. Seagrass individuals were maintained in aquaria at the University of North Florida greenhouse in congruence with the methods described in Bishop (2013).

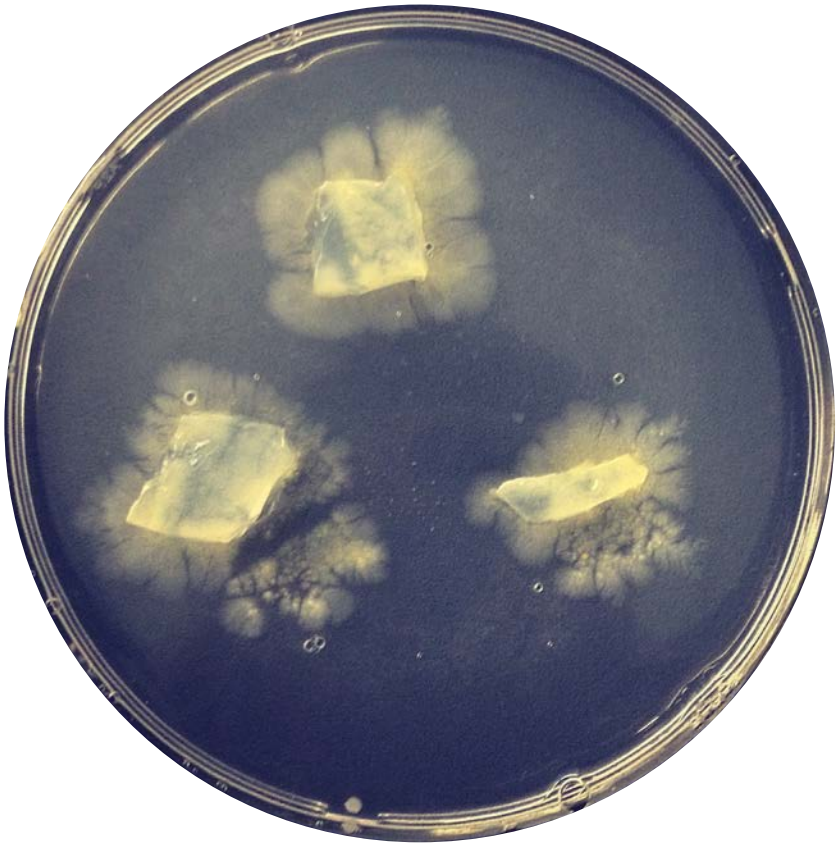

Figure 2-3. *Labyrinthula* strain 8b growing in culture on serum-seawater agar plates at room temperature. This image represents approximately 20 days of growth in culture.

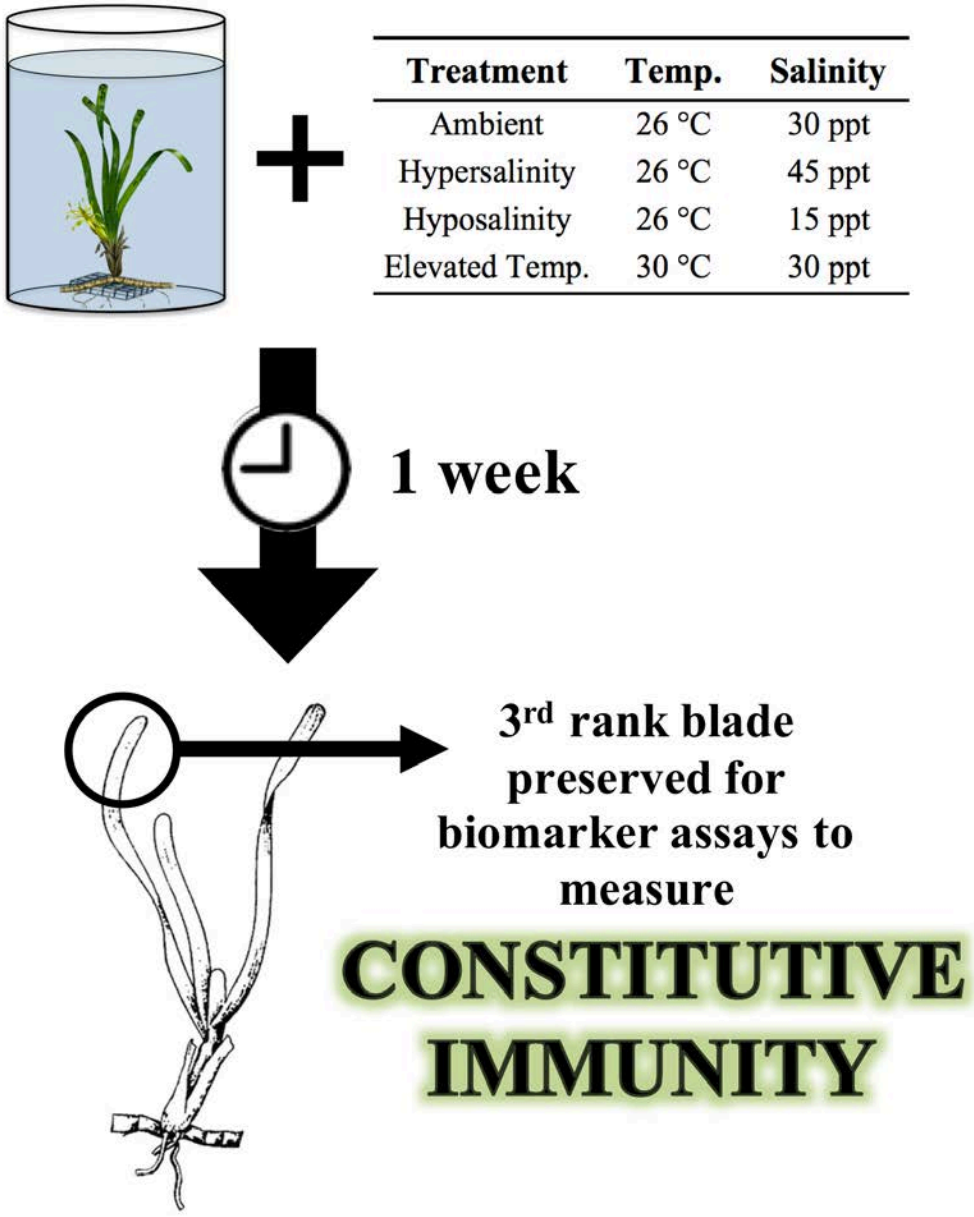

Figure 2-4. Diagram depicting the work-flow associated with the first stress-response experiment, which subjected *T. testudinum* individuals to abiotic stressors for one week under controlled lab conditions. The table displays conditions of each experimental treatment group. Sample size of n=5 per treatment.

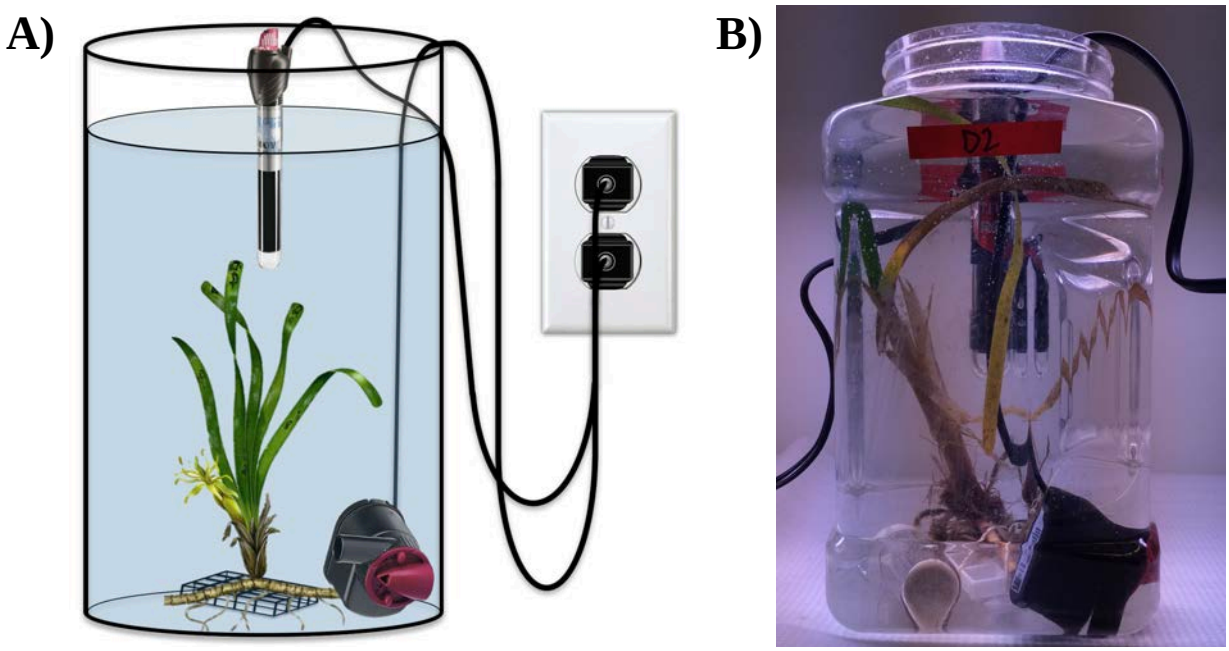

Figure 2-5. [A)] Diagram and [B)] photograph depicting the microcosm environment which housed *T. testudinum* individuals in controlled stress-response experiments, with heater (elevated temperature treatment only) and mini aquaria pump to promote circulation (all treatments).

(Hydor©, Sacramento, CA, US). Instant Ocean Sea Salt (Instant Ocean®) was used to create all desired salinities used in this study. Lighting was maintained at a photoperiod ratio of 12:12 hr light:dark (~200 μm $m^{-2}s^{-1}$) , using full spectrum Power-FLO T5 HO bulbs (Hagen, West Yorkshire, UK). After seven days under assigned conditions, tissue samples were extracted and processed. Processing involved isolating the third rank blade from each individual, with one shoot corresponding to one individual (figure 2-4). The blade was split longitudinally using a scalpel; although only one half was retained (in a 15-ml falcon conical centrifuge tube and stored at -80°C) for use in biomarker assays. This process was employed to maintain consistency with tissue processing in the second stress-response experiment, where the other half of the blade was preserved for qPCR-based pathogen loading analyses.

Induced Stress-Response Experiment

In order to determine the stress-response of *T. testudinum* due to abiotic stressors followed by pathogen-challenge, an experiment similar to the first was conducted, with the following differences: After one week under assigned conditions (figure 2-6), all individuals were returned to ambient conditions (26°C, 30 ppt seawater) and infected with *Labyrinthula* according to the methods outlined by Steele et al. (2005) (figure 2-7). After one week of infection, tissue samples from the experiment were processed by splitting the third rank blade longitudinally; one part was placed in a 15-ml falcon tube and stored at -80°C for use in biomarker assays aimed at measuring immune status and the other was preserved in Drierite® (Sigma Aldrich, Darmstadt, Germany) for downstream qPCR procedures, which served to quantify pathogen loading in experimental samples.

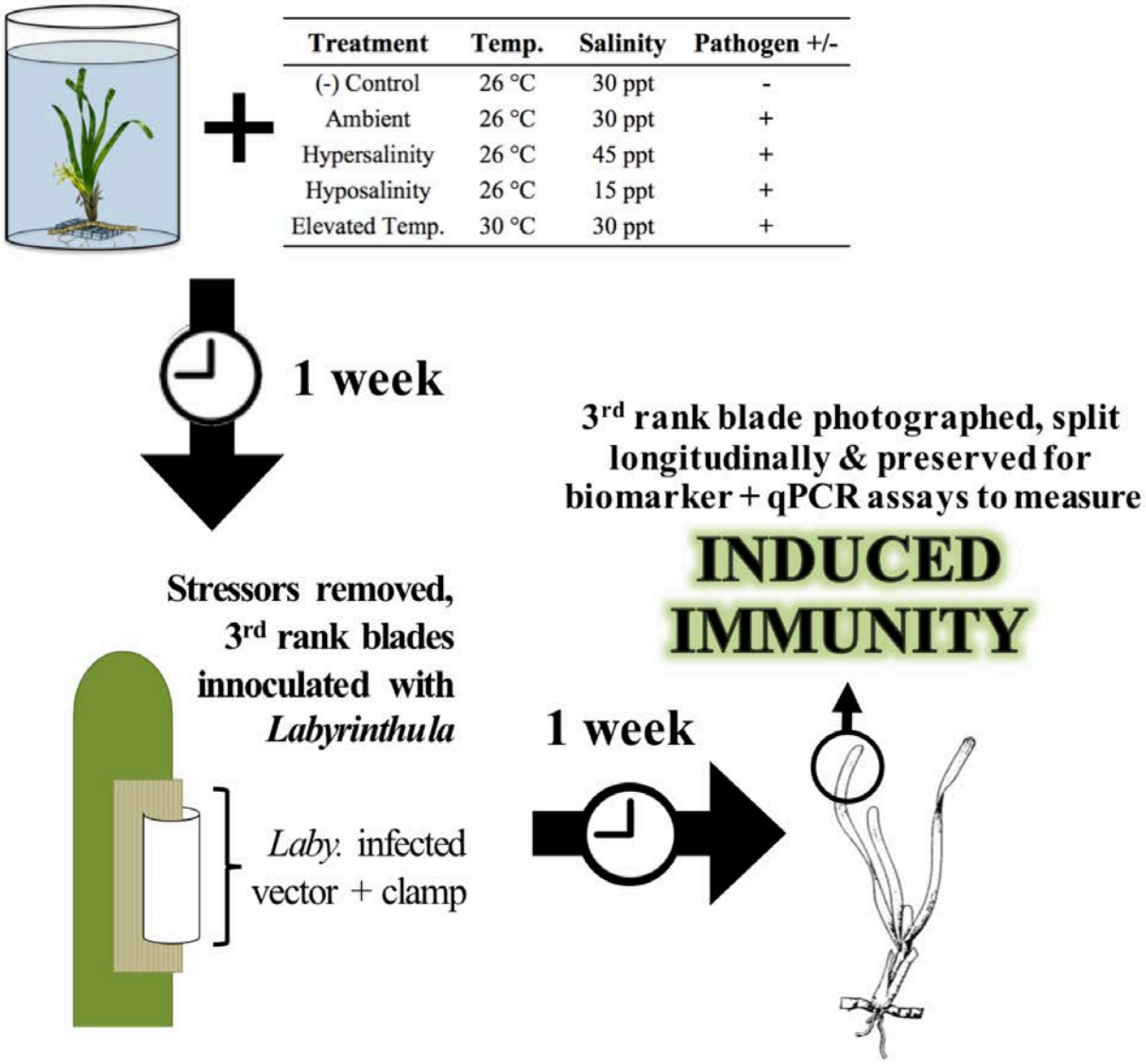

Figure 2-6. Diagram depicting the work-flow associated with the second stress-response experiment, which subjected *T. testudinum* individuals to abiotic stressors for one week under controlled lab conditions, followed by disease inoculation for one week. The table displays conditions of each experimental treatment group. Sample size of n=5 per treatment.

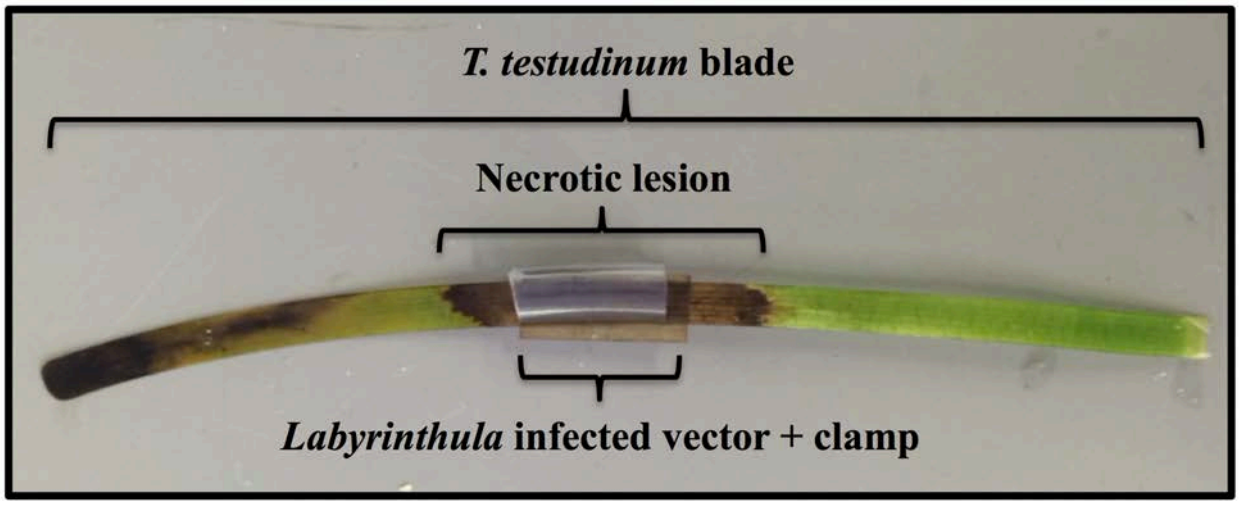

Figure 2-7. Characteristic necrotic lesion spreading through *T. testudinum* blade after *Labyrinthula* exposure using infection vector and clamp method (Steele et al. 2005).

Quantification of Pathogen Loading in Seagrass Tissue

In an effort to more reliably and precisely quantify the degree of infection in seagrass tissue by *Labyrinthula* spp., both within the context of this investigation and in future studies, a novel quantitative polymerase chain reaction (qPCR)-based approach was established. Primers were designed to amplify a common DNA marker, the internal transcribed spacer (ITS) region of the ribosomal RNA gene complex, for *Labyrinthula* based on publicly available sequences (GenBank 2016). Specifically, we targeted a 256 bp sequence within the ITS1 region, located between the 18s and 5.8s ribosomal subunits (18S-ITS1-5.8S) with novel, unpublished primers (ITS1-F: 5'- AAC TCA ATG AAT ATC TTG GTT TCC -3'; ITS1-R: 5'- GAT ATG CTT AAA TTC AGG GAG T -3') corresponding to sequences that were conserved among isolates belonging to the putatively pathogenic clade identified in Martin et al. (2016) (figure 2-8). Two *Labyrinthula* isolates, 8b and 316b (table 2-1) served as the primary strains utilized during method development of the qPCR assay. Both isolates are robust, pathogenic and readily virulent in their respective hosts *T. testudinum* (8b) (Martin et al. 2016) and *Zostera marina* (316b) (D. Martin, pers. comm.), and have been maintained on serum-seawater agar plates for 12 and five years (respectively). After the procedure was optimized using these *in vitro* cultures, the method was expanded upon by testing its ability to detect pathogenic cells within *T. testudinum* infection lesions and across a vast collection of 39 *Labyrinthula* strains (courtesy of D. Martin), both putatively pathogenic and non-pathogenic, collected opportunistically around the globe from a variety of temperate and tropical hosts (table 2-1; figure 2-9) (Martin et al. 2016).

```
1   TCTAANACTAAACGAGGCGAAAGCCTACCTATTTTAAACTAAAACACCAATTAAACAACT
61  CAATGAATATCTTGGTTTCCGTATCTTTGAAAAACGTAACTAGACACGCAAATTTGTATG
121 ATCTGTGATCTCTGAAAATACTTGTTTTTGAACGTAACATTCGACTTTCGTCGATTTTGT
181 GGACGAGTGTGTTTTGTAAACCTACCCAAGAAGACCGCTTCATGCGTGTCGCTGACTAAT
241 GAAACAAACAAACAACTAACACCAAACTTACTCCTCGTCCACAAACGAGCACTCCCTGAA
301 TTTAAGCATATCAATAA
```

Figure 2-8. Consensus sequence of the ITS1 region in pathogenic *Labyrinthula* isolates (written from 5' to 3'). Primers (underlined nucleotides) flank the 256 bp sequence (highlighted in blue) target.

Table 2-1. Twelve (12) pathogenic ("P") and 27 non-pathogenic ("N") *Labyrinthula* isolates of various origins were used to test the effectiveness of the qPCR assay. Isolate host/substrate code: ZM = *Zostera marina*; ZP = *Zostera pacifica*; PT = *Phylospadix torreyi*; PO = *Posidonia oceanica*; CN = *Cymodocea nodosa*; SI = *Syringodium filiforme*; HW = *Halodule wrightii*; TT = *Thalassia testudinum*; PS = *Phylospadix scouleri*; ML = detrital mangrove leaves; Px = *Phylospadix* sp.

Isolate ID Code	Isolate Host/ Substrate Code	Putative Functional Clade	Seagrass Bioregion Climate	Location	Count
107b	ZM	P	Temperate	US, NY, Long Island, Fisher Island	
113b	ZP	P	Temperate	US, CA, Refugio Beach	
142b	ZP	P	Temperate	US, CA, Anacapa Island	
140b	PT	P	Temperate	US, CA, Goleta, Coal Oil Point	
302b9	PO	P	Temperate	Spain, Alicante Bay	
287b	CN	P	Temperate	Spain, Cabrera Island, Port Cabrera	
180b3	SI	P	Tropical	Australia, Brisbane, N. Stradbroke Island	
74b	HW	P	Tropical	US, FL, Key West	
160b1	TT	P	Tropical	Panama, Playa Longosta	
8b	TT	P	Tropical	US, FL, Perdido Key	
316b	ZM	P	Temperate	US, OR, Newport	
347b	ZM	P	Temperate	US, VA	**12**
30b	PS	N	Temperate	US, WA, San Juan Island, Cattle Point	
282b	ML	N	Tropical	Belize, Twin Cay	
229b	TT	N	Tropical	Bahamas, Exuma Cay, Big Point	
109b	ZM	N	Temperate	Portugal, Ria Formosa	
75b	HW	N	Tropical	US, FL, Key West, 2	
84b	HW	N	Tropical	US, FL, Perdido Key	
239b	ZM	N	Temperate	US, WA, Sucia Island, Shallow Bay	
243b	ZM	N	Temperate	US, WA, Sucia Island, Shallow Bay	
250b	Px	N	Temperate	US, CA, Cayucos	
255b	ZM	N	Temperate	US, CA, Morro Bay	
267b	Px	N	Temperate	US, CA, Cayucos	
271b	ZM	N	Temperate	US, WA, Shaw Island, Picnic Cove	
50w	ZM	N	Temperate	US, WA, Shaw Island, Picnic Cove	
51b	ZM	N	Temperate	US, CA, San Diego Bay, Shelter Island	
214b	ZM	N	Temperate	US, VA, Chesapeake Bay, Cape Charles	
254b	ZM	N	Temperate	US, CA, Morro Bay	
237b	ZM	N	Temperate	US, WA, Lopez Island, Shoal Bay	
295b	ML	N	Tropical	Belize, Twin Cay	
345b	ZM	N	Temperate	US, VA	
66b	TT	N	Tropical	US, FL, Marquesas	
77b	HW	N	Tropical	US, FL, Marquesas	
48b	PS	N	Temperate	US, CA, La Jolla Shores	
52b	Px	N	Temperate	US, CA, La Jolla Shores	
279b	TT	N	Tropical	Belize, Twin Cay	
98b	ZM	N	Temperate	US, WA, San Juan Island, Mosquito	
161b3	ML	N	Tropical	Panama, Playa Longosta	
284b	ML	N	Tropical	Belize, Twin Cay	**27**

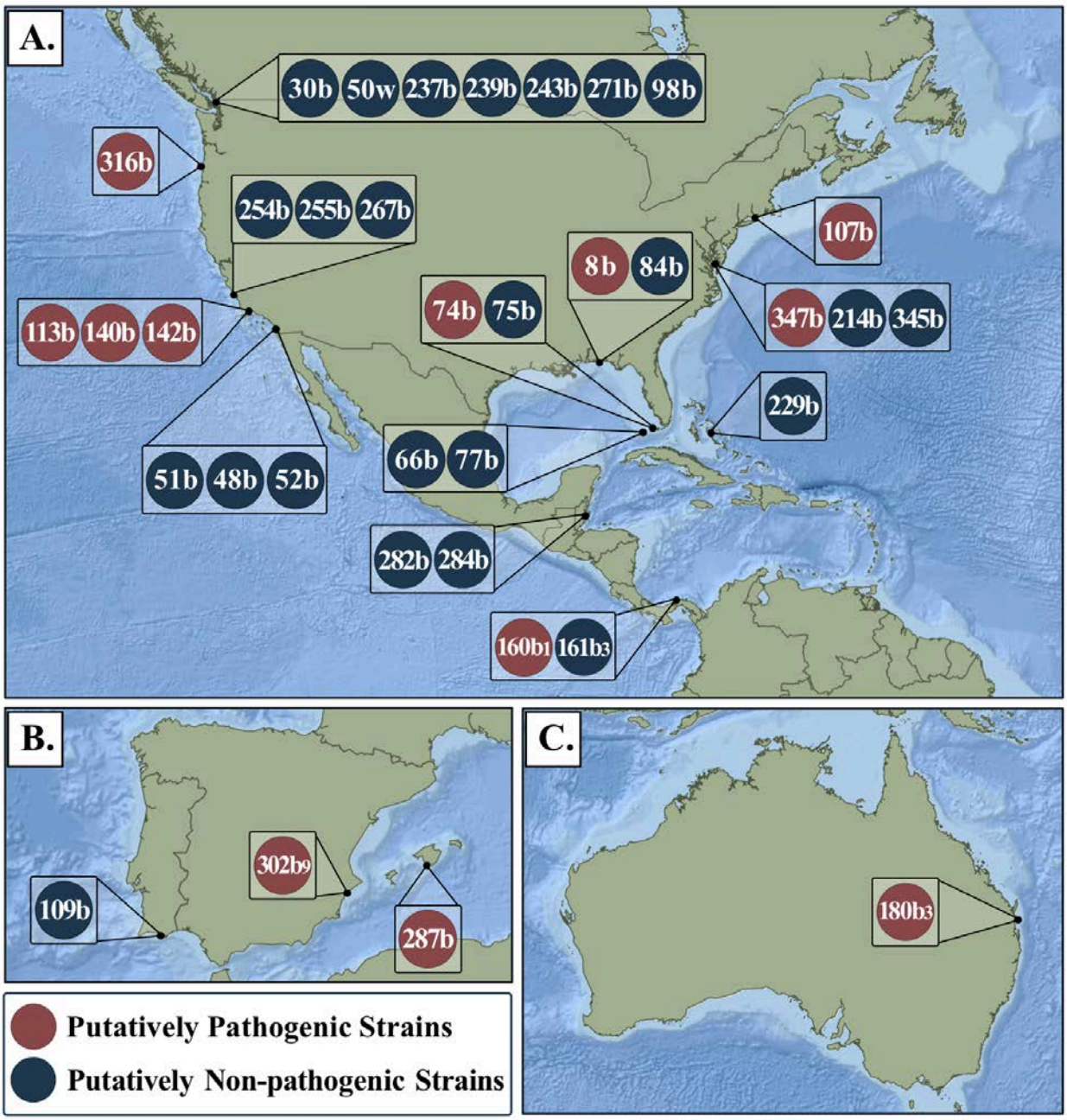

Figure 2-9. Geographic distribution (spanning throughout regions of [A)] North & Central America, [B)] Spain, and [C)] Australia) of the 39 *Labyrinthula* isolates used to test the effectiveness of the qPCR assay. Isolates samples courtesy of Dan Martin. Regions are not to scale across parts A, B, and C. Base map obtained using ArcGIS software (ESRI, Version 10.5.1.).

DNA Extraction

Whole tissue seagrass samples were preserved in Drierite® prior to DNA extraction. Extractions were performed by combining longitudinal half-leaf sections with three steel homogenizing beads in a microcentrifuge tube and disrupted using a FastPrep®-24 Tissue Homogenizer (MP Biomedicals, Solon, OH, USA), at a speed of 4.0 m/sec, repeated at one-minute intervals until the mixture resembled a fine powder. Next, DNA was extracted from ~0.5 mg subsample of the pulverized tissue using an Invisorb® spin tissue mini kit (Stratec Molecular, Berlin, Germany), according to the published manufacturer's protocol, adding 40 µL of 10 mg/mL RNase (Thermo Fisher Scientific™, Waltham, MA, US) when indicated to each sample. The resulting eluent was purified using a OneStep™ PCR Inhibitor Removal Kit (Zymo Research, Irvine, CA) to give a final DNA product. Prior to use in qPCR assays, the concentration of each DNA sample was measured using the Epoch™ Microplate Spectrophotometer (BioTek Instruments, Winooski, VT) and adjusted to reflect a standardized concentration of 10 ng/µL, aside from pure *Labyrinthula* samples of variable concentrations for use in the standard curve.

qPCR Protocol

The qPCR reaction consisted of 2 µL of DNA sample template (at 10 ng/µL), 1 µL each of the forward (ITS1-F) and reverse (ITS1-R) primers (both at 0.5 µM), 0.27 µL of BSA (at 0.2 µg/µL) and 10 µL of iTaq SYBR Green Supermix (Bio-Rad Laboratories, Hercules, CA, USA). The final volume was taken to 20 µL using UltraPure™ DNase/RNase-Free water (Invitrogen™ of Thermo Fisher Scientific™, Waltham, MA, US). Reactions were run on a CFX Connect™ Real-Time PCR Detection System (Bio-Rad Laboratories, Hercules, CA,

USA) using the following protocol: 95ºC for five minutes, followed by 45 rounds of a two-step thermocycling protocol (95ºC for 30 seconds, 63ºC for 60 seconds). At the end of each cycle, fluorescent signals were read and recorded. Finally, a melting curve step was performed (65-95ºC, at 0.5 ºC increments) to verify the identity of the amplicon within the sample. All samples were run in triplicate.

Cell Counts/Standard Curve

The quantity of *Labyrinthula* cells within seagrass tissue was estimated through the generation of a standard curve, consisting of a series of dilutions of *Labyrinthula* strain 8b growing *in vitro*. Cell counts were performed on *Labyrinthula* cells which had been transferred from the standard, long-term serum-seawater agar media to a liquid medium (formulated using the same ingredients as stated in the section on *Labyrinthula* culture maintenance, minus the agar component). The cultures were allowed to grow for 24 hours at room temperature, gently scraped off the surface of culture plates, and resuspended in a small volume of liquid culture (e.g. 1 mL for five growth plates) containing 2% Tween 80® (Sigma Aldrich, Darmstadt, Germany) followed by a 15 second vortex to mix. Using a Neubauer-improved hemocytometer grid (at 400x), 10 µL of the cell culture was loaded into the chamber, and four of the nine 0.1 µL grid cells were counted. This process was repeated with a total of 28 aliquots to generate a 1x standard solution of ~1,293 cells per microliter (µL). Following DNA extraction, this stock solution was then used to generate a geometric series of preparations containing DNA in volumes that corresponded to *Labyrinthula* cells ranging from 1,293.66 to 7.71 x 10^{-5} cells μL^{-1}.

Wasting Index Lesion Measurements

In addition to quantifying *Labyrinthula* loading in seagrass tissue via qPCR, wasting disease was quantified in post-treatment experimental samples using a modified version of the Wasting Index method (Burdick et al. 1993). Necrotic lesions appearing on inoculated tissue (representative lesions visible in figure 2-7) were photographed in high resolution and the proportion of diseased blade area was measured using ImageJ software (Schneider et al. 2012).

Immune Profiling through Cellular Biomarker Assays

Buffer controls with the substrate alone were included in each biomarker assay (POX, EXOC, PPO, and LYS) and subtracted from final absorbance values. All assays were performed in clear, flat-bottom Fisherbrand® 96-well plates (Thermo Fisher Scientific™, Waltham, MA, US) unless otherwise noted.

Isolation of Crude Protein from Seagrass Tissue

Crude protein extract was isolated from *T. testudinum* tissue following Couch et al. (2008), with modifications. A small section (~0.1 g) of each seagrass blade sample (third rank blade, split longitudinally) was combined with three steel homogenizing beads in a microcentrifuge tube, followed by the addition of 250 μL of extract buffer. The extract buffer contained 0.2 M phosphate and 5 mM β-mercaptoethanol in HPLC-grade water adjusted to a final pH of 7.8. Samples were homogenized using a FastPrep®-24 Tissue Homogenizer, at a speed of 4.0 m/sec, repeated at one-minute intervals until the mixture resembled a fine paste with no large particles. The samples were then centrifuged for 10 minutes at 17,000 ×g, and the resulting supernatant was transferred to a new tube, avoiding pelleted cellular debris. Following a

second centrifugation for 15 minutes at 17,000 ×g, the supernatant, containing the crude extract product, was transferred to a final tube and stored at -20°C for use in subsequent biomarker assays.

BCA Protein Assay

Crude extract protein concentrations were obtained using the Pierce BCA Protein Assay Kit according to the published manufacturer's protocol (Thermo Fisher Scientific™, Waltham, MA, US), with slight modifications. Briefly, crude extracts were diluted to an 8% solution using extract buffer and protein concentrations were measured at 562 nm using a Synergy™ HT Multi-Detection Microplate Reader (BioTek Instruments, Winooski, VT). Occasionally, samples exceeded the maximum absorbance read. In this event, the BCA protein assay was repeated with a 1% crude extract stock solution. Individual dilution factors were accounted for in calculating the final crude extract protein concentration of each sample. All enzyme assays were normalized by protein content.

Peroxidase Activity

Peroxidase activity in seagrass samples was measured following a modified version of the 96-well plate assay described in Couch et al. (2008). Crude extracts were diluted to a 10% solution by combining 5 µL sample extract and 45 µL of a 0.01 M phosphate buffer (pH 6.0). Forty-seven microliters of 0.01 M phosphate buffer (pH 6.0) was added to each well. Subsequently, 50 µL of 25 mM guaiacol (0.01 M phosphate buffer, pH 6.0) and 10 µL of the 10% extract solution were added. Finally, the reaction was initiated when 8 µL of 20 mM hydrogen peroxide (in 0.01 M phosphate buffer, pH 6.0) was added to each reaction well.

Sample absorbance values were measured at one-minute intervals for 20 minutes at 470 nm using a Synergy™ HT Multi-Detection Microplate Reader. Peroxidase activity for each sample was determined by taking the slope of the linear phase of the resulting enzymatic activity curve (figure 2-10) expressed as the change in absorbance at 470 nm per minute, per μg of total crude protein.

Exochitinase Activity

The activity of exochitinase was quantified in experimental samples in accordance with the assay methods published in Douglas et al. (2006), with modifications. Initially, 22.5 μL of assay buffer (100 mM sodium acetate, 0.1% SDS, 0.1% Triton X-100, 10 mM EDTA, 10 mM β-mercaptoethanol in HPLC-grade water, pH 5.0) was added to each microplate reaction well (black 96-well assay plate). Subsequently, 22.5 μL of crude sample extract was added to each well. along with 45 μL of 0.5 mM 4-methylumbelliferyl *N*-acetyl-β-D-glucosaminide (Sigma Aldrich, Darmstadt, Germany) in sodium acetate buffer (pH 5.0). The contents of the wells were gently perturbed, with care taken to ensure that no bubbles were present, after which the plate was covered in aluminum foil and incubated at 37° C for 30 minutes. Following incubation, fluorescence of the liberated product, 4-methylumbelliferone, was detected on the FLx800 Fluorescence Microplate Reader (BioTek Instruments, Winooski, VT) with excitation and emission wavelengths of 360 nm and 460 nm, respectively. Sample fluorescence values were compared to a standard curve which featured a dilution series (0 nM, 1 nM, and 20 nM to 100 nM in increments of 20) of free methylumbelliferone, which is commercially available. Exochitinase activity was represented as the number of nanomoles (nmol) of 4-methylumbelliferone (MU) released per microgram (μg) of total crude protein.

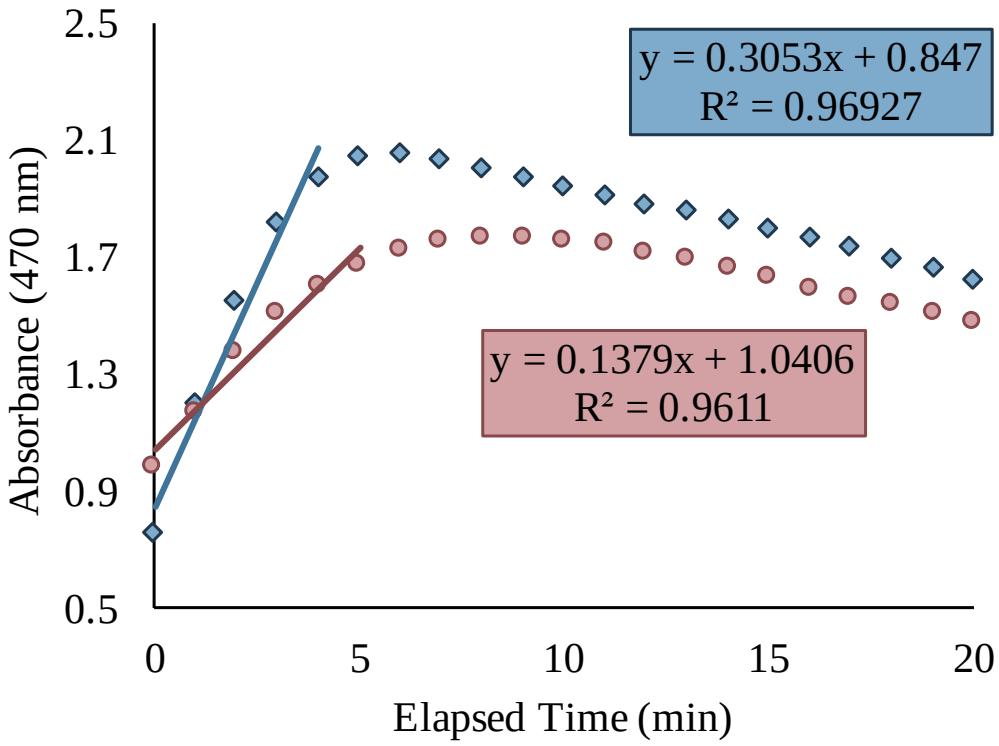

Figure 2-10. Enzymatic activity curves depicting peroxidase (POX) activity of two representative samples. The value for each sample was determined by manually fitting the linear phase of the reaction curve with a line in Excel. The slope of the resulting equation of the line (in the format y = mx + b, where m is the slope) was recorded as the level of POX activity in a given sample. For example, POX activity for the red and blue representative samples would be 0.1379 and 0.3053 (respectively), divided by crude protein concentrations to give final activity values expressed as the change in absorbance at 470 nm per minute, per µg of total crude protein.

Polyphenol Oxidase Activity

The level of polyphenol oxidase activity for each sample was estimated utilizing a modified version of the assay described in Gertzen and Escobar (2014). First, a 100 mM sodium phosphate assay buffer (pH 7.0) was created by combining a mixture that was 9.522 g/L monosodium phosphate (Na_2HPO_4) and 5.921 g/L disodium phosphate (NaH_2PO_4) in HPLC-grade water. The sodium phosphate buffer was then utilized to dissolve the substrate, 3,4-Dihydroxy-L-phenylalanine (L-DOPA), to a concentration of 20 mM. Next, 0.15% SDS was added, after which the mixture was heated to fully solubilize the substrate. Heat applied to the solution was minimized through frequent inversion and immediately removed once the powder was fully dissolved. A very small volume (one medium-size pipette tip dipped in catalase powder per 10 mL solution) of catalase was added to the cooled solution. A 96-well assay plate was obtained and 200 µL of the substrate-containing solution was combined with 30 µL of crude sample extract; one well per plate was reserved as a blank/negative control, which contained a volume of extract buffer in place of sample extract. The enzymatic conversion of L-DOPA to the dopachrome product via oxidation (Couch et al. 2008) was quantifiable via a color change (colorless to deep purple-black), and absorbance was measured at two-minute intervals for 3.5 hours at 490 nm using a Synergy™ HT Multi-Detection Microplate Reader. Polyphenol oxidase activity was quantified as the slope of the line during the linear phase of enzymatic activity (figure 2-11) expressed as the change in absorbance at 490 nm per minute, per microgram (µg) of total crude protein.

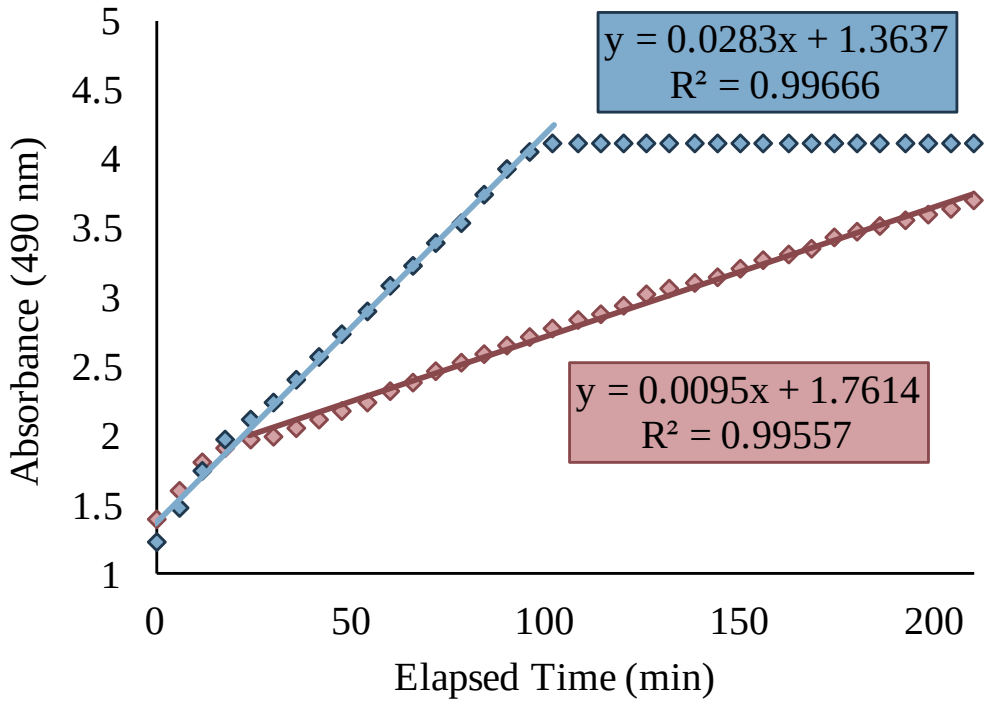

Figure 2-11. Enzymatic activity curves depicting polyphenol oxidase (PPO) activity of two representative samples. The value for each sample was determined by manually fitting the linear phase of the reaction curve with a line in Excel. The slope of the resulting equation of the line (in the format y = mx + b, where m is the slope) was recorded as the level of PPO activity in a given sample. For example, PPO activity for the red and blue representative samples would be 0.0095 and 0.0283 (respectively), divided by crude protein concentrations to give final activity values expressed as the change in absorbance at 470 nm per minute, per µg of total crude protein.

Lysozyme Activity

Lysozyme and lysozyme-like activity was measured by monitoring the inhibition of *Micrococcus luteus* bacteria growth in the presence of crude sample extract, following a modified version of the assay protocol described in Couch et al. (2008). First, a 10 mM phosphate buffer with a pH of 7.4 was created by combining a mixture that was 1.277 g/L monosodium phosphate (Na_2HPO_4) and 0.316 g/L disodium phosphate (NaH_2PO_4) in HPLC-grade water. The sodium phosphate buffer was then utilized to dilute reactivated *M. luteus* bacteria (previously freeze-dried MicroKwik Culture®, Carolina Biological Supply, Burlington, NC, USA) to a concentration of 30% *M. luteus* (in rehydration media, provided in MicroKwik Culture® kit). Two 96-well plates (per 93 samples run) were obtained; in the first set of wells, 100 µL of the diluted *M. luteus* solution was combined with 25 µL crude sample extract. The second plate served as a set of parallel blanks for each sample; in this case, the *M. luteus* solution was replaced with 100 µL of the 10 mM phosphate buffer (pH 7.4). The remaining three wells of plate #1 were filled with the diluted *M. luteus* solution without any extract added in order to estimate the average uninhibited growth rate of the bacteria over the course of the assay. The absorbance of each sample/well was recorded at the start of the assay, and after approximately 24 hours of incubation at room temperature, using the Synergy™ HT Multi-Detection Microplate Reader at 405 nm. For the lab experiment studies, lysozyme activity was quantified as the percent inhibition of *M. luteus* growth conferred by an individual's crude protein extract (per µg of total crude protein), standardized by presenting the value as a function of the uninhibited growth of *M. luteus* in the absence of crude extract run as a control group during the same assay.

Correlating Individual Immune Responses and Pathogen Loading

In order to address the potential role of individual variation in the host response to abiotic stressors and/or susceptibility to wasting disease, the association between biomarker (POX, EXOC, PPO, and LYS) activity and pathogen loading was assessed by pooling together all individuals from the second stress-response experiment, regardless of experimental treatment. This data was used to [A)] correlate activity levels at each biomarker with pathogen loading and [B)] create a heat map that allowed for the visualization of relative values for each individual at the five parameters measured (POX activity, EXOC activity, PPO activity, LYS activity, and pathogen load) at the same time. Measurements for each parameter (POX activity, EXOC activity, PPO activity, LYS activity, and pathogen load) were adjusted to reflect a proportional value between 0 and 1 by dividing all values within a parameter by the highest value detected in that parameter set. Next, values were assigned shades along a color gradient that corresponded with their magnitude (dark red and white = highest and lowest value of the set, respectively). Finally, individuals were reordered from lowest to highest pathogen loading values to view subsequent trends in the corresponding immune markers paired by individual.

Statistical Analyses

All statistical tests were performed with 95% confidence intervals ($\alpha = 0.05$) on data that were normally distributed according to Kolmogorov-Smirnov and Sharpiro-Wilk normality tests, unless otherwise stated. All statistical tests were computed using IBM SPSS® Statistics 25 software (International Business Machines Corp., Armonk, NY, USA) unless otherwise stated.

Treatment Effects in Stress-Response Experiments

For both experiments (abiotic stressors only and abiotic stressors followed by pathogen inoculation) one-way ANOVAs were conducted to test for differences among treatment groups on measurements representing either POX activity, EXOC activity, PPO activity, LYS activity, and, in the second experiment only, pathogen loading. Following one-way ANOVA tests, individual treatment groups were compared pairwise by multiple comparisons LSD posthoc tests ($\alpha<0.05$). All biomarker raw values were not normally distributed, so natural log transformations were used to transform the data sets such that they met the assumptions of normality. In the second experiment, LYS values could not be transformed to meet the assumptions of normality, but ANOVA was considered robust enough to handle this violation (as demonstrated in Blanca et al. 2017).

Correlational Analyses

When comparing biomarker activity with pathogen loading using the pooled values across all treatments from the second stress-response experiment, POX, EXOC, and PPO values were transformed using natural log to meet the assumptions of normality, and Pearson product-moment correlation coefficients, along with coefficient of determination (R^2) and p-values, were calculated using these transformed variables. However, LYS values, again, violated and could not be transformed to meet the assumptions of normality. Thus, the two variables (measuring pathogen loading and LYS activity) were ranked and the Spearman's rho nonparametric equivalent was utilized to assess the strength of their linear relationship.

2.4 Results

Effectiveness of the qPCR Procedure

Standard Curve

The dilution series created using known cell counts of the pathogenic *Labyrinthula* strain 8b were utilized to assess the efficiency and precision of the novel qPCR assay presented herein by analyzing whether the assay results (C_T values) were proportional to the known cell number from which the DNA template was extracted. The resulting standard curve generated an R^2 value of 0.98 and the extraction efficiency was 88.3% (figure 2-12). Additionally, the qPCR assay reliably amplified the highest dilution within the series, indicating that the assay was capable of detecting pathogen DNA equivalent to approximately 0.0095 *Labyrinthula* cells μL^{-1}. ($Log_2[0.0095] \approx -6.72$; figure 2-12)

Isolate/Clade Specificity

In order to generate a qPCR assay capable of detecting a broad suite of pathogenic *Labyrinthula* strains with accuracy and precision, we tested our qPCR assay on 39 strains within the genus; 31% (n = 12) of the isolates were putatively pathogenic strains and 69% (n = 27) were putatively non-pathogenic strains we did not wish to amplify (figure 2-13, 2-14). The qPCR assay reliably amplified 100% (12 of 12) of the putatively pathogenic stains (figure 2-13, 2-14). Of the 27 putatively non-pathogenic strains, 19 (70%) were never amplified, 4 (15%) were reliably amplified, and 4 (15%) were weakly amplified (figure 2-13, 2-14); that is, they were amplified 50% of the time with an average C_T value of 38.80 (data not shown).

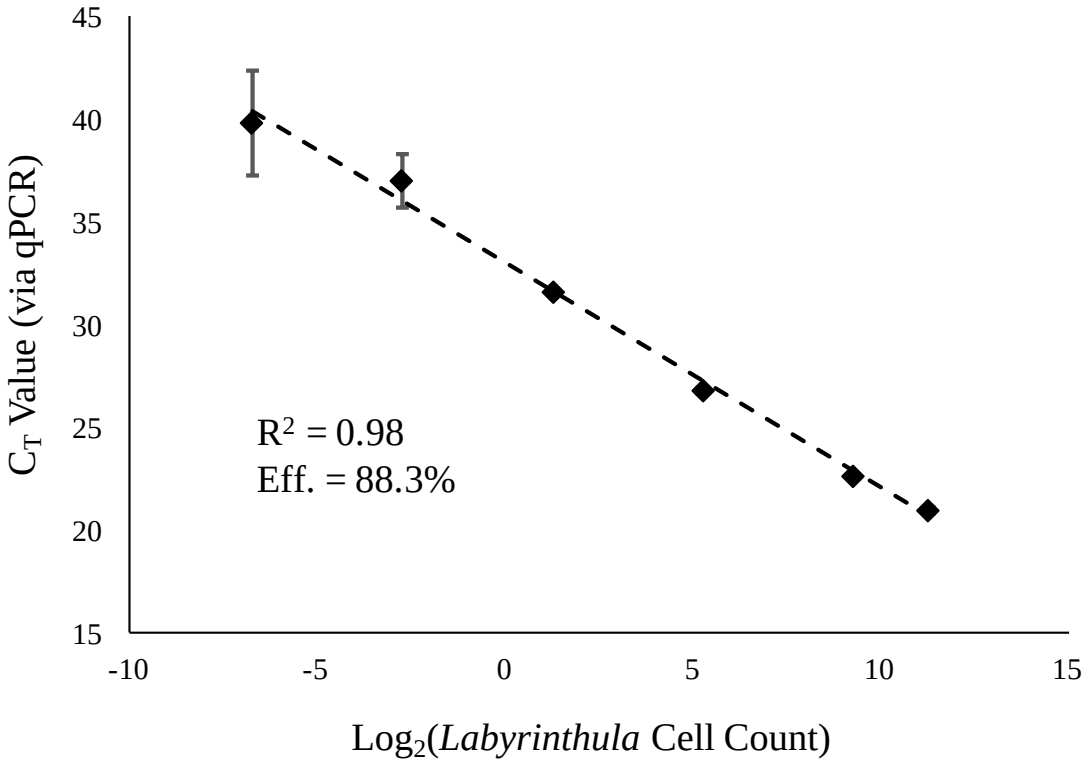

Figure 2-12. Representative standard curve for qPCR assays, generated using a cell dilution series and used to calculate extraction efficiency. The number of *Labyrinthula* cells μL^{-1} (log_2) was plotted against threshold (C_T) values automatically calculated via CFX Connect BIORAD software using fluorescence curves generated for each sample run. Each sample was analyzed in triplicate. Error bars reflect ±1 SEM across q-PCR assay replicates.

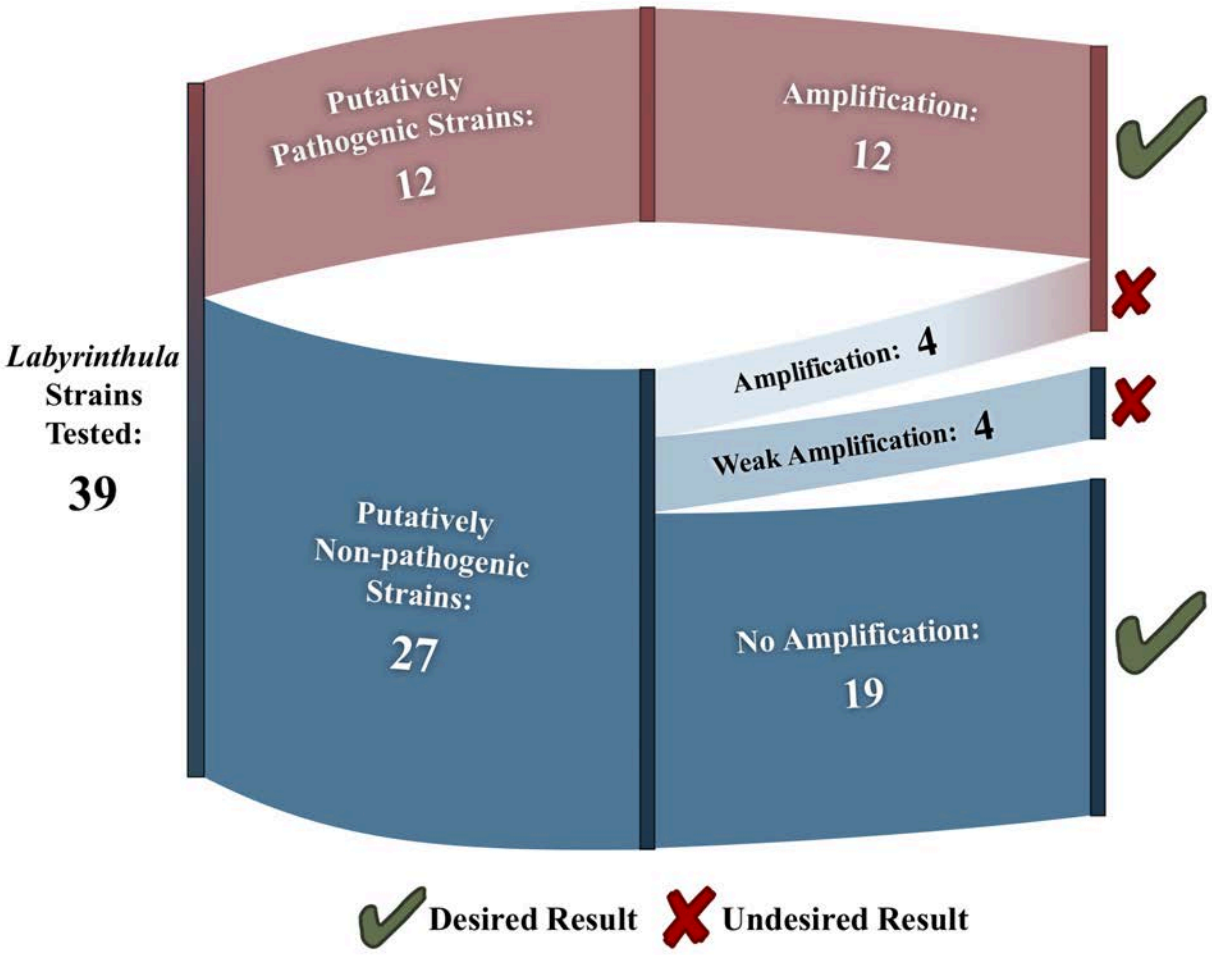

Figure 2-13. Schematic diagram summarizing the results of the 39 *Labyrinthula* strains tested using the qPCR-based pathogen detection assay. Sankey diagram generated using the SankeyMATIC tool available at http://sankeymatic.com/build/.

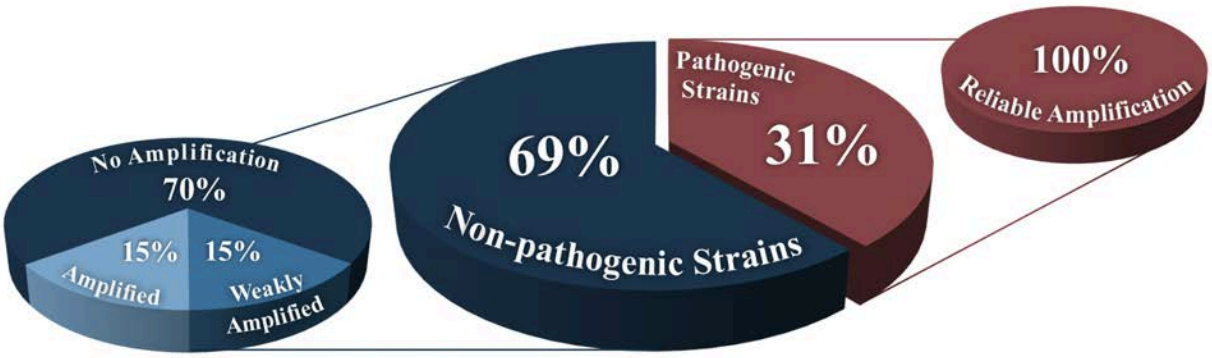

Figure 2-14. Pie-chart summarizing the results of the 39 *Labyrinthula* strains tested using the qPCR-based pathogen detection assay.

Quantification in Inoculated Seagrass Tissue

The novel qPCR assay presented here was successful in quantifying *Labyrinthula* prevalence and severity in host tissue, as evidenced by the results of the second laboratory experiment. The assay detected background-level quantities of *Labyrinthula* negative control treatment individuals (n = 4) that were, on average, six orders of magnitude lower than individuals inoculated with the pathogen (n = 20) ($4.61 \times 10^{-3} \pm 3.72 \times 10^{-3}$ cells μL^{-1} and 28.27 ± 3.39 cells μL^{-1} in non-infected and infected seagrass tissue, respectively; figure 2-15)

Comparison of Wasting Disease Quantification Methods

The novel qPCR-based pathogen quantification method presented in this chapter was compared with the historical Wasting Index (WI) method by performing correlations between *Labyrinthula* cell count values obtained through qPCR (pathogen loading) and percent leaf area coverage of induced lesions as determined through WI methods. There was a significant positive relationship between estimates of pathogen loading and percent leaf coverage of induced lesions (p-value = 0.000; $R^2 = 0.53$) (figure 2-16 A); however, when the lower 50% (based on pathogen loading values) of the data points were removed, the two variables were no longer significantly associated with one another (p-value = 0.255; $R^2 = 0.127$) (figure 2-16 B).

Constitutive Immunity of Seagrass Exposed to Abiotic Stressors

The immune metric procedures described herein were utilized to quantify the immune status of individuals at four biomarkers which measured peroxidase (POX), exochitinase (EXOC), polyphenol oxidase (PPO), and lysozyme-like (LYS) activity in *Thalassia testudinum* individuals exposed to either ambient (26ºC, 30 ppt seawater), hypersaline (26ºC, 45 ppt seawater),

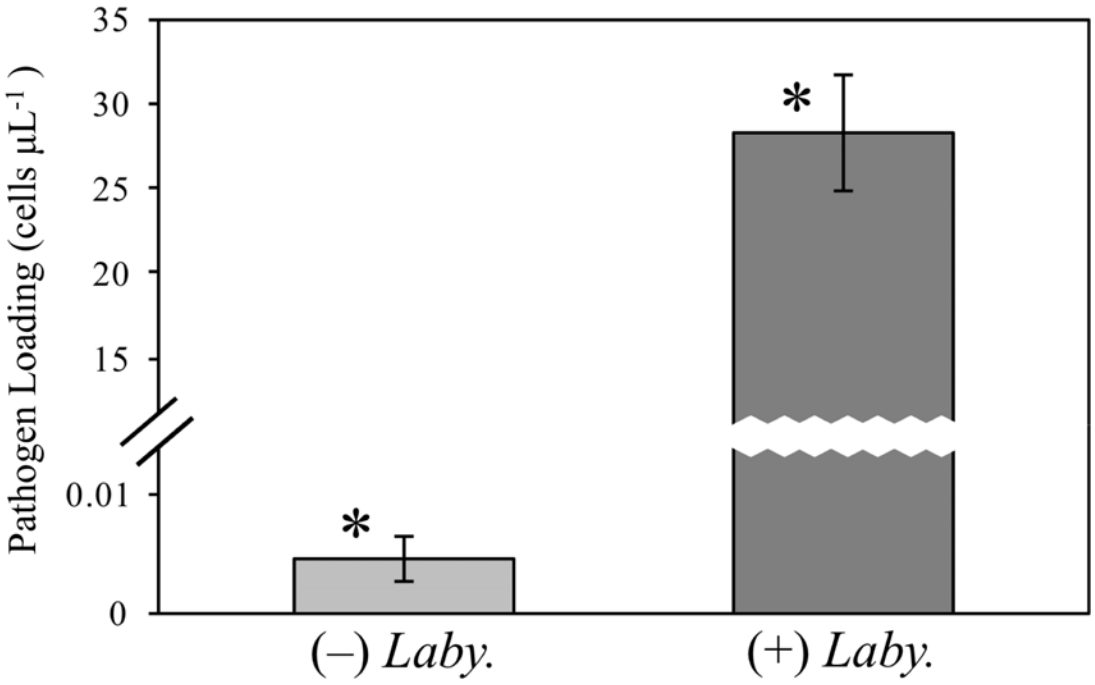

Figure 2-15. Results of qPCR assays measuring pathogen loading (number of *Labyrinthula* cells per ng DNA) in tissue of *T. testudinum* individuals from the second stress-response experiment, under control [no *Labyrinthula,* or (-) *Laby.*] and pathogen-exposed [inoculated with *Labyrinthula,* or (+) *Laby*] conditions. Error bars reflect ±1 SEM. Asterisk (*) represents two-tailed significant difference at $\alpha = 0.01$. Sample size n = 4 and n = 20 individuals for (-) *Laby*. and (+) *Laby* groups, respectively.

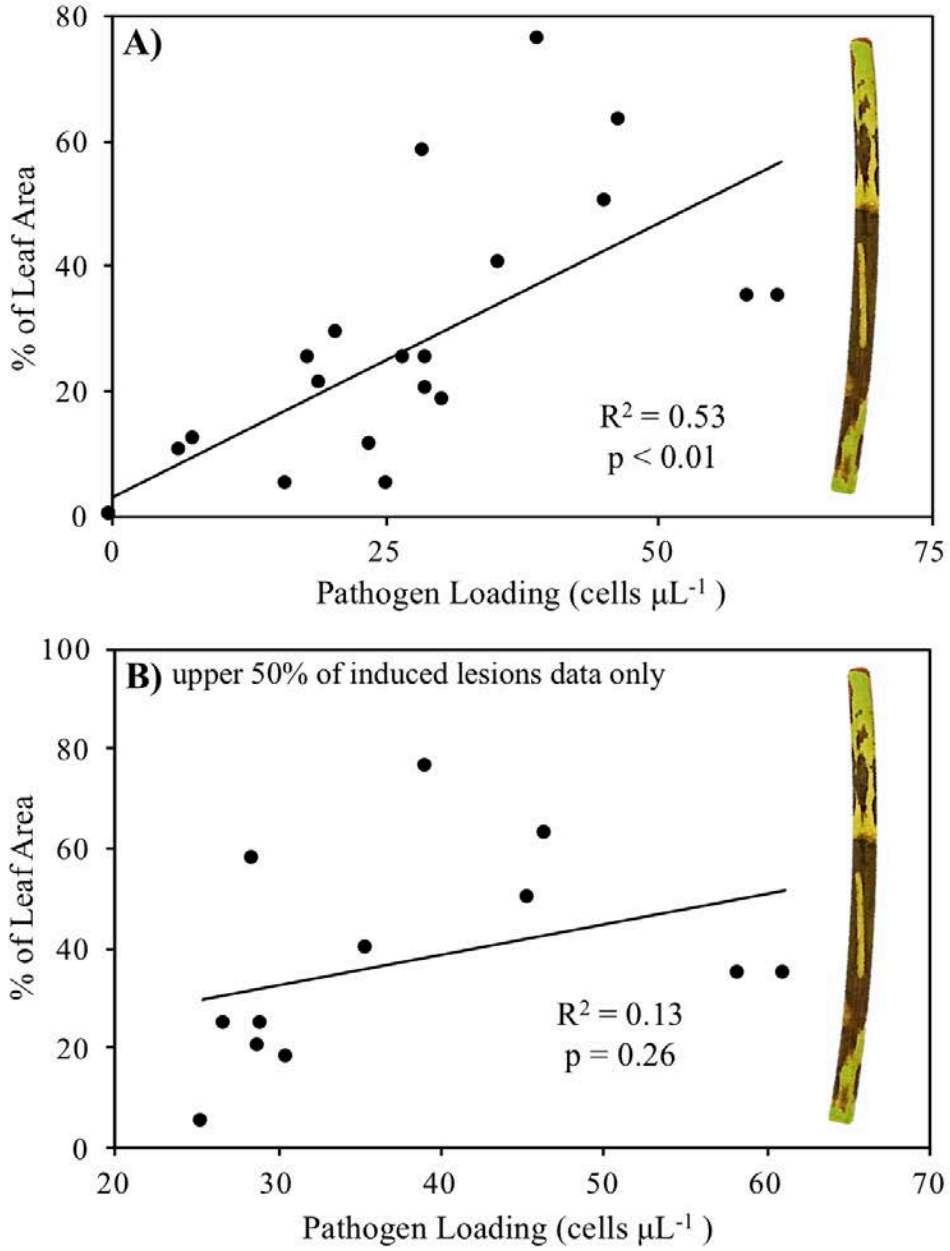

Figure 2-16. Scatterplots displaying the relationship between *Labyrinthula* cell count values obtained through qPCR (pathogen loading) and percent leaf area coverage of induced lesions as determined through WI methods. Part A displays pairwise values across all 23 individuals from the second stress-response experiment. Part B displays a subset of the 23 individuals; more specifically, the 11 samples with the lowest pathogen loading values were removed, such that the pairwise values being displayed represent only the upper ~50% of the data quantifying induced lesions. The overall sample size was reduced from 25 individuals to 23 individuals; one sample was discarded due to errors in the qPCR procedure, and the other due to errors in the WI methods.

hyposaline (26ºC, 15 ppt seawater), or elevated temperature (30ºC, 30 ppt seawater) conditions for one week (figure 2-4).

Two samples (replicate 3 from the hypersaline treatment and replicate 3 from the elevated temperature treatment) were removed from subsequent analyses due to outlier BCA protein concentrations, whose statistically extreme values distorted immune assay activity levels when divided by it. Thus, the ambient and hyposaline treatment groups each consisted of five replicates (n = 5), while the hypersaline and elevated temperature treatment groups were reduced to four replicates (n =4) each.

There were no significant differences among treatment groups as a function of POX, EXOC, and LYS activity (figure 2-17 A, B, D). However, PPO activity differed significantly between ambient and hyposaline ($p = 0.019$) and elevated temperature and hyposaline ($p = 0.047$) treatment groups (figure 2-17 C).

Induced Immunity of Seagrass Exposed to Abiotic Stressors Followed by Pathogen Exposure

Immune metric panels were generated using peroxidase (POX), exochitinase (EXOC), polyphenol oxidase (PPO), and lysozyme-like (LYS) activity assays for *T. testudinum* individuals exposed to either ambient (26ºC, 30 ppt seawater), hypersaline (26ºC, 45 ppt seawater), hyposaline (26ºC, 15 ppt seawater), or elevated temperature (30ºC, 30 ppt seawater) conditions for one week, followed by disease inoculation with *Labyrinthula* vectors to induce wasting disease conditions for a second week (figure 2-6).

One outlier, an EXOC value belonging to an individual within the hyposalinity treatment group, was removed from subsequent analyses due to its extremity. Therefore, the EXOC activity values within the hyposalinity treatment group was reduced to four replicates (n = 4),

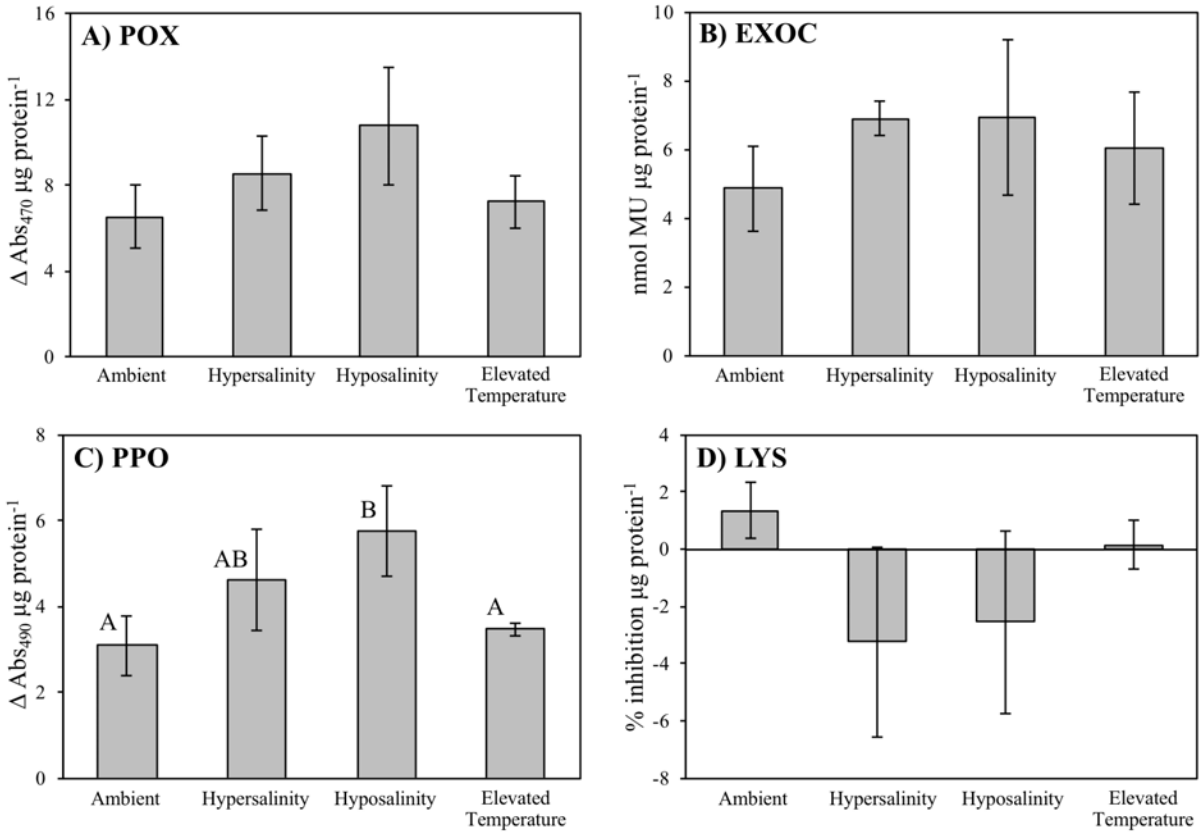

Figure 2-17. Results of biomarker assays measuring stress biomarker activity levels (parts A-D: peroxidase, exochitinase, polyphenol oxidase, and lysozyme, respectfully) of *T. testudinum* individuals from the constitutive stress response experiment under various treatments (control/ambient, hypersalinity, hyposalinity, or elevated temperature). Error bars reflect ±1 SEM. Letters (A & B) represents significant difference in mean activity levels between two treatment groups as determined by ANOVA analyses, followed by multiple comparisons LSD posthoc tests (two-tailed, $\alpha = 0.05$). Sample size n = 5, with the following exceptions: hypersalinity and elevated temperature groups, n = 4 each.

while all other treatment groups measured at each biomarker consisted of five replicates each (n=5).

While PPO activity failed to show any significant differences among treatment groups (figure 2-18 C), both POX (figure 2-18 A) and EXOC (figure 2-18 B) showed significantly lower activities The immune activity differed significantly at both the POX (figure 2-18 A) and EXOC (figure 2-18 B) biomarkers in hypersaline (+ *Labyrinthula*) treated individuals when compared to elevated temperature (+ *Labyrinthula*) stress treatments (POX activity p-value = 0.049; EXOC activity p-value = 0.041). Additionally, individuals which were exposed to ambient conditions but not the pathogen (– *Labyrinthula*) differed significantly from both [1)] those exposed to ambient conditions (+ *Labyrinthula*) and [2)] those exposed to elevated temperature (+ *Labyrinthula*) at two biomarkers: EXOC ([1)] p-value = 0.034; [2)] p-value = 0.007) (figure 2-18 B) as well as the LYS ([1)] p-value = 0.028; [2)] p-value = 0.025) (figure 2-18 D).

Differential Pathogen Loading as a Function of Experimental Treatment

The novel quantitative polymerase chain reaction (qPCR) assay presented in this chapter was utilized to measure the degree of pathogen loading in diseased tissue from the inoculation experiment (figure 2-6) through detection of *Labyrinthula* cells down to a specific cell count. An error in the DNA extraction procedure resulted in the removal of one individual from the ambient treatment group which was not exposed to *Labyrinthula*, reducing the sample size of this group down to four replicates (n = 4), while all other treatment groups retained five replicates (n = 5).

Our qPCR-based method detected an abundance of *Labyrinthula* cells that were several orders of magnitude lower in individuals belonging to the negative control treatment (ambient

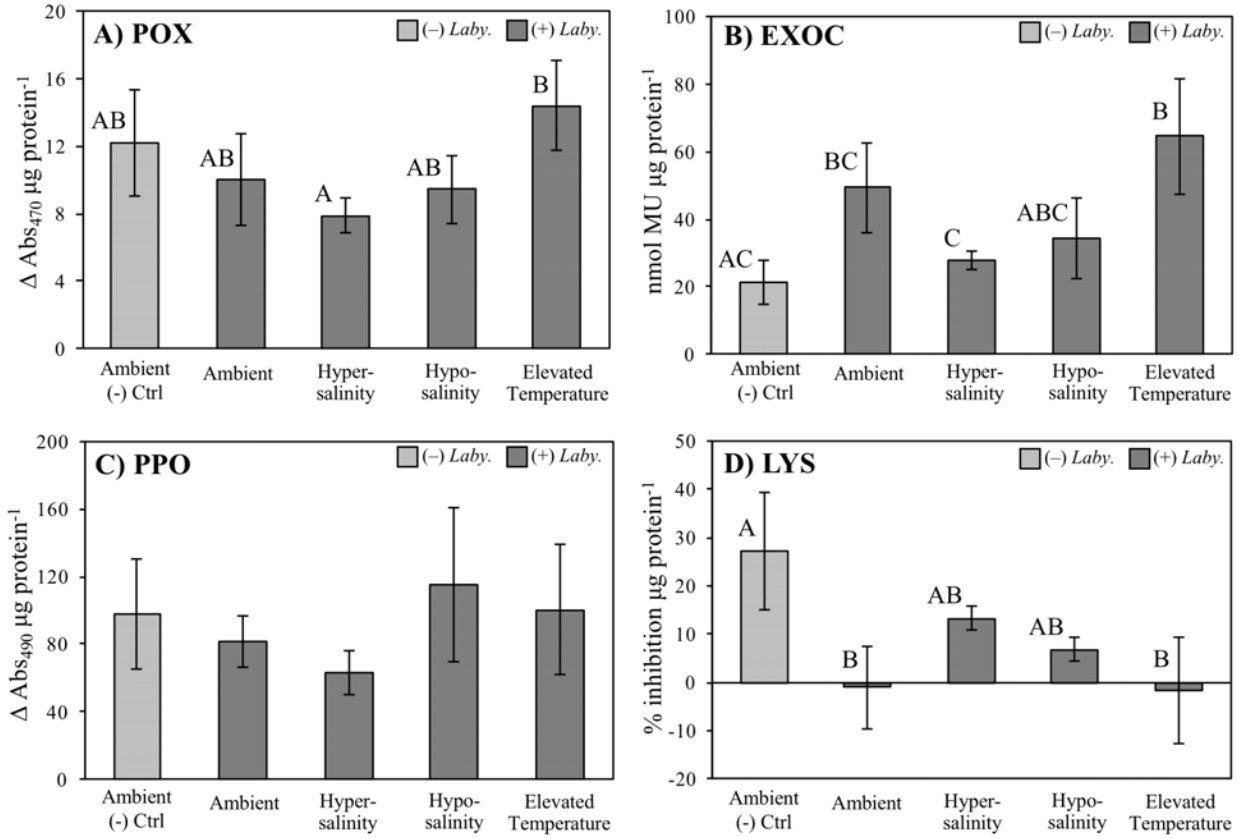

Figure 2-18. Results of biomarker assays measuring stress biomarker activity levels (parts A-D: peroxidase, exochitinase, polyphenol oxidase, and lysozyme, respectfully) of *T. testudinum* individuals from the induced stress response experiment under various treatments [control/ambient (-) *Laby.*; ambient (+) *Laby*; hypersalinity (+) *Laby*; hyposalinity (+) *Laby*; elevated temperature (+) *Laby.*]. Error bars reflect ±1 SEM. Different letters (A, B, & C) represents significant differences in mean activity levels between two treatment groups as determined by ANOVA analyses, followed by multiple comparisons LSD posthoc tests (two-tailed, $\alpha = 0.05$). Sample size n = 5, with one exception: part B, hyposalinity treatment, n = 4.

conditions, – *Labyrinthula*), when compared to all other treatment groups (ambient, hypersalinity, hyposalinity, and elevated temperature, all + *Labyrinthula*) (p-value = 0.005, 0.004, 0.036, and 0.001, respectively) (figure 2-19; table 2-2). Additionally, there was a significant difference between individuals belonging to the hyposalinity (+ *Labyrinthula*) and the elevated temperature (+ *Labyrinthula*) treatment groups (figure 2-19; table 2-2). However, there were no detectable differences between any of the abiotic stress treatments and the ambient control exposed to *Labyrinthula* during the second week of the experiment (figure 2-19; table 2-2). Furthermore, a subsequent ANOVA analysis in which the significantly different negative control group (ambient conditions, **–** *Labyrinthula*) was removed revealed that the sum of square values within groups vastly exceeded that which measured between group variation (SS = 3482.063 verses 457.595, respectively) among individuals who were introduced to the pathogen (table 2-3).

Immune Status and Pathogen Loading as Functions of Individual Variation

In an effort to address potential variation among individuals in the second stress-response experiment, regardless of treatment group, we tested the strength of relationships between each biomarker and *Labyrinthula* cell count as a function of each individual. Correlative analyses revealed that there was a positive relationship between individual pathogen loading and POX activity ($R^2 = 0.18$) that was significant, with 95% confidence ($\alpha = 0.05$; p-value = 0.04) (figure 2-20 A) and between individual pathogen loading and EXOC activity ($R^2 = 0.33$) that was significant, with 99% confidence ($\alpha = 0.01$; p-value = 0.04) (figure 2-20 B). The relationships between pathogen loading and PPO activity and pathogen loading and LYS activity were not significant (figure 2-20 C, D).

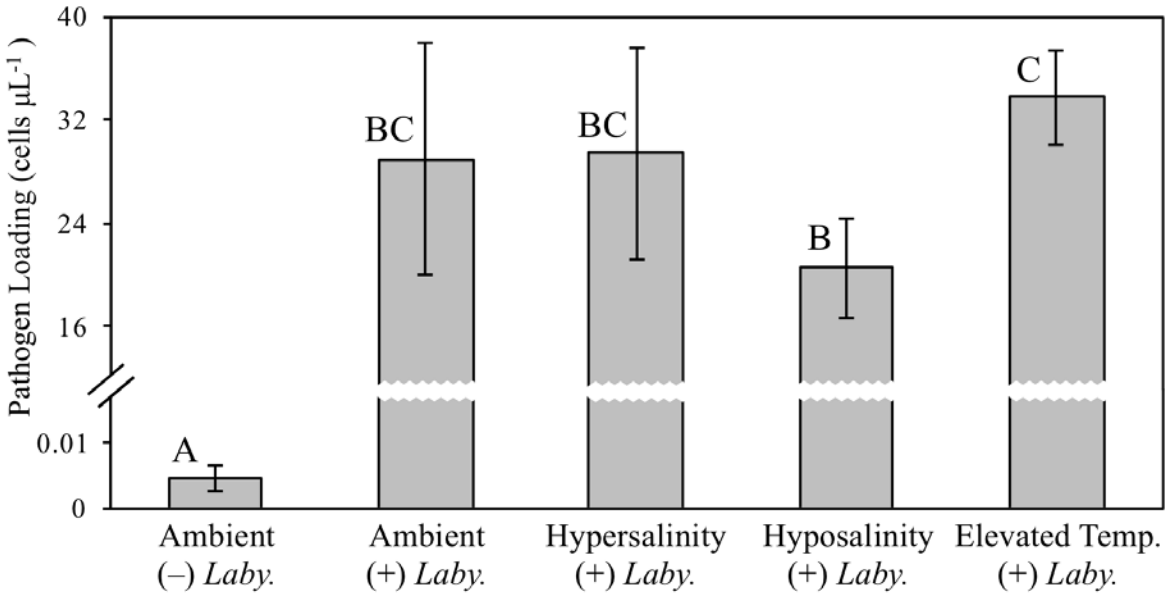

Figure 2-19. Results of qPCR assays measuring pathogen loading (number of *Labyrinthula* cells per ng DNA) in tissue of *T. testudinum* individuals from the second stress-response experiment, under control [no *Labyrinthula*, or (-) *Laby.*] and pathogen-exposed [ambient (+) *Laby*; hypersalinity (+) *Laby*; hyposalinity (+) *Laby*; elevated temperature (+) *Laby.*] conditions. Error bars reflect ±1 SEM. Asterisk (*) represents two-tailed significant difference at $\alpha = 0.01$. Sample size n = 5, with one exception: Ambient (-) *Laby*. treatment, n = 4.

Table 2-2. Results of multiple comparisons LSD posthoc tests (p-values) comparing pathogen loading (*Labyrinthula* cells ng DNA^{-1}) pairwise between treatment groups [control/ambient (-) *Laby*.; ambient (+) *Laby*; hypersalinity (+) *Laby*; hyposalinity (+) *Laby*; elevated temperature (+) *Laby*.] in the second stress-response experiment. One and two asterisks (*, **) represent two-tailed significance at $\alpha = 0.05$ and $\alpha = 0.01$, respectfully. Insignificant differences between treatments are shaded in gray.

	Ambient (-) *Laby.*	**Ambient**	**Hyper-salinity**	**Hypo-salinity**	**Elevated Temp.**
Ambient (-) *Laby*	—	0.005**	0.004**	0.036*	0.001*
Ambient	—	—	0.961	0.336	0.586
Hypersalinity	—	—	—	0.313	0.620
Hyposalinity	—	—	—	—	0.037*
Elevated Temperature	—	—	—	—	—

Table 2-3. One-way ANOVA results of treatment effect on pathogen loading (*Labyrinthula* cells ng DNA^{-1}) in the second stress-response experiment.

	Sum of Squares	df	Mean Square	F	Sig.
Between Groups	457.595	3	152.532	0.701	0.565
Within Groups	3483.063	16	217.691		
Total	3940.658	19			

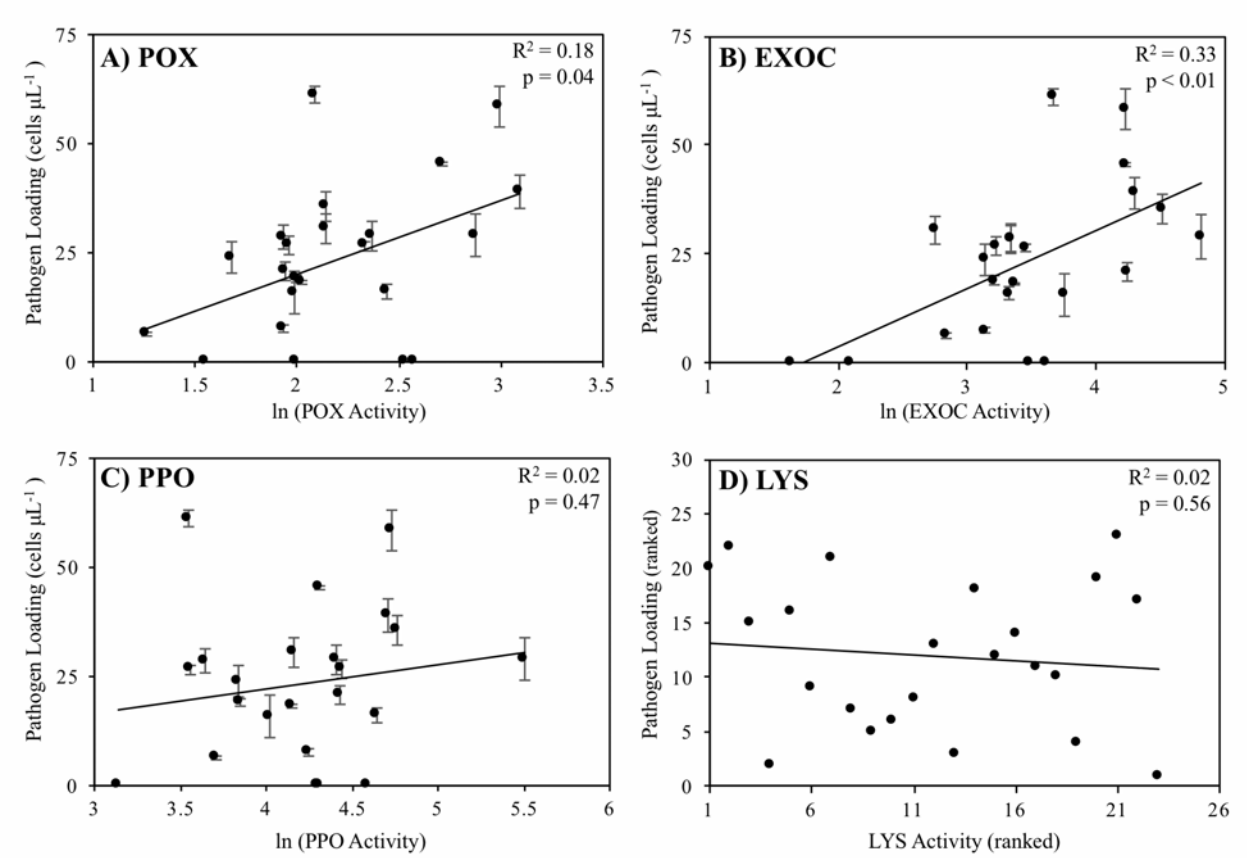

Figure 2-20. Results of correlation analyses between quantified pathogen load (*Labyrinthula* cells μL^{-1}) and stress biomarker activity levels (parts A-D: peroxidase, exochitinase, polyphenol oxidase, and lysozyme, respectfully) of *T. testudinum* individuals from the second stress response experiment. Significance (p-values) are based on Pearson product-moment correlation coefficients (A-C) or Spearman's rho correlation coefficients (D). Error bars reflect ±1 SEM for pathogen loading values (A-C). Error bars are not present in Part D because the variables are displayed as ranked values due to the non-parametric nature of the LYS activity data set. The sample size in all parts (A-D) was reduced from 25 individuals to 24 individuals, as one sample was discarded due to errors in the qPCR procedure. The sample size was further reduced to 23 individuals in Part B due to an error in the EXOC assay.

Variation among individuals was also graphically represented as a heat map, where individual values were converted to proportionally pigmented colors and displayed as a matrix (figure 2-21); each column represents the relative pathogen loading or activity at each of the four biomarkers and each row represents one individual from the second stress-response experiment (in ascending order of pathogen loading from top to bottom). Though statistically untested, several points of interest emerge. The individual possessing the highest LYS activity (individual "1") also exhibits the lowest relative *Labyrinthula* cell count in its tissue (figure 2-21). Likewise, the two lowest LYS activity values belong to individuals ("20" and "22") who are among the most infected (that is, among the highest pathogen loading values) (figure 2-21). Seagrass individual "17" has relatively high enzyme activity, overall, and is the 7th most infected with *Labyrinthula* cells (figure 2-21). In contrast, individual "3" has relatively low POX, EXOC, and PPO activity levels and exhibits a very low degree of pathogen loading (the first four individuals have pathogen loading values that fall within a range that have been attributed to "background noise") (figure 2-21).

2.5 Discussion

Elucidating the relationship between aquatic species and their pathogenic diseases is pertinent in the field of marine ecology because infection outbreaks have the potential to drastically alter ecosystem functionality (Blakesley et al. 2002, Burge et al. 2014). However, these pathosystems are usually complex and dynamic, and our understanding of the mechanisms that underpin disease etiology is often hindered by a paucity of basic information on the host and/or pathogen involved. In the case of seagrass wasting disease, this hindrance may be partially attributed to

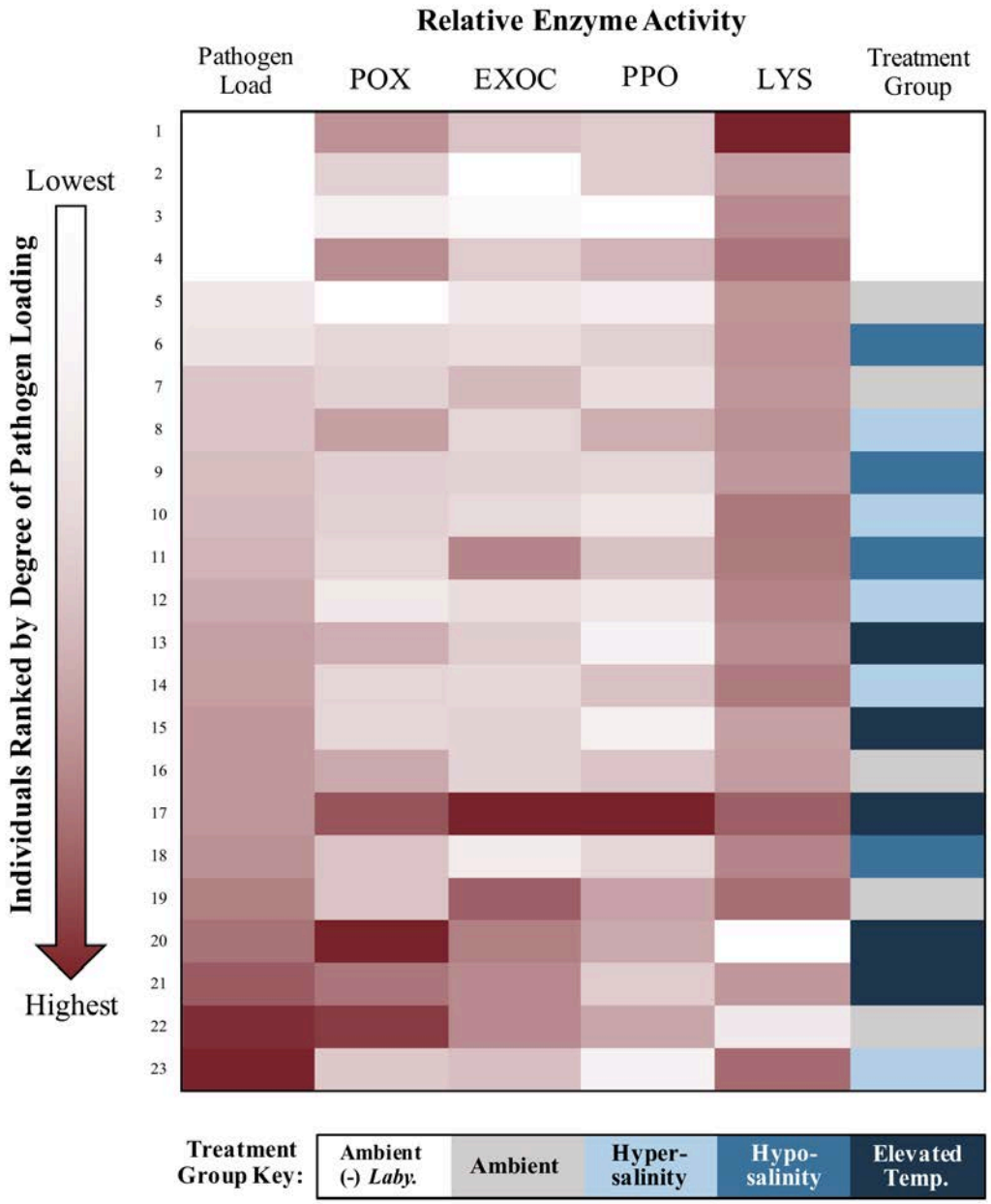

Figure 2-21. Heat map displaying relative values at the five parameters measured (POX activity, EXOC activity, PPO activity, LYS activity, and pathogen load) in *T. testudinum* individuals of the second stress-response experiment [subjected to control/ambient (-) *Labyrinthula*, ambient (+) *Labyrinthula*, hypersalinity (+) *Labyrinthula*, hyposalinity (+) *Labyrinthula*, or elevated temperature (+) *Labyrinthula*, shaded white, gray, light blue, blue, and dark blue, respectively. Each column represents the relative pathogen loading or activity at each of the four biomarkers and each row represents one individual from the second stress-response experiment (in ascending order of pathogen loading from top to bottom). The shade assigned to each individual at a given parameter reflects the proportional activity at that parameter, as compared to the entire data set, with white representing the lowest value of the set and dark red representing the highest.

outdated pathogen quantification techniques within host tissue and the absence of a practical method to generate immune status profiles in seagrass individuals, both of which are needed to test the hypothesis that disease susceptibility is intimately linked to the ability of the host to initiate defense responses. This study sought to develop and implement the methodologies necessary to investigate the role of environmental stressors in dictating host immunocompetence and susceptibility to seagrass wasting disease.

Pathogen Detection via the qPCR Assay is Valid and Broadly Applicable

This chapter presents, and validates the use of, a real-time quantitative polymerase chain reaction (qPCR) technique that is capable of detecting and quantifying the pathogen, *Labyrinthula*, in pure culture samples and, more importantly, in host seagrass tissue. While previous studies have established similar qPCR methodologies to measure pathogen cells in wasting disease tissue, their primers were tailored to one species, *Labyrinthula zosterae*, which is host-specific to the temperate seagrass *Zostera marina* (Bergmann et al. 2011, Bocklemann et al. 2013). Our results indicate that the qPCR assay presented herein is capable of detecting a broad range of globally distributed *Labyrinthula* strains, isolated from within both temperate and tropical regions. Furthermore, our assay preferentially amplifies putatively pathogenic isolates, increasing the likelihood that, when used on field-collected individuals, amplification values will be reflective of the quantity of pathogenic (and not non-pathogenic) strains, which is desirable as only the former are capable of producing disease in host tissue.

The ability to resolve small quantities of template DNA (in this case, belonging to pathogenic *Labyrinthula*) is an important component to consider when implementing a successful qPCR assay. Our assay consistently and reliably detected standard curve dilutions

containing DNA concentrations that were at and above 4.75×10^{-3} cells per microliter (μL). This estimate is an order of magnitude more sensitive than the detection limit of the *L. zosterae*-specific assay (Bergmann et al. 2011), suggesting that it is certainly sensitive enough to dependably pick up ecologically relevant quantities from within host seagrass tissue. Additionally, the extraction/amplification efficiency estimate was within the range of accepted values as published in previous studies (86.2% to 104.0%, Bergmann et al. 2011).

Quantitative PCR methods serve as a more direct measurement of infection in the plant host tissue, as compared to the indirect proxy method, known as Wasting Index, which relies on visually assessing the percent of the tissue covered by necrotic lesions (Burdick et al. 1993). To validate this assumption, we utilized both methods to assign relative disease quantities in 19 blades which were inoculated with *Labyrinthula* and displayed wasting disease symptoms, and four blades which were not deliberately inoculated with the pathogen. The results indicate that, while the two methods appear to be comparable to one another across a broad range of infection levels (Fig. 2-16A), the correlation between the two methodologies deteriorates at higher levels of disease (Fig. 2-16B). This discrepancy may be explained by the findings of a study conducted by Muehlstein et al. (1991) who found *Labyrinthula* cells in apparently healthy, green tissue up to 5 mm from visibly blackened lesion tissue. Later studies further advanced the notion that WI may underestimate both the number of pathogen cells present and the areal extent of damage inflicted on a region of host tissue, based on the observation that photosynthesis was significantly impaired in green eelgrass tissue beyond the local lesion sites (Ralph & Short 2002). Furthermore, “browning” could be a function of host necrosis or programmed cell death in response to pathogen infection as opposed to serving as an actual reflection of true pathogen

load (Greenberg et al. 1994, Ma & Berkowitz 2011). Finally, Muehlstein (1992) described that *Labyrinthula* cells were more abundant along the margins of disease lesions, suggesting that total areal measures of lesions may not be appropriate to quantify of the degree of *Labyrinthula* infection. Consequently, the results of the present study contribute to the body of evidence which collectively suggests that a shift from historical WI methods to qPCR-based detection techniques is warranted, as they arguably produce more accurate estimates of the true virulence of the parasite and susceptibility of the host.

Biomarkers are Constitutively Active and Variable Among Individuals, Regardless of Treatment

The first step in elucidating the role of environmental stressors in dictating the ability of *Thalassia testudinum* to mount an immune response to pathogen invasion was to establish quantifiable measures of seagrass immunity, then identify constitutive and inducible immunity expression patterns following exposure to selected abiotic stressors.

The results of the biomarker assays testing innate stress-responses of the host in the presence of abiotic stressors indicated that peroxidase (POX), exochitinase (EXOC), and polyphenol oxidase (PPO) were constitutively active in *T. testudinum* experimental individuals. Lysozyme-like activity was variable in individuals among and within treatment groups; the crude protein extract of some samples appeared to inhibit bacterial growth, while others promoted it (figure 2-17 D). In those samples where LYS activity was negative, meaning the addition of protein extract promoted growth of the bacteria, it is likely that the apparent benefit of other proteins within the crude extract simply outweighed negligible LYS activity, whereas positive LYS activity measurements might indicate that the inhibitory effects of LYS activity on growth offset any advantage conferred by the crude protein amalgam.

It was hypothesized that constitutive expression of the chosen biomarkers in seagrass tissue may be compromised or suppressed in the presence of selected abiotic stressors. However, the results of the innate stress-response experiment show that POX, EXOC, and LYS activity levels were not significantly affected by the stressors imposed (hypersalinity, hyposalinity, and elevated temperature) when compared to control groups (ambient). The only biomarker whose expression varied significantly between treatments was PPO (figure 2-17 C). Individuals exposed to hyposaline conditions had significantly higher PPO expression compared to those in either ambient or elevated temperature treatments. Much of the literature on PPO expression in plants revolves around its role in the inducible immune response to pathogen exposure (Li & Steffens 2002, Mayer 2007), but it has been proposed that PPO may play a role in the generation of reactive oxygen species (ROS) (Thipyapong et al. 2004). Furthermore, Trevathan-Tackett (2011) noted that ROS production was upregulated in *T. testudinum* individuals following exposure to sub-optimal salinity conditions in a controlled laboratory setting similar to the methods of this study. Thus, previous findings support the trend observed in this study, and suggest that osmotic stress (e.g. hyposalinity) may upregulate enzymes, such as PPO, that are involved in the ROS-induction pathway (Thipyapong et al. 2004, Trevathan-Tackett 2011).

Complex Immune Responses Driven by Pathogen Exposure

In order to test the commonly-held hypothesis that stress imposed by the environment reduces overall fitness and defense responses in plants, thereby increasing an individual's susceptibility to subsequent disease infection, we explored the competing roles of abiotic stressors, plant immunity, and pathogen exposure in our model pathosystem. Previous studies have indicated that when environmental stressors are applied in conjunction with *Labyrinthula* inoculation, any

negative impacts on the host may be outweighed by the sensitivity of pathogen. More specifically, Bishop et al. (2016) noted that elevated salinity suppressed the severity of wasting disease in *T. testudinum* individuals, but this response was attributed to the sensitivity of *Labyrinthula* to hypersaline conditions, rather than a compromised ability of the host to fight infection. Thus, in this experiment, we simulated a scenario where the environmental stressor is lifted as the pathogen is introduced in an attempt to isolate the impact of stressors on the host seagrass species, and not the pathogen. This scenario is plausible, considering the high degree of stochasticity in the coastal marine environments where both species are found. A system habitually exposed to hypersaline conditions, for example, may actively suppress the virulence in an omnipresent, yet dormant, *Labyrinthula* species while simultaneously imposing chronic stress on the long-lived seagrass host. A short-term shift in environmental conditions, such as a sudden increase in rainfall due to a tropical storm, may shift the favor from host to pathogen, whereby the opportunistic, fast-growing parasite takes immediate advantage of optimal conditions, while adjustments occurring in the host, such as a revitalization in its ability to resist pathogen invasion, likely occur over a longer time frame.

The results of this study highlight the complexity of plant immune responses. In general, immune activity varied considerably within and among experimental treatment groups; as a result, visual trends often lacked statistical significance (figure 2-18).

In contrast to the findings of first stress-response experiment, PPO activity did not vary significantly among treatment groups; expression levels were not differentially affected by the addition of the pathogen (ambient conditions +/– *Labyrinthula*) or by the presence of abiotic stressors followed by pathogen inoculation (ambient conditions versus hypersaline, hyposaline,

and elevated temperature treatments) (figure 2-18 C). This observation is in contrast to previous findings, which suggest that PPO plays a role in the defense and resistance of plants against pathogen invasion (Li & Steffens 2002, Thipyapong et al. 2004).

The results detailing POX expression are equally perplexing in the context of differential expression among treatment groups, as a number of studies have found positive relationships between a specific subclass of POX enzymes and resistance to disease (Lovrekovich & Farkas 1965, Simons & Ross 1970, Mydlarz & Harvell 2006, and reviewed in Hiraga et al. 2001). Consequently, it was hypothesized that there would be a significant induction of POX activity in *Labyrinthula*-infected individuals as compared to the control group (– *Labyrinthula*), which was not the case (figure 2-18 A). However, this lack of differential expression trends among treatment groups is likely due to sample size limitations, supported by the emergence of significant trends when all samples were pooled together (figure 2-20, discussed in more detail within the next section)

EXOC activity appears to have been upregulated in response to pathogen exposure, but only when preceded by ambient or elevated temperature treatments. These results are interpreted as a component of the induced immune response. The lack of a difference between the no-pathogen control and the hyper- and hypo-salinity treatments which were exposed to *Labyrinthula* suggest that stress due to either sub-optimal saline condition may have impaired the seagrasses' ability to mount a defense response, via the upregulation of EXOC activity, when later challenged with the pathogen. Interestingly, Douglas et al. (2006) noted that EXOC levels decreased in sea fans following stressful events (via injury, agitation, or tissue manipulation); however, they observed a concurrent, transient increase of this enzyme in samples taken from the

water column adjacent to the fans. They proposed that EXOC is actually synthesized constitutively as a protection against opportunistic infections and that specific stressors can trigger the release of EXOC enzymes into the surrounding environment (Douglas et al. 2006). Therefore, it is possible that a similar EXOC release event occurred in the hyper- and hypo-salinity-stressed individuals during the first week of the lab experiment and, as microcosm water was discarded and replaced with ambient (30 ppt) seawater just before the pathogen was introduced at the start of the second week, EXOC would have been absent from both the water column and the plant tissue in these individuals at the time of collection. Future studies should perform EXOC activity assays on water samples collected during similar experiments in order to explicitly test this hypothesis.

Interestingly, the results of the LYS assay produce similar trends as those observed in EXOC activity, but in the opposite direction, with respect to the conditions which downregulated the immune response parameter under comparison. LYS activity was significantly reduced in response to pathogen exposure, but only when preceded by hypersaline or hyposaline treatments. As LYS levels are higher in individuals which were not exposed to the pathogen, activity at this biomarker is interpreted, in this context, as a component of the constitutive immune response. A potential explanation of these results, in conjunction with the trends observed in EXOC activity, is that LYS activity was reduced in ambient and elevated temperature treatment individuals due to resource reallocation and a shift away from investment in the constitutive immune response via LYS, which may have been necessary in order to successfully upregulate EXOC activity in response to pathogen invasion. Furthermore, the absence of this activity shift in individuals belonging to the hyper- and hypo-saline treatment groups may suggest a differential (and

possibly compromised) capacity to respond to pathogen challenge in an immune system which has become overwhelmed by specific abiotic stressors. Indeed, immunity is a costly process to invest in (Armitage et al. 2003), suggesting that tradeoffs must occur, and individuals who can effectively allocate resources, and dynamically shift those allocations as new threats are posed, confer a fitness advantage over those who cannot. Whether or not this differential allocation paid off depends on the resulting degree of infection within these individuals.

Thus, in addition to validating the assumption that the treatment group which was not exposed to the pathogen (Ambient, **–** *Labyrinthula*) was, indeed, void of ecologically significant *Labyrinthula* cell counts, our analysis of differential pathogen loading as a function of treatment group revealed several important patterns. If the selected environmental stressors contributed to increased prevalence and severity of wasting disease in seagrass tissue, as predicted based on previous observations (Blakesley et al. 2002, Trevathan-Tackett et al. 2015, Bishop et al. 2017), the treatment group inoculated with *Labyrinthula* but held at ambient temperature (26°C) and salinity (30 ppt) should have resulted in significantly lower pathogen loading values as compared to one or more of the treatments which paired an abiotic stressor with subsequent infection. However, this was not the case; the hypersalinity, hyposalinity, and elevated temperature treatments (all + *Labyrinthula*) did not vary significantly from the ambient (+ *Labyrinthula*) group with respect to the number of pathogenic cells infecting their tissue. One possible explanation for this deviation from our expectations, and those predicted by the findings of past work, lies in the high degree of within-group variation as compared to variation that existed between groups. Variability among individuals may exist for a variety of reasons beyond those explicitly accounted for in the experimental design (e.g. genetic variation); given the limited

sample size within groups ($4 \leq n \geq 5$), it is plausible that the wide degree of inherent (or otherwise unaccounted for) variability we observed in both immune response parameters and pathogen loading masked any true differences that existed between experimental factors. The second trend which emerged was that that there was a significant difference between *Labyrinthula* infection among the hyposalinity and elevated temperature treatments. More specifically and on average, individuals exposed to elevated temperature followed by pathogen inoculation were more susceptible to infection than individuals exposed to the hyposalinity treatment. The pathogen loading differences among these treatment groups will be examined in the following section, within the context of a proposed mechanism which helps explain this pattern observed.

Individual Variation Trends Support a Potential Trade-Off Mediated Immune Response

In an attempt to extricate meaning from the considerable variation in experimental samples that was not due to treatment effects, the values estimated for each parameter (including POX, EXOC, PPO, LYS, and *Labyrinthula* cell loading) were pooled together and treated as one data set to examine trends that might exist between immune metric values and pathogen loading as a function of variation among individuals. In this manner, correlative analyses revealed significant positive relationships between wasting disease severity and immune status at two of our chosen biomarkers. The results suggest that both POX and EXOC activity is upregulated as pathogen loading increases in *T. testudinum* tissue (figure 2-20 A, B).

While this association does not guarantee that elevated POX and/or EXOC activity causes increased susceptibility to wasting disease (or, conversely, that disease proliferation throughout host tissue directly results in the upregulation of POX and/or EXOC enzymes), it

does highlight interesting patterns, especially when viewed in a context provided by other aspects of this study. More specifically, it may be valuable to revisit the proposed explanation detailing a perceived resource allocation shift in certain treatment groups (ambient and elevated temperature) from constitutively expressed LYS activity to the induction of EXOC activity in response to pathogen invasion. The positive association between EXOC activity and wasting disease severity, however, may imply that the investment in EXOC activity-based defenses did not pay off, a gamble which resulted in a compromised system that was susceptible to infection. Alternatively, it is possible that this shift occurs *after* pathogen loading reaches a certain threshold level in host tissue, and that samples containing the highest prevalence of *Labyrinthula* tissue had not yet succumbed to the disease, but were captured in a state of active defense facilitated by the shift from their first line of defense (constitutively expressed proteins, e.g. LYS) to a more sophisticated and context-dependent attack (via enzymes, like EXOC, induced in response to specific cues).

The presence of a tradeoff-mediated immune response, mechanistically similar to the one proposed here, is further supported by the differential pathogen loading estimates observed between the hyposaline and elevated temperature treatment groups. The reallocation of resources by the elevated temperature treatment, as indicated by the observed decrease in the apparent constitutive expression of LYS activity coupled with the induction of EXOC enzymes, may be evidence that these individuals are responding to pathogen invasion, whereas a reallocation in defense responses has not been initiated in the hyposalinity treatment as evident by trends in LYS and EXOC activity that were the inverse of those seen in the elevated temperature treatment.

However, the basis as to why elevated temperature, but not hyposaline, individuals may have been compelled to reallocate immune response tools remains unclear. Earlier in this discussion, it was proposed that the immunity of individuals exposed to sub-optimal hyposaline conditions may have been compromised by their assigned stressor, preventing them from facilitating the shift in chemical defense from LYS to EXOC, but, given that hyposalinity-treated individuals had less pathogen loading than those of the elevated temperature group, the possibility exists that the latter group, not the former, was the group which experienced compromised immunity. Perhaps some untested component of the seagrasses' constitutive immune response was actively weakened by the temperature stress treatment, allowing the pathogen to gain a foothold in its host, who then responded via an alternative pathway such as EXOC (and/or POX) activity. The absence of this shift in hyposalinity treatment individuals may, then, be indicative of a successful first line of defense (the constitutive immune response) in deterring the pathogen. This would explain the observed differences in both immune markers and pathogen loading estimates between these two groups. However, as neither of these treatments differed significantly from the ambient group (+ *Labyrinthula*) in terms of disease prevalence and severity, the extent to which we can explain differences in this manner are limited.

The heat map was included in our results to visually demonstrate the complex and variable response across experimental individuals at the parameters we assessed. In the most general sense, there appears to be a loose, statistically invalid, inverse relationship between pathogen load and LYS activity, as some of the lowest LYS values are found in individuals with the highest pathogen load and vice versa. However, the statistical power of this potential trend is

lost in the high degree of LYS activity variation observed in the individuals with moderate estimates of pathogen loading (individuals “5” through “18”, figure 2-21). In other words, individuals within our experiment did not appear to have a mechanistic response that was consistent enough among replicates to be detected by our dependent variables.

Once again, variation within the sample population of seagrass appears to obscure potential findings and produce inadequate conclusions of observed phenomenon. Thus, it is necessary to address the limitations of this study. Notably, the design of this experiment assumed that one week of applied stressors was sufficient to elicit a differential response. Indeed, early attempts were made to prolong the duration of experiment, but were deemed impossible due to rapidly deteriorating conditions of all experimental samples around the two-week mark. Not only did this hinder the length of the experiment and introduce the possibility that the period of stress was too brief to produce detectable changes, but it also implied that all experimental units faced stressful conditions that were artifacts of the experiment and independent of the applied abiotic stressors. Consequently, the ambient treatment may not have accurately simulated an environment that was void of stressors; in other words, there may have been a lurking variable which stressed all individuals to the point where the effects of the chosen stressor applied on top of it were negligible by comparison. In order to address these concerns and parse out details and/or trends that were not discernible in this experiment, future studies should focus on improving experimental microcosm conditions in an effort to extend the longevity of the treatment period and minimize stress imposed on the individual, ideally such that it represents only stressors deliberately implemented. Furthermore, sample size within treatment groups

should be significantly increased in order to compensate for the high degree of individual variation we observed among replicates.

CHAPTER 3: INVESTIGATING PATTERNS BETWEEN TURTLEGRASS PATHOGEN LOADING, IMMUNE STATUS, LEAF MORPHOLOGY, AND WATER QUALITY IN FLORIDA BAY

3.1 Abstract

Florida Bay is a shallow subtropical estuary located between the mainland of Florida and the Florida Keys. *Thalassia testudinum* dominates this highly productive region, but the spatiotemporal heterogeneity of the system and recent hydrological changes, among other human impacts, impose a variety of stressors on this seagrass species. Seagrass wasting disease, caused by a genus of protists known as *Labyrinthula*, represents an understudied aspect in the efforts which have been made to predict the future health of *T. testudinum* meadows in Florida Bay. This study used a novel qPCR-based detection method to quantify *Labyrinthula* loading in *T. testudinum* tissue collected from 15 sites throughout the bay, as well as a set of biomarker assays to generate an immune profile for each individual sampled. Additionally, the history of leaf morphology and important water quality parameters at the sites sampled were obtained through long-term monitoring networks. The results, which involved a series of univariate and multivariate analyses searching for meaningful patterns among data, revealed that both pathogen loading and immune status varied as a function of location in Florida Bay. Furthermore, based on the trends observed among and between sites with regards to pathogen loading, immune status, leaf morphology and water quality, a mechanism in which all four of these parameter sets interact is proposed as a potential explanation for the differences observed in *Labyrinthula* prevalence and severity within the bay. The findings of this study have important implications for management strategies of *T. testudinum* beds in Florida Bay, and may be useful in predicting future outbreaks of seagrass wasting disease.

3.2 Introduction

Marine organisms living within coastal habitats are routinely exposed to an onslaught of disturbances of both natural and anthropogenic origin. System hydrodynamics, stratification, species composition and distribution, nutrient availability, sporadic weather patterns and storms, changes in volume and duration of freshwater input, and algal blooms are just a few of the inherent factors contributing to the spatiotemporal variation within these ecosystems (Blakesley et al. 2002, Fourqurean et al. 2003, Hackney & Durako 2004, Greenwood et al. 2006). Many of these factors exhibit temporal variation across years, seasons, or even tidal cycles at a single location- and spatial differences are often as great, or greater. The inhabitants of these regions have developed a broad set of adaptations to deal with this environmental stochasticity, but, even so, it is not uncommon for a species to find itself at or near the limits of its physiological tolerance (Bricker et al. 2011). Anthropogenic impacts exacerbate these stressful conditions. The proximity of coastal ecosystems to human activity results in significant exposure to associated disturbances including physical damage and habitat modification, overharvesting of important species, freshwater source withdrawal and diversion, climate change, coastal development, non-native and invasive species introduction, and nutrient loading (Orth et al. 2006, Madden et al. 2009).

Seagrass meadows form the benthic habitat of some of the most globally significant and ecologically diverse communities in the aquatic realm (Robblee et al. 1991, Zieman et al. 1999, Orth et al. 2006). As foundation species and autogenic engineers, seagrasses provide a broad array of ecosystem functions, including erosion control, carbon fixation and export, oxygen production, nutrient cycling, and most notably, three-dimensional structure and habitat for

species across virtually every taxon (Short et al. 2000, Dawes et al. 2004, Orth et al. 2006). Unfortunately, the distribution of seagrasses throughout subtropical and temperate coastal regions makes them especially vulnerable to ecological permutations- so much so that they are often utilized as bio-indicators of ecosystem health (Hackney & Durako 2004). These vascular plants are especially sensitive to light availability, salinity, water movement and wave action, nutrient availability, sediment accumulation, and temperature (Waycott et al. 2009); however, as an artifact of their terrestrial origin, the high light requirement of seagrasses is thought to be the dominant factor which limits their distribution (Hackney & Durako 2004).

Florida Bay is a notable example of a system which is dominated by and relies upon seagrass communities; they form the primary physical structure of this shallow (average depth <2 m; Schomer & Drew, 1982), semi-enclosed and roughly triangular-shaped estuary situated between the Everglades, the Florida Keys and the Gulf of Mexico (figure 3-1) (Hall et al. 2007, Bricker et al. 2011, Herbert et al. 2011). This unique geographical position, in conjunction with the limited hydrological connectivity between basins (or regions of the bay which are semi-isolated by shallow carbonate mud-banks), translates to a spatially and temporally heterogeneous lagoon; highly variable water quality, species composition, and even morphological characteristics within a single species (e.g. *T. testudinum,* Bricker et al. 2011) characterize different locations of the bay (Nuttle et al. 2000, Rudnick et al. 2005, Lee et al. 2006, Hall et al. 2007). Florida Bay has historically supported some of the most extensive seagrass meadows in the world (Fourqurean & Robblee 1999, Hackney & Durako 2004, Madden et al. 2009, Bricker et al. 2011), and the three most abundant seagrasses are (from most to least prevalence): the

Figure 3-1. Map detailing the location of the study site, Florida Bay, in relation to the mainland of Florida and several large US cities. Base map obtained using ArcGIS software (ESRI, Version 10.5.1.).

long-lived, climax species *Thalassia testudinum*, followed by *Halodule wrightii* and *Syringodium filiforme* species (Hall et al. 2007, Hammerstrom et al. 2007, Cole 2017). Throughout modern history of the bay, however, the abundance of *T. testudinum* has vastly outweighed that of the other two species; a study conducted in 1989 reported that turtlegrass occupied about 2000 km^2 of the bay's 2100 km^2 (Zieman et al. 1989). While ecosystem stability is a commonly implied benefit of climax species, like *T. testudinum*, it is important to note that some degree of species diversity is considered desirable to attain habitat complexity in a system that is resilient and productive (Boström et al. 2006, Ray et al. 2014). Historically, Florida Bay appeared to exemplify an ideal balance between mono- verses polytypic seagrass communities (Hall et al. 2007, Hammerstrom et al. 2007, Cole 2017).

However, the past 30 years have seen a series of drastic changes which have altered the community structure of seagrass communities in the bay and, consequently, threaten the future of this once-productive and stable ecosystem. These changes are largely due to anthropogenic-induced disturbances, but have been exacerbated by the natural morphology of the system (Hall et al. 1999). Generally speaking, and like most other marine ecosystems at the land-water interface, Florida Bay has experienced loss of biodiversity, eutrophication and algal blooms, habitat loss and degradation, as well as the looming consequences associated with global climate change (Vitousek et al. 1997, Hall et al. 1999, Blakesley et al. 2002, Waycott et al. 2009, Hoegh-Guldberg & Bruno 2010). A disturbance more unique to this system, however, revolves around significant changes in the timing and volume of freshwater draining from the Everglades watershed into Florida Bay (Madden et al. 2009). More specifically, the hydrological dynamics of freshwater inflow have been significantly modified through drainage of natural marsh habitats

for development and agricultural/consumptive use. As a result of these anthropogenic manipulations, the overall flow into the bay has decreased by at least 60% over the past century (Boyer et al. 1999, Madden et al. 2009). This drastically altered the salinity of the estuary, as well as the flux of organic matter (Fourqurean et al. 2003). The bathymetry of Florida Bay further aggravated these hypersaline conditions because the shallow banks which create the distinct basins of the bay also restrict circulation and, therefore, facilitate evaporative processes (Nuttle et al. 2000, Madden et al. 2009).

These changes due to freshwater diversion were recognized among state management groups, and in an effort to better understand the resulting changes in seagrass distribution and abundance over time in Florida Bay, the Fisheries Habitat Assessment Program (FHAP) was initiated in 1995. Funded by the Florida Fish and Wildlife Conservation Commission (FWCC), this long-term monitoring program has since recorded the benthic coverage of seagrass at 15 sites throughout the bay, as well as the water quality and drift algal composition in these locations (Fourqurean et al. 2003, Madden et al. 2009). It was through this program, and others like it, that researchers identified a change in the overall character of the area in a direction generally referred to as the "marinization" of Florida Bay, which, in turn, altered the benthic species composition; conditions shifted favoritism towards *T. testudinum* and away from other, more sparsely present seagrass species (Madden et al. 2009). Restoration plans arose from these observations, including a project known as the Comprehensive Everglades Restoration Program (CERP, established in 2005). A primary objective of CERP was to decrease salinity in the bay to reflect historic conditions by restoring water flow patterns that existed before significant human

diversion projects. Figure 3-2 provides a visual of the changes proposed by CERP with respect to freshwater inflow into the Florida Bay region.

The availability of extensive benthic habitat and water quality (funded and conducted by the South Florida Water Management District, SFWMD) monitoring data amid these drastic changes provide a tantalizing framework for answering ecological questions about this important marine system. Indeed, many studies have been published in recent years that explore the possible shifts in community structure predicted to occur in response to the reversion of hydrological characteristics back to a historical state in Florida Bay. Many of these investigations predict shifts in seagrass community composition and distribution in favor of species that competitively exclude *T. testudinum* in the absence of hypersalinity stress (e.g. *H. wrightii* and *S. filiforme*) (Fourqurean et al. 2003, Lirman & Cropper 2003). However, one additional factor worth considering is the potential role of disease in dictating the abundance and distribution of *T. testudinum* in Florida Bay.

More specifically, we propose a potential population control mechanism among the largely monotypic stands of turtlegrass which exist in Florida Bay, in the form of seagrass wasting disease. Caused by pathogenic parasites of genus *Labyrinthula*, seagrass wasting disease has been implicated as a major contributor to a significant historic die-off event occurring in this region in the late 1980s. The threat of mass-wasting due to *Labyrinthula* outbreaks in this region is plausible considering two additional principles:

1) *Labyrinthula* isolates (see chapter 2 for more detail) are often host-specific and the presence of dense, monotypic seagrass meadows in Florida Bay provides an ideal scenario for the rapid spread of SWD via blade-to-blade contact.

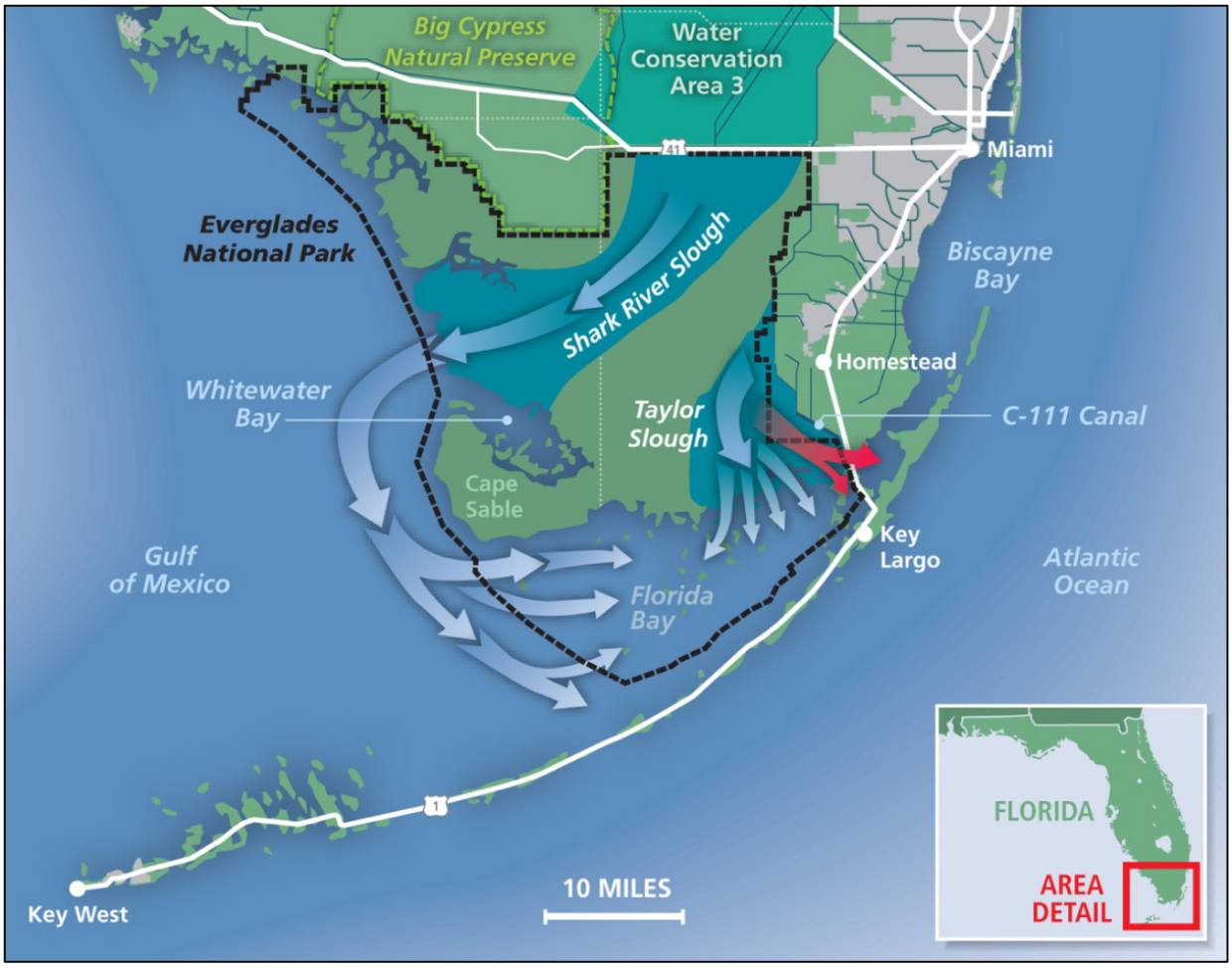

Figure 3-2. Map of South Florida, and specifically, the Everglades watershed, showing the reduced freshwater flow which lead to the marinization of Florida Bay (red arrows) over the 20th century as well as restoration efforts to return the watershed back to its historic state (blue arrows) in terms of the volume, timing and distribution of freshwater flow. Image obtained at: https://www.evergladesfoundation.org/florida-bay-a-unique-everglades-estuary/

2) Pathogenic strains of *Labyrinthula* are thought to behave opportunistically. They co-exist with their host in the aquatic community, and there is evidence to suggest that they only become virulent (or capable of producing infection) when the host species' immunity becomes compromised or suppressed. In light of the modern hydrological changes occurring in the bay (reviewed herein), it is likely that *T. testudinum* populations will be experiencing chronic stress due to unfavorable fluctuations in water quality parameters.

Our field-based study addressed these predictions within the context of a larger effort to identify patterns existing between *Labyrinthula* prevalence/severity and immune status biomarkers as a function of the available historical morphometric and water quality monitoring data. In May 2015, we sampled 15 sites in Florida Bay that were associated with both FHAP (morphometric data) and SFWMD (water quality data) monitoring stations. These samples were analyzed using the qPCR-based pathogen quantification and immune biomarker assay methods established in Chapter 2. With this data, several questions were asked:

1) Are there pathogenic *Labyrinthula* isolates present in the samples collected from Florida Bay in 2015?
2) Is there a relationship between the prevalence/severity of seagrass wasting disease and selected immune biomarker activity levels in the field-collected samples?
3) Is there variation in the prevalence/severity of seagrass wasting disease as a function of location among the 15 different sites surveyed from Florida Bay in 2015?
    a) Can variation in morphology help explain any patterns observed in pathogen loading across sites?

b) Can variation among historical water quality parameters help explain any patterns observed in pathogen loading across sites?

4) Are there differences in immune status as a function of enzyme biomarkers among the 15 different sites surveyed from Florida Bay in 2015?
    a) Can variation in morphology help explain any patterns observed in immune status at the site-level?
    b) Can variation among historical water quality parameters help explain any patterns observed in immune status at the site-level?

This study used a variety of graphical and statistical methods to generate answers to these questions. Our findings validate the practicality of long-term management initiatives such as FHAP, and the efforts presented here contribute to our understanding of the local biotic and abiotic factors which dictate the abundance and distribution of an important foundation species over time.

3.3 Methods

Study System

Florida Bay (ca. 25˚05′ N, 81˚45′ W) is a shallow estuarine system located on the inner-continental shelf, bordering the southern tip of the south Florida watershed and adjacent to Biscayne Bay, which lies northeast, and the Gulf of Mexico, which lies to the west. Shoals, vegetated embankments, and submerged soft-sediment banks restrict the hydrology of the system, creating approximately 50 interior basins with unique water quality characteristics. For the scope of this study, 15 sites within representative basins dispersed throughout the bay were

considered (figure 3-3). Table 3-1 details information on the basin/site name, site abbreviation/code, and coordinate location for each of the 15 sites surveyed.

Turtlegrass Sampling Methodology

A survey of 15 *Thalassia testudinum* beds was conducted across Florida Bay between May 25th and May 31st of 2015 (table 3-1) in tandem with the spring 2015 Florida Fisheries Habitat Assessment Program (FHAP) survey of the region (see long-term seagrass survey section, below, for more details). At each permanent FHAP transect site, 10 turtlegrass individuals were obtained haphazardly by sampling first at the stern, then traveling clockwise around the research vessel. Plants were collected within an approximately 30-meter radius area around the vessel, and no two individuals were chosen within ~10 meters of one another to reduce the likelihood that samples were ramets, or physically connected by rhizomes. Individuals were bagged, placed in an ice cooler, and processed on land no more than four hours after collection. Tissues were processed by isolation of the first and third rank blades from each individual, with the first "rank" allocated to the youngest blade present within the shoot (figure 3-4 A). The first rank blade was preserved in Drierite® (Sigma Aldrich, Darmstadt, Germany) for genotyping analysis (not included within the scope of this study), while the third rank blade was split longitudinally using a scalpel; one part was immediately placed in a conicle tube and stored at -80°C for use in biomarker assays and the other was preserved in Drierite® for qPCR procedures (figure 3-4 B).

Long-Term Turtlegrass Morphometric Surveys

Seagrass abundance surveys were conducted every spring (May) and fall (September and/or October), in coordination with the end of the dry and wet seasons, respectively, in the bay

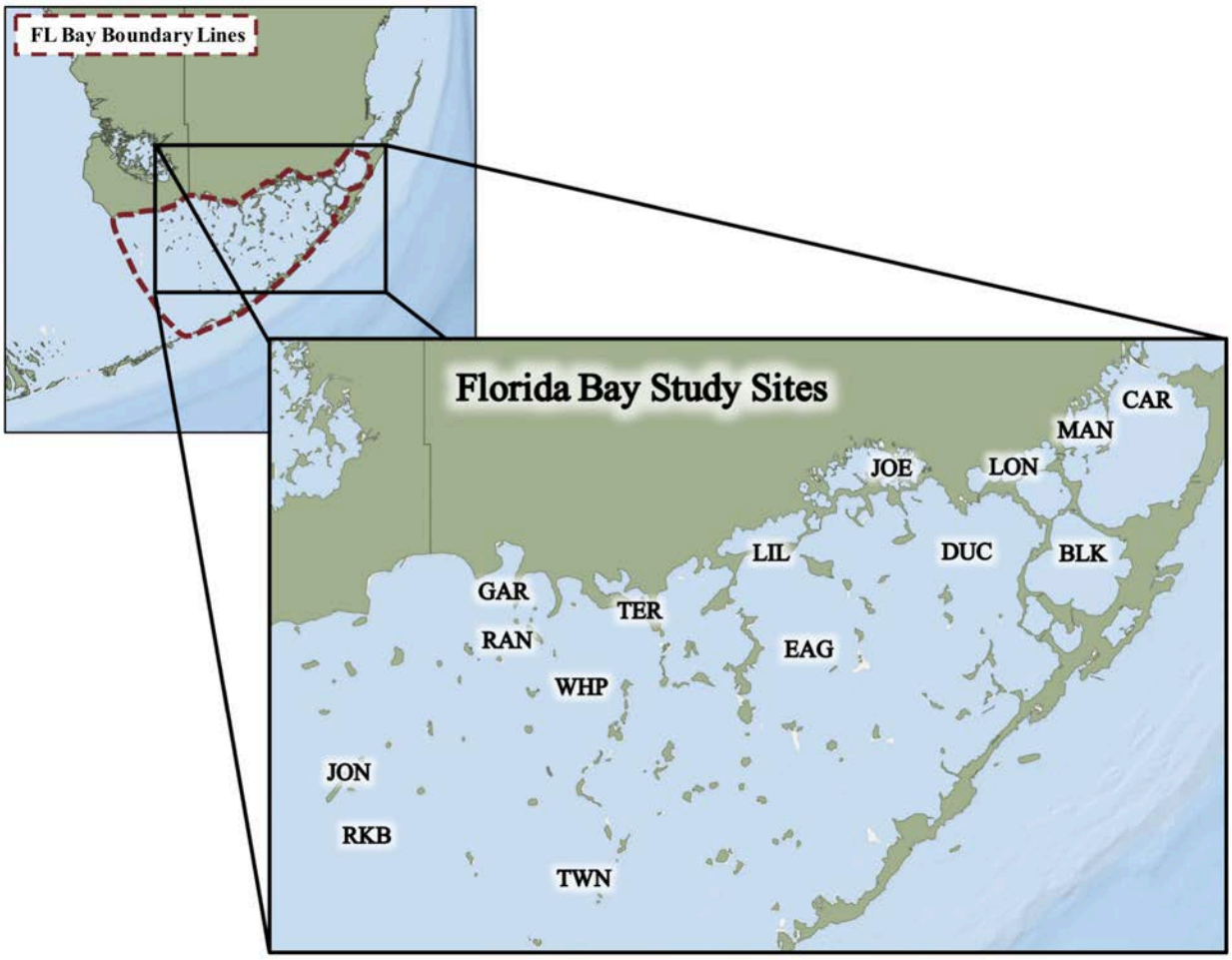

Figure 3-3. Map detailing the 15 locations surveyed within Florida Bay during May of 2015. Base map obtained using ArcGIS software (ESRI, Version 10.5.1.).

Table 3-1. Site information (full site name, abbreviation, collection date, and decimal coordinates) for the 15 locations surveyed in Florida Bay during May of 2015.

Site/Basin Name	Site Code	Collection Date	Location	
			Latitude	Longitude
Johnson Key Basin	JON	5/26/15	25.04247	-80.91482
Rabbit Key Basin	RKB	5/30/15	25.00242	-80.9001
Garfield Bight	GAR	5/25/15	25.15048	-80.80922
Rankin Lake	RAN	5/25/15	25.12138	-80.80288
Whipray Basin	WHP	5/26/15	25.09142	-80.75478
Twin Key Basin	TWN	5/30/15	24.97767	-80.75352
Terrapin Bay	TER	5/26/15	25.14037	-80.71612
Little Madeira Bay	LIL	5/27/15	25.17517	-80.62692
Eagle Key Basin	EAG	5/27/15	25.11797	-80.59972
Joe Bay	JOE	5/31/15	25.22447	-80.53658
Duck Key	DUC	5/29/15	25.17707	-80.49157
Long Sound	LON	5/28/15	25.22737	-80.46167
Blackwater Sound	BLK	5/28/15	25.17405	-80.42308
Manatee Bay	MAN	5/29/15	25.25103	-80.41517
Card Sound Bridge	CAR	5/29/15	25.27355	-80.37458

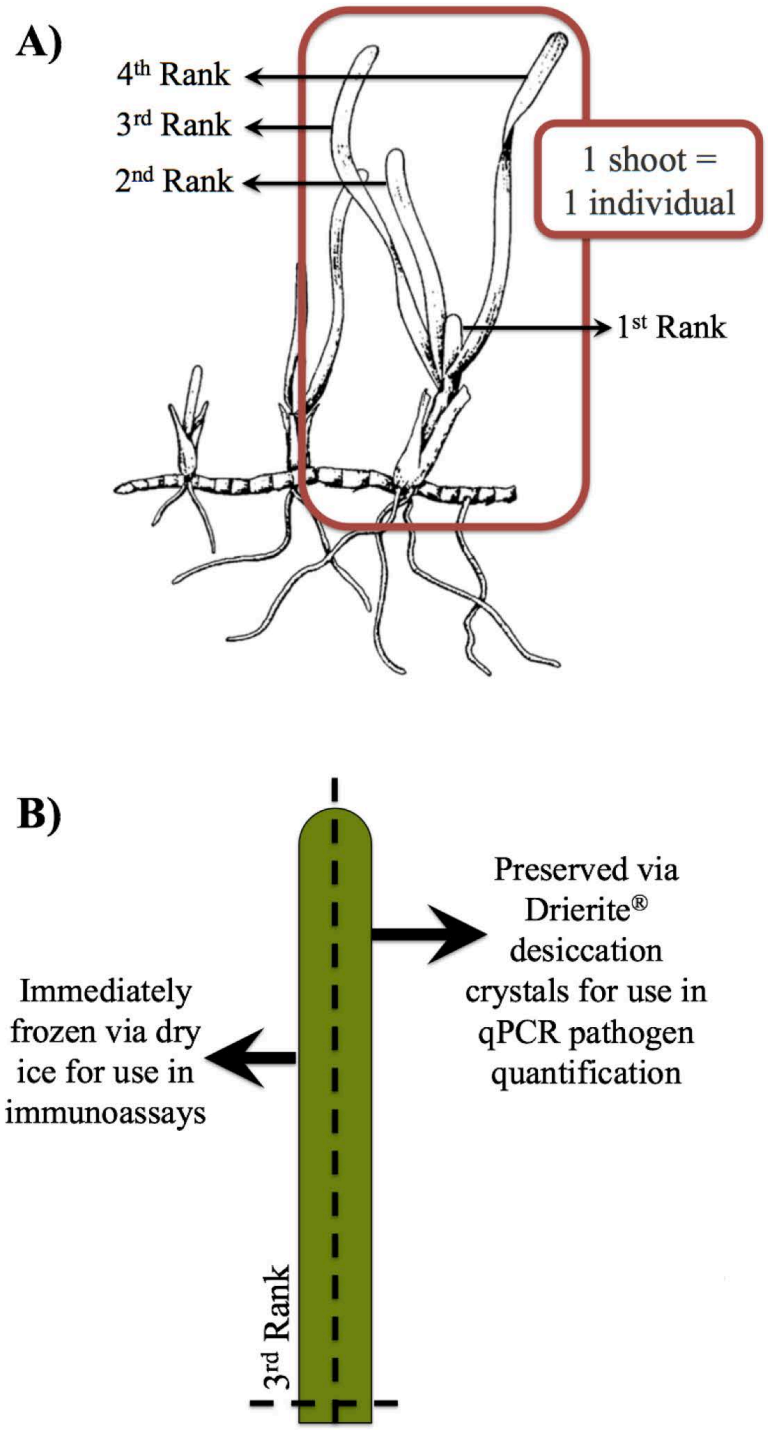

Figure 3-4. Supplementary diagrams detailing [A)] the method of ranking blades within a seagrass individual, or shoot, and [B)] the methods by which tissue from third rank blades of experimental *T. testudinum* individuals were collected for use in immunoassay and qPCR procedures.

through the FHAP program. Starting at the exact coordinate location of the site (table 3-1) a 50-meter transect line was haphazardly subsampled 10 times within a 0.25 m^2 quadrat. A number of variables were subsampled along the transect in this manner, including macrophyte cover-abundance data (using a modified Braun-Blanquet technique, as detailed in Fourqurean et al. 2003), shoot density, standing crop, epiphyte biomass, and leaf morphometrics for 10 *T. testudinum* individuals (sampled haphazardly). For the scope of this investigation, leaf morphometric and canopy data was of particular interest as this is considered an important aspect of disease ecology (see Burdon & Chilvers 1982). Important characters included the mean number of leaves per shoot, the mean height (cm) of the longest leaves from the 10 shoots, and the mean total area (cm^2) per shoot. Although these surveys have been conducted biannually since 2006, only the data collected between spring 2010 and spring 2015 were considered, as this time frame most directly reflects the conditions of the current standing crop of *T. testudinum*.

Long-Term Water Quality Monitoring Database

A long-term water quality monitoring program, funded and conducted by the South Florida Water Management District (SFWMD), was utilized to obtain information about historical water quality patterns at each site included in the turtlegrass survey (table 3-1) through the SFWMD website using the public DBHYDRO tool (https://www.sfwmd.gov/science-data/dbhydro). Although the original database included 36 water quality variables, the subset utilized in this study were first reduced by removing 22 parameters, based on the variable inclusion criteria described in Cole et al. (2018). The 14 remaining variables were further reduced based on large gaps and/or inconsistencies within the time frame chosen for this study

(2010-2015). Thus, six final parameters were considered in our analyses: dissolved oxygen, nitrate levels, phosphate levels, pH, salinity, conductivity, temperature and turbidity. Dissolved oxygen was measured in milligrams per liter (mg/L) using an oxygen electrode *in situ*. Salinity and temperature were also measured *in situ*, in parts per thousand (ppt) and degrees Celsius (°C), respectively, 10 cm beneath the surface using a combination salinity-conductivity-temperature probe. Water samples were collected at a depth of 10 cm and analyzed later in a laboratory setting for nitrate (in milligrams per liter, mg/L), total phosphorous (in mg/L), pH, and turbidity (in nephlometric turbidity units, NTUs) levels. Water sample transport techniques and specific methodologies used to measure each parameter are available in Cole et al. (2018). Although this monitoring system has been in place since 1989, only the data collected between January 2010 and May 2015 were considered relevant to the scope of this study. Unfortunately, only 13 of the 15 sites had sufficient data to perform the analyses of this study; consequently, CAR and MAN were not included in any water quality parameter investigations.

Pathogen Loading and Immune Status Profiling in Field-Collected Turtlegrass Tissue

Pathogen loading and immune status profiles were measured in 150 *T. testudinum* individuals collected in 2015 from Florida Bay (15 sites, 10 samples per site) following the methods detailed in Chapter 2. Briefly, the pathogen load in seagrass tissue was determined through DNA extraction from preserved tissue followed by a qPCR-assay (all samples run in triplicate) which quantified the number of *Labyrinthula* cells present in the sample (cell count per µL template; template concentration set at 10 ng/µL DNA). Immune status profiles were generated through biomarker assays, which measured peroxidase (POX, in Δ Abs_{470} µg $protein^{-1}$), exochitinase

(EXOC, in nmol MU µg protein^{-1}), polyphenol oxidase (PPO, in Δ Abs_{490} µg protein^{-1}) and lysozyme (LYS, in % inhibition µg protein^{-1}) activity in the protein extract derived from preserved sample tissue.

Statistical, Graphing and Mapping Techniques

All statistical tests were performed with 95% confidence intervals ($\alpha = 0.05$) on data that were normally distributed according to Kolmogorov-Smirnov and Sharpiro-Wilk normality tests, unless otherwise stated. All statistical tests were computed using IBM SPSS® Statistics 25 software (International Business Machines Corp., Armonk, NY, USA) unless otherwise stated. Box plots were utilized on a number of occasions in this analysis in an effort to create visual distributions for trend identification and group comparison, and were generally created by first taking a numerical data set and calculating the minimum, third (lower) quartile, median, first (upper) quartile, and maximum quantities within it. The main box in the plot represents the interquartile range (IRQ) of the data, with a median line intersecting the box at the second quartile. The lower and upper lines (whiskers) extending from the box in either direction signify the minimum and maximum (respectively) spread of the data outside of the IRQ.

Pathogen Loading and Immune Biomarker Correlations

When comparing biomarker activity with pathogen loading using the pooled values across all sites in Florida Bay, all data sets violated and could not be transformed to meet the assumptions of normality. Thus, variables were ranked and the Spearman's rho nonparametric equivalent was utilized to assess the strength of the linear relationship between pathogen loading and each biomarker (POX, EXOC, PPO, and LYS).

Patterns Associated with Pathogen Loading

> *Pathogen Prevalence by Site*

In order to calculate pathogen prevalence, or the percent of individuals infected at each site (presence/absence), raw pathogen loading values (cell count per μL) were manipulated to remove background levels of *Labyrinthula*; in other words, only ecologically relevant quantities of pathogen loading were considered in the calculation. In order to determine what range of values should be considered ecologically irrelevant (as no reference exists in the literature), we utilized the pathogen loading quantities present in lab samples of *T. testudinum* that were not inoculated with *Labyrinthula* (these four individuals were labeled as "Ambient (-) *Labyrinthula*" in the second lab experiment; see Chapter 2). The average cell count ($\bar{x}$) of the individuals not deliberately infected with the pathogen was $4.61 \times 10^{-3} \pm 3.72 \times 10^{-3}$ cells μL^{-1}. Interestingly, the same field-collected individuals fell beneath the upper-limit "background level" threshold whether it was set at $\bar{x} \pm 1\sigma$ or $\bar{x} \pm 3\sigma$. This helps to validate the notion that the criteria we established truly captured the disparity between insignificant background levels of the pathogen and ecologically relevant quantities. Of the 150 Florida Bay-collected samples, the pathogen loading values of 28 samples fell between zero and 1.66×10^{-2} cells μL^{-1} ($\bar{x} \pm 3\sigma$) and were converted to zero prior to binomial (presence/absence) pathogen loading analyses by site.

> *Pathogen Severity by Site*

Pathogen severity is defined here as the number of pathogen (*Labyrinthula*) cells present in a sample (arithmetic mean across three qPCR assay replicates) or group of samples

(arithmetic mean across samples). Summary statistics (mean, standard error, median, minimum, maximum, 1st quartile, and 3rd quartile) were calculated for each site from the raw pathogen loading values (cell count per μL) among individuals at that site (n = 10). Box plots were utilized to visually summarize this information. Lines denoting the mean and median pathogen loading values of individuals across all sites were manually added to the graph. If there were large differences among sites that prevented adequate resolution of those in the lower range of values, scale breaks were used. A one-way ANOVA (two-tailed, $\alpha<0.05$) was performed to determine overall significance of the differences between sites as a function of pathogen severity. Finally, bubble plots were generated to visualize the relative magnitude of pathogen loading as a function of site; these relative magnitudes (denoting pathogen severity) were utilized to generate pie charts (displaying pathogen prevalence) of proportionate size. These were superimposed over a base map of the region (ArcGIS, ESRI, Version 10.5.1.) to examine spatial patterns with respect to the geography of the bay.

> *Grouping Sites into Categorical Pathogen Severity Classes*

The mean number of *Labyrinthula* cells (per μL) present among individuals at a given site were used to categorize sites into pathogen severity classes. Because no ecological definitions of *Labyrinthula* loading severity yet exist, we based our classes on the order of magnitude of cell concentration, extrapolated to cells per mL (0 = 'NONE', 1-9 = 'LOW,' 10-99 = 'MODERATE,' 100-999 = 'HIGH,' 1000-10000 = 'VERY HIGH'). Sites grouped using this logarithmic scale were assigned colors and superimposed over a base map of the region to visually assess the geographic coherence of the classifications. Box

plots were generated (with horizontal lines denoting mean and median pathogen loading values across all sites) in order to visualize the magnitude of the differences in pathogen loading among pathogen severity classes ("Very High," "High," "Moderate," "Low," and "None"), and a one-way ANOVA (two-tailed, $\alpha<0.05$) was performed to determine overall significance of the differences between these categorical groupings as a function of pathogen severity.

> *Morphological Characteristics by Pathogen Severity Class*

Summary statistics (mean, median, minimum, maximum, 1st quartile, and 3rd quartile) were calculated for each pathogen severity class ("Very High," "High," "Moderate," "Low," and "None") using seasonal (spring and fall) morphology data averaged across the time series, which extended backward five years from the collection date (spring 2010 – spring 2015). The *T. testudinum* morphometrics included in this analysis were the mean number of leaves per shoot, mean canopy height (cm), and mean leaf area per shoot (cm^2). Mean leaf length and width were excluded from this analysis as mean leaf area encompassed both these parameters (length x width = area). Box plots were generated to visually display this data in the same manner as previously described and one-way ANOVAs (two-tailed, $\alpha<0.05$) were performed to determine overall significance of the differences between groups at each parameter.

> *Water Quality Parameters by Pathogen Severity Class*

Summary statistics (mean, median, minimum, maximum, 1st quartile, and 3rd quartile) were calculated for each pathogen severity class ("Very High," "High," "Moderate," "Low," and "None") using monthly water quality parameter values averaged across the

time series; in this case, we focused on more recent water quality history, extending back ~2.5 years from the collection date (January 2013 – May 2015). The water quality parameters included in this analysis were dissolved oxygen (mg/L), nitrate (mg/L), total phosphate (mg/L), pH (field units), conductivity (field μS/cm), temperature (°C) and turbidity (NTU). Once again, box plots were generated to highlight visual differences among the data in the same manner as previously described and one-way ANOVAs (two-tailed, $\alpha<0.05$) were performed to determine overall significance of the differences between groups at each parameter.

Patterns Associated with Immune Status

> *Immune Biomarker Levels by Site*

Activity levels at each of the four biomarkers (POX, EXOC, PPO, and LYS) were compared among the 15 Florida Bay sites with the same procedures used to characterize each site by pathogen loading.

> *Grouping Sites into Categorical Immune Status Classes*

Multivariate analyses performed in PRIMER (v6) were utilized to group sites according to their overall immune status (simultaneously incorporating POX, EXOC, PPO, and LYS activity levels). First, the CLUSTER routine was used to perform a hierarchical cluster analysis, producing a dendrogram of similarity among sites based on immune status. This was followed by a similarity profile routine (SIMPROF), which is a permutation procedure intended to prevent over-dissection of subgroups (Clarke et al. 2008). The clustered divisions were supported by SIMPROF at $\alpha = 0.05$. The relative dissimilarity of

these immune groups (and the sites between and among groups) was mapped two-dimensionally in an ordination plot using non-metric multi-dimensional scaling (MDS). The three distinct groups generated through these analyses were assigned names ("Immune Class A" through "Immune Class C") and superimposed over a base map of the region to visually assess the geographic coherence of the classifications.

> *Morphological Characteristics by Immune Class*

Potential patterns in morphological characteristics as a function of immune class ("Immune Class A" through "Immune Class C") were explored in the same manner as previously described with reference to pathogen severity classes. However, due to the compelling nature of the data output, bar graphs were also generated (in addition to box plots) and the global test of significance via ANOVA was followed by LSD posthoc tests to elucidate pairwise differences groups (two-tailed, $\alpha<0.05$).

> *Water Quality Parameters by Immune Class*

Potential trends in water quality parameters among the three immune classes ("Immune Class A" through "Immune Class C") were investigated with the same procedures used to characterize water quality metrics among pathogen severity classes.

Patterns Associated with Salinity Metrics

In order to further investigate whether trends in salinity explained variation among pathogen severity and/or immune status, data corresponding to the two most extreme pathogen severity classes ("Very High" and "None") from Immune Class C were analyzed against various interpretations of monthly salinity values. More specifically, both a box plot and bar graph

were generated in an effort to compare summary statistics (mean, standard error, median, minimum, maximum, 1st quartile, and 3rd quartile) based on the sites with very high pathogen loading ("Very High") and those based on the sites with no pathogen loading ("None") within Immune Class C. Lines were manually added to the graphs to denote the mean and median pathogen loading values for both 1) individuals across both groups under comparison and 2) individuals across all sites in the bay, to provide additional context to the figures. As with the other water quality parameter analyses, only salinity measurements collected between January 2013 and May 2015 were considered. A one-way ANOVA was conducted to test for differences between the two groups under consideration (two-tailed, $\alpha<0.05$). Additionally, seasonal values of salinity were plotted individually by site in the five sites grouped together in Immune Class C in order to visualize fine-tuned temporal trends in this variable.

Finally, a broad sweep to identify potential water quality predictor variables of *Labyrinthula* loading was conducted using multivariate techniques in PRIMER (v6). First, site averages of pathogen loading were extrapolated from cells μL^{-1} to cells mL^{-1} and rounded to the nearest whole number. Next, a set of summary statistics (minimum, maximum, mean, and maximum change) were calculated among seasonal means (spring and fall) across all water quality parameters [dissolved oxygen (mg/L), nitrate (mg/L), total phosphate (mg/L), pH (field units), conductivity (field μS/cm), temperature (°C) and turbidity (NTU)] using the full 5-year data set (2010-2015). These data sets were each correlated against pathogen loading values using a Spearman rank correlation test, and those with a correlation coefficient less than the absolute value of 0.4 were discarded from subsequent analyses. Next, a CLUSTER dendrogram (autocorrelation) of correlated predictors was generated using a Spearman rank

correlation matrix, and one dendrogram with a self-similarity value of >0.90 was chosen. The 10 predictor variables selected through this process were each plotted against pathogen loading as an x-y scatterplot (figure 3-5). Only one predictor variable, maximum seasonal change in salinity, reflected a trend that could be fit to a mathematical model that was biologically justifiable (logistic regression).

3.4 Results

Correlations between Pathogen Loading and Immune Biomarkers

This study surveyed 15 sites across Florida Bay that were representative of the inherent spatial heterogeneity of the system, both in terms of seagrass communities themselves and the environmental conditions which surround them. The Spearman's rho nonparametric correlation analyses between ranked pathogen loading values and ranked activity levels at each of the four biomarkers (peroxidase, POX; exochitinase, EXOC; polyphenol oxidase, PPO; lysozyme, LYS) across all 150 individuals sampled in the survey revealed no significant linear relationships between any of the data pairs (figure 3-6).

Exploring Patterns Associated with Pathogen Loading in the Florida Bay

Labyrinthula Prevalence and Severity in Florida Bay

Table 3-2 summarizes the *Labyrinthula* prevalence and severity values quantified in *Thalassia testudinum* samples collected from each site; the relative magnitude of each value in relation to the data set (in columns) is visually demonstrated with proportionately pigmented coloration of the cells associated with each value. Prevalence and severity vary along a

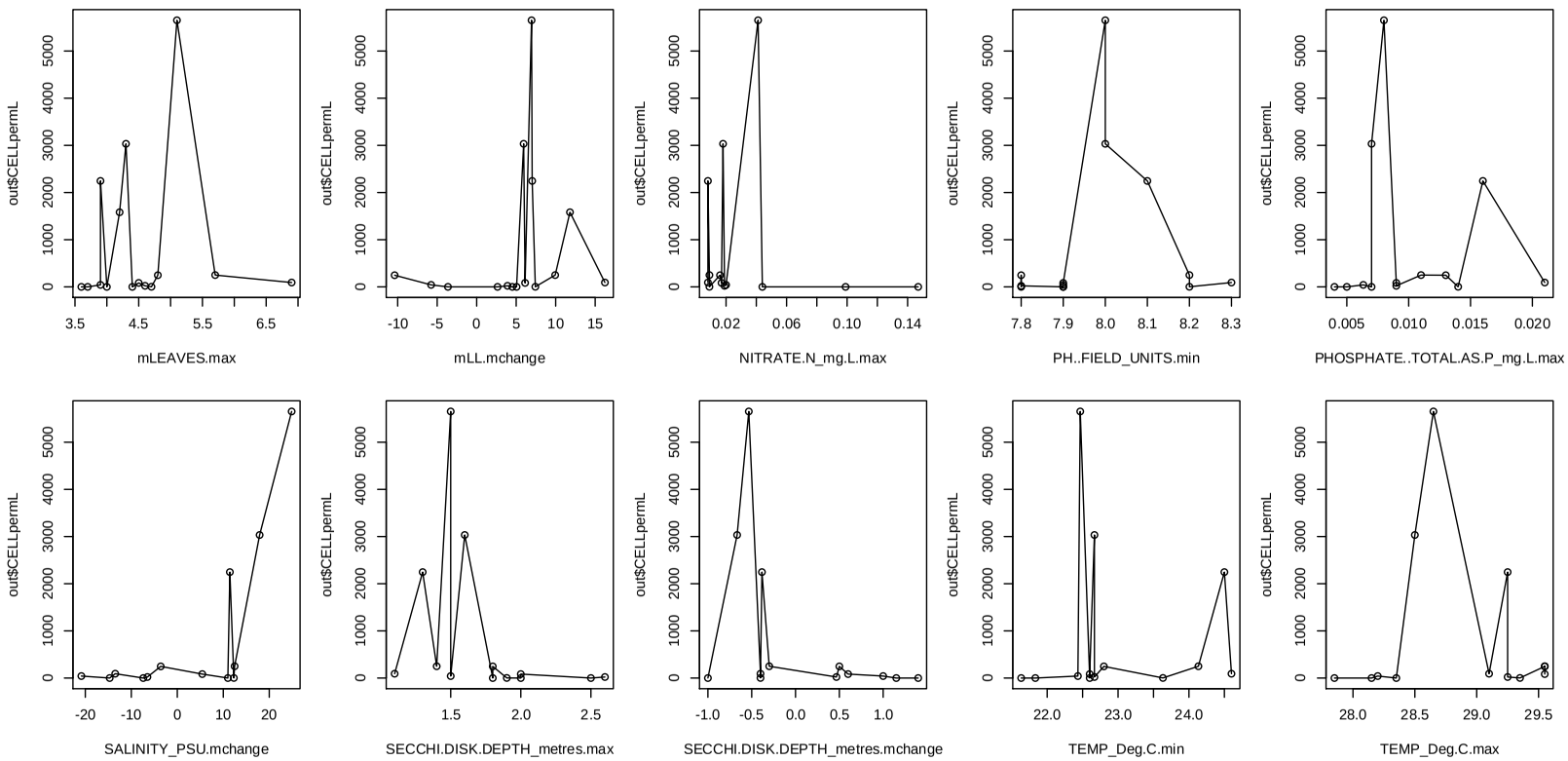

Figure 3-5. Predictor variables selected through multivariate analyses (Spearman rank correlation test, CLUSTER dendrogram) plotted against pathogen loading (cells mL^{-1}, rounded to the nearest whole number). Only one predictor variable, maximum seasonal change in salinity (bottom row, far left) was of interest, as all other trends could not be fit to a mathematical model that was biologically justifiable.

gradient of red shades (with the darkest shade denoting the highest value of the set) and standard error magnitude is represented by shades of gray (table 3-2).

The qPCR-based assay revealed that 26.67% of individuals had ecologically relevant quantities of the pathogen in their tissue. This mean value of pathogen prevalence (% infected per site) across all sites exceeded the median value (20%; finely dotted horizontal line, figure 3-7) of the same data and only four sites (JON, TER, JOE, and MAN) had pathogen prevalence greater than the mean across all sites (table 3-2, mean represented as the dashed horizontal line in figure 3-7). One site, JOE, featured a pathogen prevalence value of 100%; in other words, all individuals collected from JOE contained ecologically significant quantities of *Labyrinthula* (figure 3-7, table 3-2). Conversely, the pathogen was not detected in any samples collected (0% prevalence) at five sites (WHP, EAG, DUC, BLK and CAR) (figure 3-7, table 3-2).

In terms of pathogen severity (actual cell count per μL), the average across all 150 *T. testudinum* samples collected (10 samples each of 15 sites) was 0.882 +/- 2.920 cells μL^{-1}. Excluding the 110 individuals where no cells were detected (or cell counts within the range of background levels, and thereby considered negligible), the average severity of those infected with ecologically relevant quantities was 3.233 +/- 4.895 cells μL^{-1}. At JOE, the pathogen severity value of each individual exceeded that of the median across all individuals at all sites (0.0814 cells per μL^{-1}; fine dotted line, figure 3-8), and almost all JOE samples exceeded the mean value across all individuals at all sites (0.8818 cells μL^{-1}; dashed line, figure 3-8). TER, JOE and LON had the most variation in the severity of the pathogen among samples (table 3-

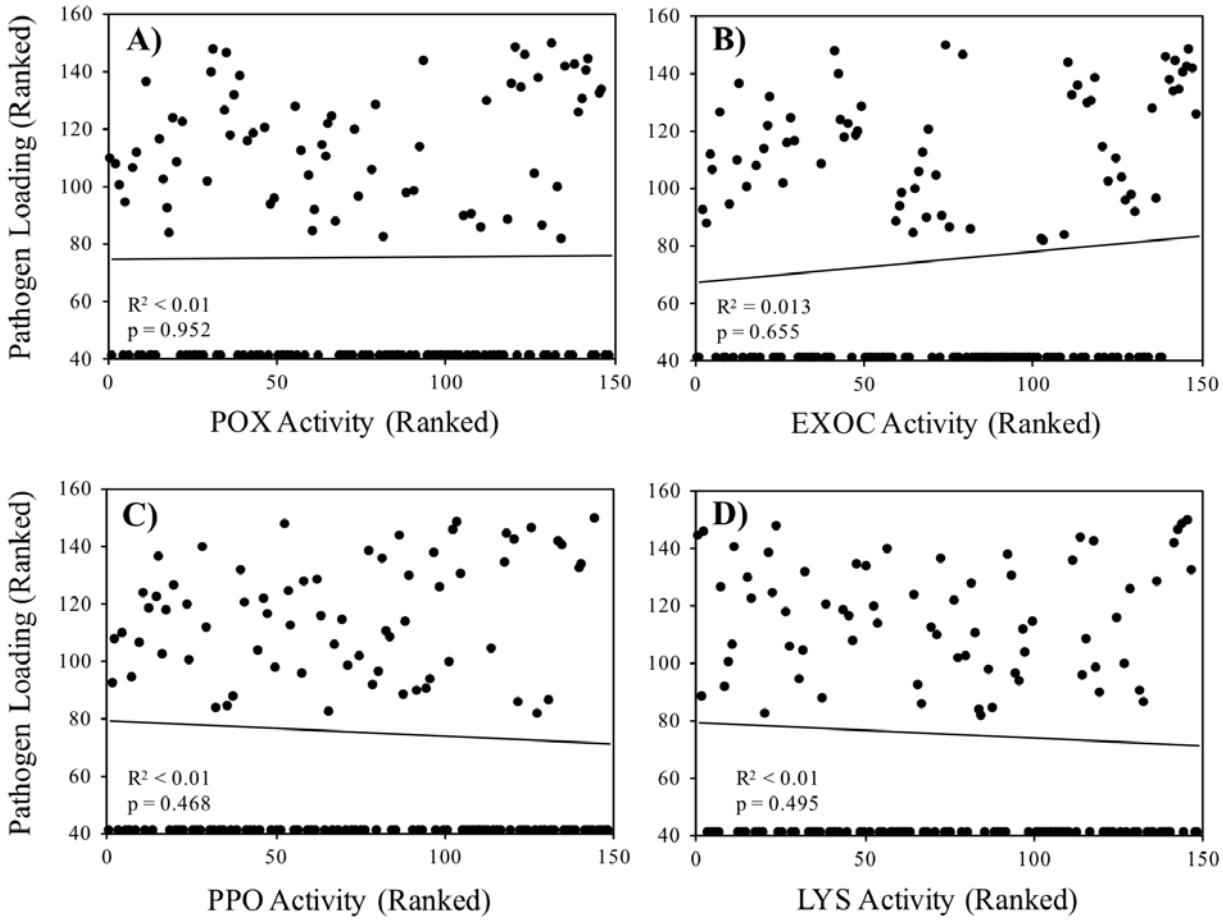

Figure 3-6. Results of correlation analyses between quantified pathogen load (*Labyrinthula* cells μL^{-1}; ranked across all individuals at all sites) and stress biomarker activity levels (parts A-D: peroxidase, exochitinase, polyphenol oxidase, and lysozyme, respectfully; ranked across all individuals at all sites) of *T. testudinum* individuals collected from Florida Bay in May 2015. Significance (p-values) are based on Spearman's rho correlation coefficients (A-D) with 95% confidence ($\alpha = 0.05$). Sample size n = 150 (A-D).

Table 3-2. Pathogen prevalence (percent of samples out of 10 infected with ecologically significant quantities of *Labyrinthula*) and severity (average and standard error of cell count μL^{-1} across 10 individuals collected at a given site) as a function of collection site within Florida Bay. The shade assigned to each site at a given parameter reflects the proportional value at that parameter, as compared to the entire data set, with white representing the lowest value of the set and dark red (or gray, in the case of SE values) representing the highest value of the set. Sample size n = 10 individuals per bay site. Samples collected in May 2015.

Bay Site	*Laby.* Prevalence (% infected)	*Laby.* Severity (cell count μL^{-1})	
		Mean	SE
JON	60	0.247	0.129
RKB	10	0.083	0.083
GAR	10	0.081	0.081
RAN	20	0.247	0.241
WHP	0	0.000	0.000
TWN	20	0.020	0.014
TER	80	2.246	1.604
LIL	20	0.039	0.029
EAG	0	0.000	0.000
JOE	100	5.652	1.601
DUC	0	0.000	0.000
LON	20	3.031	2.072
BLK	0	0.000	0.000
MAN	60	1.582	0.685
CAR	0	0.000	0.000

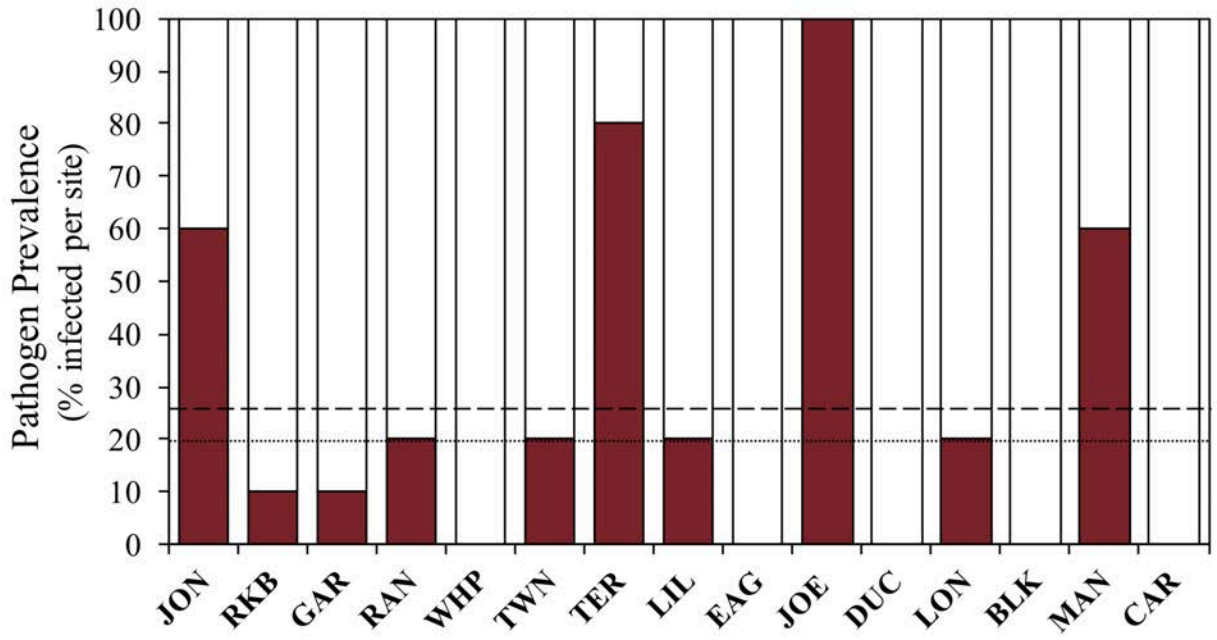

Figure 3-7. Pathogen prevalence (percent of samples out of 10 infected with ecologically significant quantities of *Labyrinthula*) as a function of collection site within Florida Bay. The coarse dashed line represents the mean pathogen prevalence across all sites and the fine dotted line represents the median pathogen prevalence across all sites (mean = 26.667; median = 20.000). Sample size n = 10 individuals per bay site. Samples collected in May 2015.

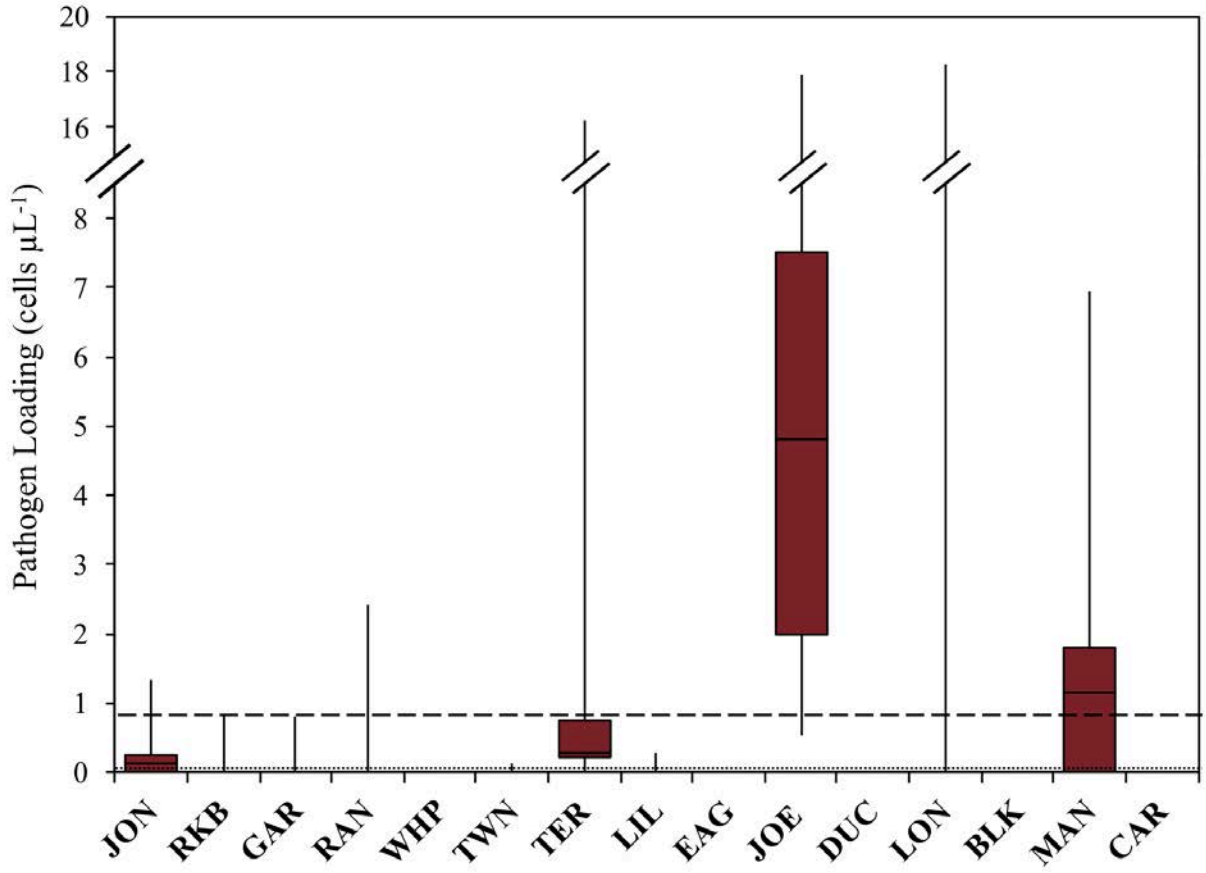

Figure 3-8. Box plots displaying pathogen loading, or severity (*Labyrinthula* cell count μL^{-1} across 10 individuals collected at a given site) as a function of collection site within Florida Bay. The main box in each plot represents the interquartile range (IRQ) of the data, with a median line intersecting the box at the second quartile. The lower and upper lines (whiskers) extending from each box in either direction signify the minimum and maximum (respectively) spread of the data outside of the IRQ. The coarse dashed line represents the mean pathogen prevalence across all sites and the fine dotted line represents the median pathogen prevalence across all sites (mean = 0.882; median = 0.082). Sample size n = 10 individuals per bay site. Samples collected in May 2015.

2). The overall differences between pathogen loading values across sites was significant at a 99% confidence interval ($\alpha = 0.01$; $p = 0.00001$).

Figure 3-9 displays the geographic distribution of *Labyrinthula* across the region in terms of both prevalence (pie chart) and severity (relative magnitude of the pie chart). The pathogen is present across all main geographic regions of the bay (western, central, and north-eastern).

Another map (figure 3-10) introduces the five pathogen severity classes: EAG, DUC, BLK, and CAR are shaded in dark blue to denote the class where no pathogen was detected ("None"); WHP represents the "Low" pathogen loading class (light blue shading); RKB, TWN, and LIL were grouped together, in yellow, based on their "Moderate" pathogen loading values; JON, GAR, and RAN belong to the "High" pathogen severity class (shaded in orange); finally, coastal basins TER, JOE, LON, and MAN are shaded in red and are classified as having "Very High" pathogen loading values. Box plots displaying summary statistics of pathogen loading for each severity class illustrate the order of magnitude which separates each group from one another (figure 3-11). The mean pathogen loading (0.884 cells μL^{-1}; dashed line, figure 3-11) is greater than the maximum value found in the three least severe classes ("Moderate," "Low," and "None," figure 3-11 A, B), but is almost equivalent to the median value of the "Very High" pathogen severity class (figure 3-11 A). The overall differences between pathogen loading values across pathogen severity classes was significant at a 99% confidence interval ($\alpha = 0.01$; $p < 0.00001$).

Morphological Characteristics across Pathogen Severity Classes

Box plots were generated to visually display the spread of data for *T. testudinum* morphological characteristics, grouped as a function of pathogen severity (figure 3-12). In

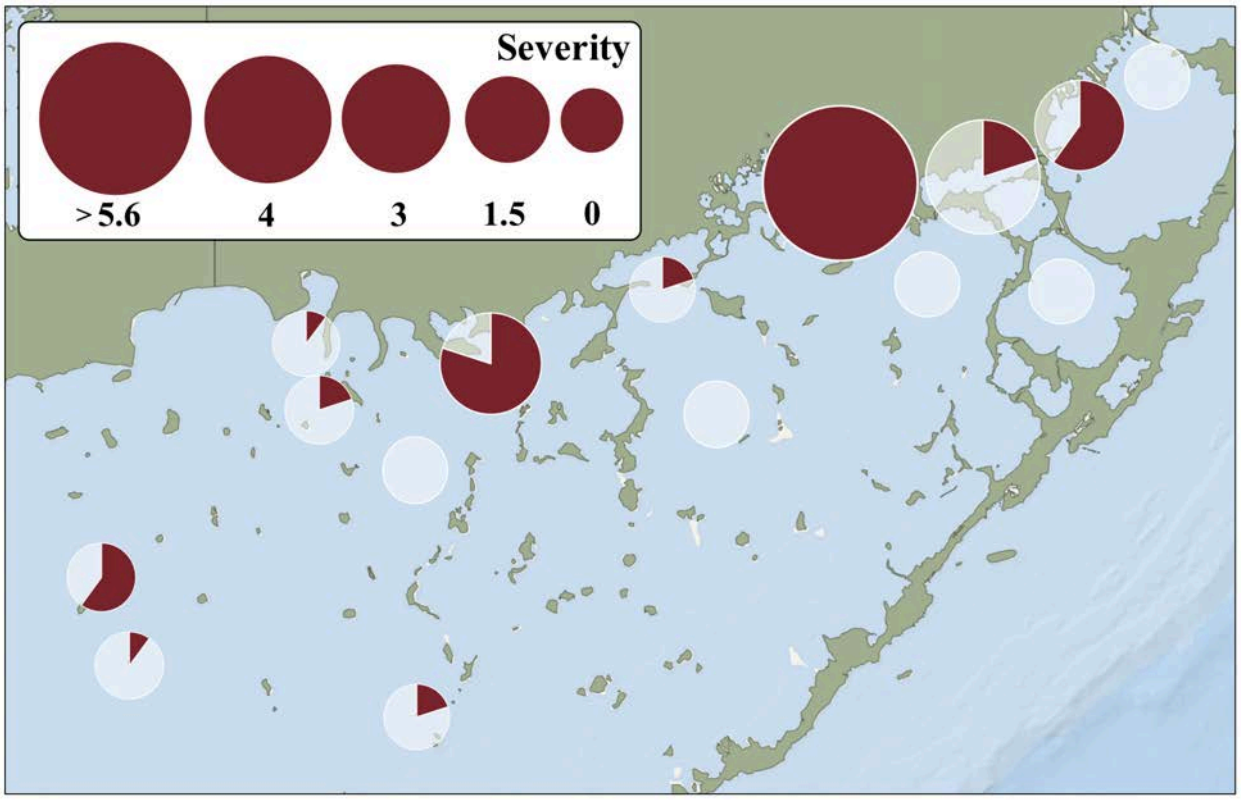

Figure 3-9. Map displaying the prevalence and severity of *Labyrinthula* as a function of the geographic distribution in Florida Bay. The pie chart layered over the location of a site represents disease prevalence (percent of samples out of 10 infected with ecologically significant quantities of *Labyrinthula*) at that site. The magnitude of the circle/pie chart represents the average severity (*Labyrinthula* cell count μL^{-1}) across 10 individuals collected at that site. Sites with no *Labyrinthula* cells detected (meaning prevalence and severity both equal zero) are represented as a small white circle. Sample size n = 10 individuals per bay site. Samples collected in May 2015. Base map obtained using ArcGIS software (ESRI, Version 10.5.1.).

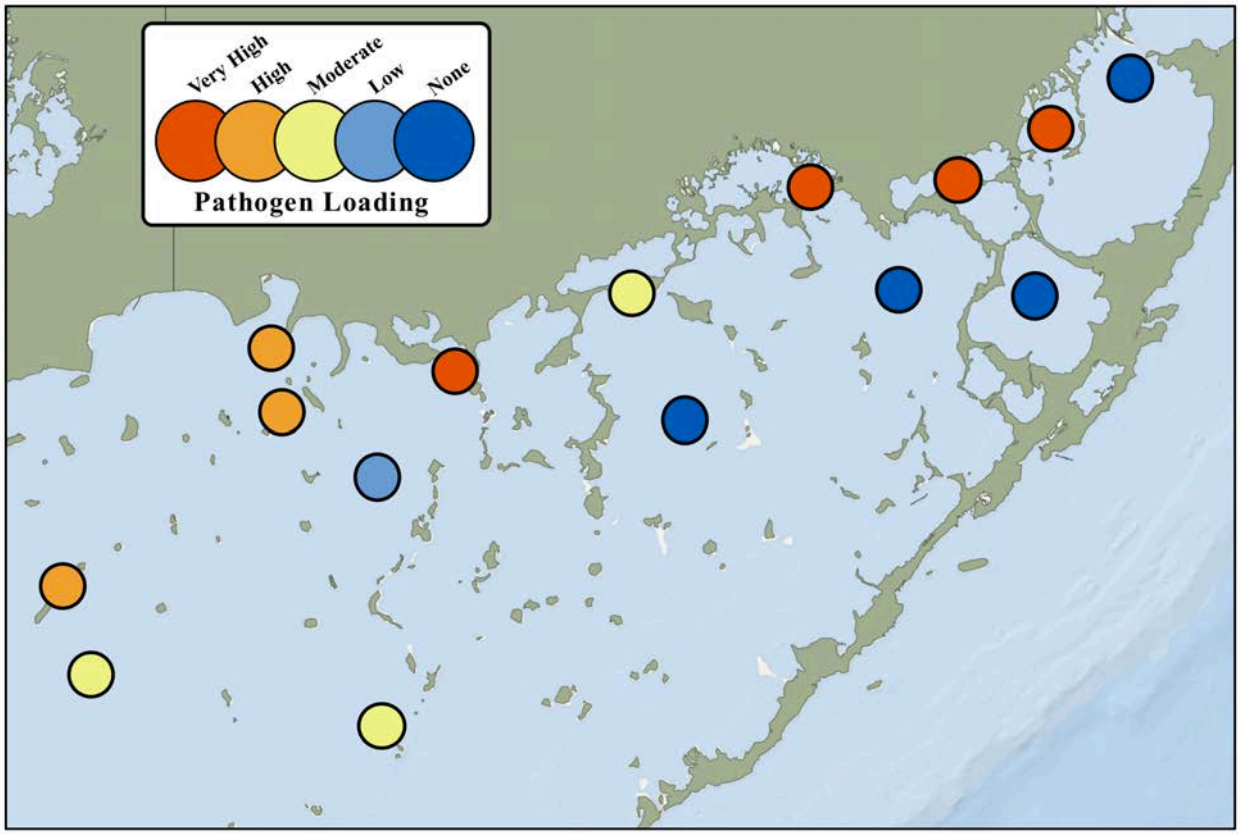

Figure 3-10. Map displaying the pathogen severity classes as a function of the geographic distribution in Florida Bay. Sites were grouped according to the order of magnitude of *Labyrinthula* cell concentrations averaged across individuals (n = 10) collected at a given site and extrapolated to cells per mL (0 = 'NONE', 1-9 = 'LOW,' 10-99 = 'MODERATE,' 100-999 = 'HIGH,' 1000-10000 = 'VERY HIGH'). Samples collected in May 2015. Base map obtained using ArcGIS software (ESRI, Version 10.5.1.).

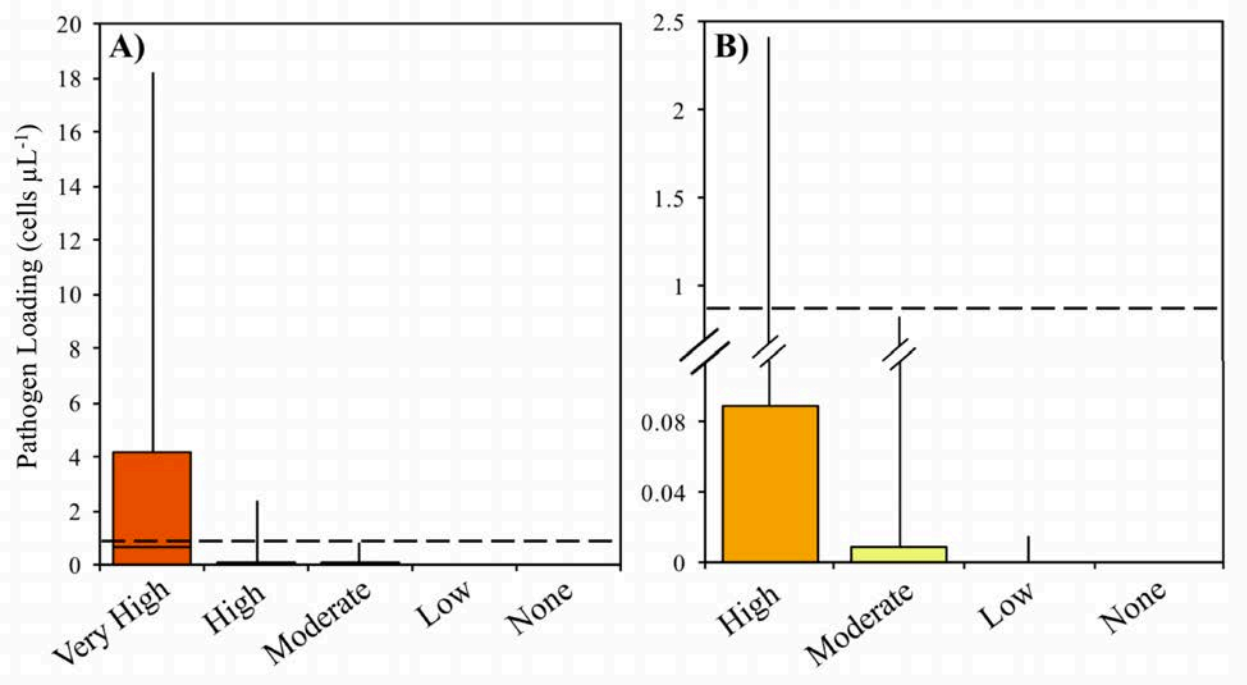

Figure 3-11. Box plots displaying pathogen loading, or severity (*Labyrinthula* cell count μL^{-1}, averaged across all individuals of the sites within a severity class) as a function of pathogen severity class. Part A displays all five severity classes, while the "Very High" severity class was removed in part B to increase the resolution of differences between the other four classes. Sample sizes as follows: "Very High," n = 40; "High," n = 30; "Moderate," n = 30; "Low," n = 10; "None," n = 40. The coarse dashed line represents the mean pathogen prevalence across all sites (mean = 0.882). Samples collected in May 2015 from Florida Bay.

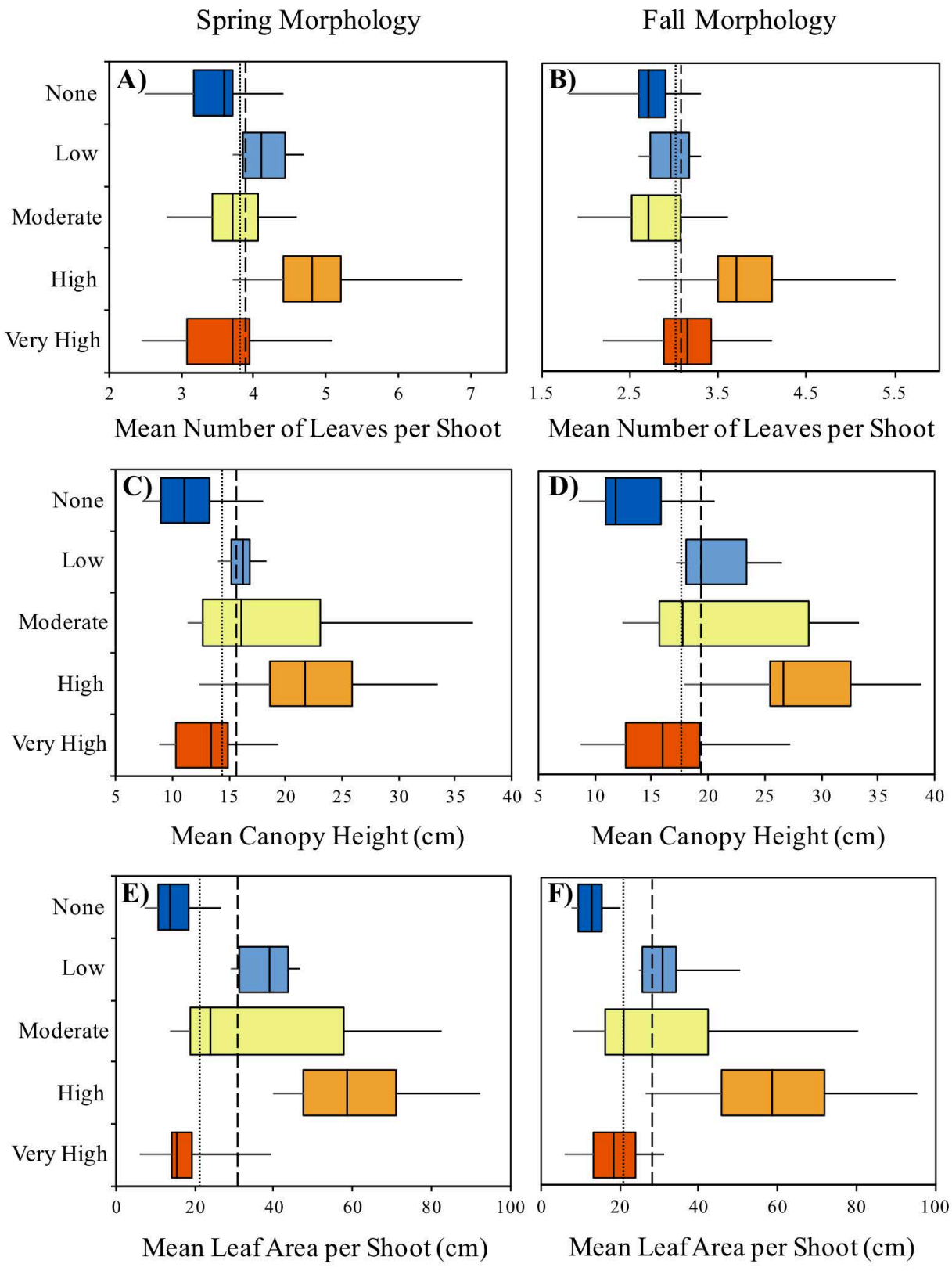
Spring Morphology
Fall Morphology
A)
B)
None
Low
Moderate
High
Very High
2
3
4
5
6
7
1.5
2.5
3.5
4.5
5.5
Mean Number of Leaves per Shoot
Mean Number of Leaves per Shoot
C)
D)
5
10
15
20
25
30
35
40
Mean Canopy Height (cm)
Mean Canopy Height (cm)
E)
F)
0
20
40
60
80
100
Mean Leaf Area per Shoot (cm)
Mean Leaf Area per Shoot (cm)

Figure 3-12 (*previous page*). Box plots displaying *T. testudinum* leaf morphometrics data [parts A & B: number of leaves per shoot; parts C & D: mean canopy height (cm); parts E & F: mean leaf area per shoot (cm^2)] collected biannually during the spring (A, C, E) and fall (B, D, F) from January 2010 to May 2015 as a function of pathogen severity class. Sample sizes as follows: "Very High," n = 24; "High," n = 18; "Moderate," n = 18; "Low," n = 6; "None," n = 24. The main box in each plot represents the interquartile range (IRQ) of the data, with a median line intersecting the box at the second quartile. The lower and upper lines (whiskers) extending from each box in either direction signify the minimum and maximum (respectively) spread of the data outside of the IRQ. The coarse dashed line represents the mean value at that parameter across all sites during that season and the fine dotted line represents the median value at that parameter across all sites during that season (part A: mean = 3.889, median = 3.800; part B: mean = 3.075, median = 3.000; part C: mean = 15.693 cm, median = 14.220 cm; part D: mean = 19.249 cm, median = 17.722 cm; part E: mean = 30.460 cm^2, median = 20.366 cm^2; part F: mean = 28.225 cm^2, median = 20.224 cm^2). Data obtained through FHAP survey database (M. Durako, pers. comm.).

general, and across all pathogen severity classes, turtlegrass individuals possessed more leaves and greater leaf area per shoot in the spring (mean leaf count = 3.889; mean leaf area = 30.460 cm^2) than in the fall (mean leaf count = 3. 075; mean leaf area = 28.225 cm^2) (figure 3-12 A, C), but mean canopy height and leaf area was greater among samples measured in the fall (spring/fall mean canopy height = 15.693/19.249 cm) (figure 3-12 B). Other noteworthy trends include the observation that the interquartile range (IQR) of individuals with no pathogen loading ("None", shaded dark blue) fell beneath the bay-wide mean and median at all six morphological characteristics (figure 3-12). Conversely, the interquartile range of individuals with high pathogen loading (shaded orange) exceeded the mean and median across all sites at all six parameters (figure 3-12). Additionally, morphometric variation appeared greatest among individuals with moderate and high pathogen loading (yellow and orange, respectively; figure 3-12). Interestingly, the two most extreme classes ("Very High" and "None"; red and dark blue, respectively) exhibit general trends more similar to one another than any other group (figure 3-12). The differences between values across pathogen severity classes were significant at every morphometric characteristic in both seasons, with a 99% confidence interval ($\alpha = 0.01$; $p < 0.00001$).

Water Quality Characteristics across Pathogen Severity Classes

Box plots were generated to visually display the spread of data at six water quality parameters [dissolved oxygen (mg/L), nitrate (mg/L), total phosphate (mg/L), pH (field units), conductivity (field μS/cm), temperature (°C) and turbidity (NTU)], grouped as a function of pathogen severity (figure 3-13). Of these characteristics, mean temperature was the most similar among pathogen severity classes (figure 3-13 G) and was the only water quality

parameter where the overall differences between groups was not significant ($\alpha = 0.05$; $p = 0.997$). Additionally, the IQR of all classes coincided with the mean and median lines measuring mean dissolved oxygen (figure 3-13 A), but differences among pathogen severity classes were significant, in this case, with a 95% confidence interval ($\alpha = 0.05$; $p = 0.022$), along with turbidity ($\alpha = 0.05$; $p = 0.043$). All other water quality parameters (nitrate, phosphate, pH, salinity and conductivity) exhibited highly significant differences as a function of pathogen severity group with a 99% confidence interval ($\alpha = 0.01$; $p < 0.00001$). IQR nitrate levels were highest in the sites categories with very high and no ("None") pathogen loading, although the "None" class displayed upper whisker (figure 3-13 B). The spread of site salinity measurements in the "Very High" severity class vastly exceeded that of any other group, and the median value of this group was less than the lower quartile of any other group (figure 3-13 E).

Exploring Patterns Associated with Immune Status in Florida Bay

Immune Biomarker Activity by Site in Florida Bay

The average immune and standard error of biomarker activity is tabulated in table 3-3. The variation among individuals is demonstrated through the conversion of values to proportionately pigmented colors; all standard error measurements are shaded along a gray gradient (with dark gray representing the highest value of the set) and POX, EXOC, PPO and LYS average activity levels are shaded in the same manner, with the darkest pink, blue, red, and green corresponding (respectively) to the highest activity level in that set (table 3-3). The x-axes of the box plots generated for POX, EXOC, PPO and LYS biomarkers were plotted such that sites were ordered (roughly) geographically from west-to-east locations (read from

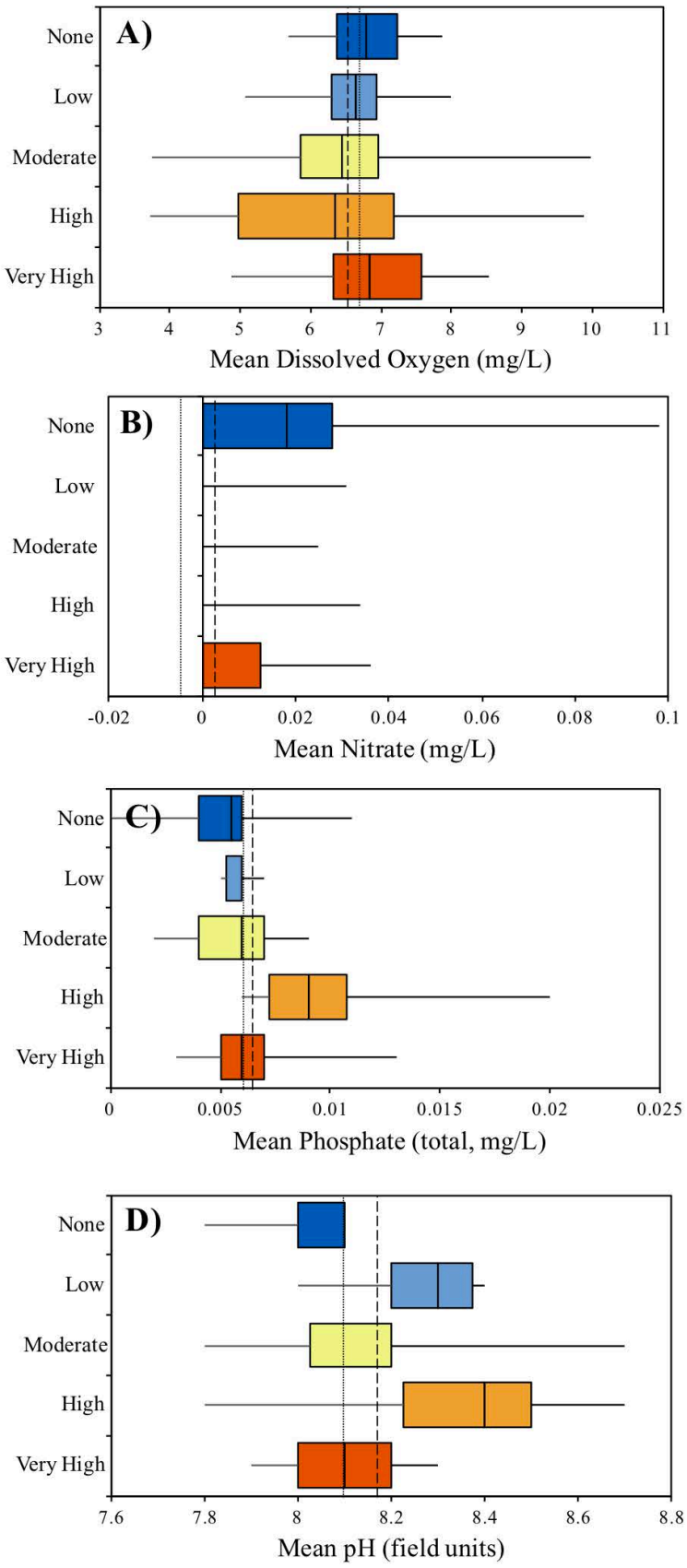
A)
None
Low
Moderate
High
Very High
3
4
5
6
7
8
9
10
11
Mean Dissolved Oxygen (mg/L)
B)
None
Low
Moderate
High
Very High
-0.02
0
0.02
0.04
0.06
0.08
0.1
Mean Nitrate (mg/L)
C)
None
Low
Moderate
High
Very High
0
0.005
0.01
0.015
0.02
0.025
Mean Phosphate (total, mg/L)
D)
None
Low
Moderate
High
Very High
7.6
7.8
8
8.2
8.4
8.6
8.8
Mean pH (field units)

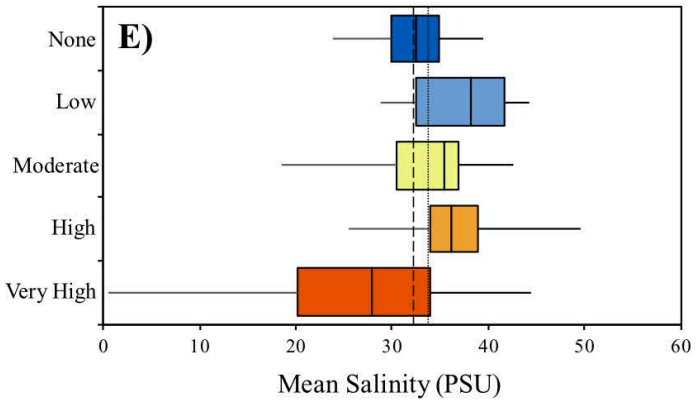
E)
None
Low
Moderate
High
Very High
0
10
20
30
40
50
60
Mean Salinity (PSU)

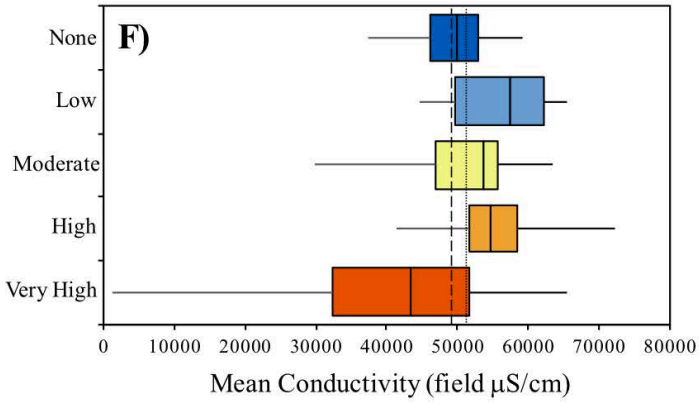
F)
None
Low
Moderate
High
Very High
0
10000
20000
30000
40000
50000
60000
70000
80000
Mean Conductivity (field µS/cm)

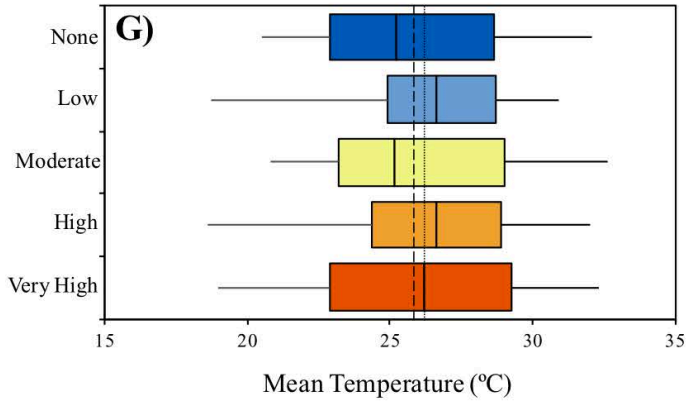
G)
None
Low
Moderate
High
Very High
15
20
25
30
35
Mean Temperature (ºC)

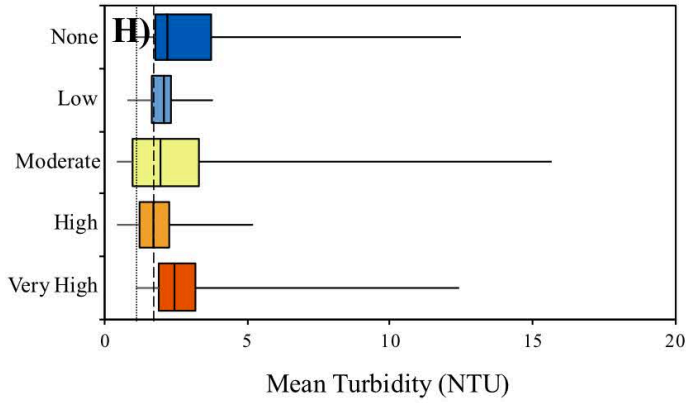
H)
None
Low
Moderate
High
Very High
0
5
10
15
20
Mean Turbidity (NTU)

Figure 3-13 (*previous two pages*). Box plots displaying water quality parameter characteristics [part A: dissolved oxygen (mg/L); part B: nitrate (mg/L); part C: phosphate (total, mg/L); part D: pH (field units); part E: salinity (PSU); part F: conductivity (μS/cm); part G: temperature (°C); part H: turbidity (NTU)] collected monthly from January 2013 to May 2015 at the 15 Florida Bay sites analyzed in this study. Sample sizes (reflecting removal of CAR and MAN sites) as follows: "Very High," n = 42; "High," n = 42; "Moderate," n = 42; "Low," n = 14; "None," n = 42. The main box in each plot represents the interquartile range (IRQ) of the data, with a median line intersecting the box at the second quartile. The lower and upper lines (whiskers) extending from each box in either direction signify the minimum and maximum (respectively) spread of the data outside of the IRQ. The coarse dashed line represents the mean value at that parameter across all sites and the fine dotted line represents the median value at that parameter across all sites (part A: mean = 6.537 mg/L, median = 6.640 mg/L; part B: mean = 0.003 mg/L, median = -0.005 mg/L; part C: mean = 0.006 mg/L, median = 0.006 mg/L; part D: mean = 8.171 field units, median = 8.100 field units; part E: mean = 32.267 PSU, median = 33.900 PSU; part F: mean = 49212.900 μS/cm, median = 51568.000 μS/cm; part G: mean = 25.926 °C, median = 26.100 °C; part H: mean = 2.693 NTU, median = 2.050 NTU). Data obtained through the DBHYDRO tool (https://www.sfwmd.gov/science-data/dbhydro) funded and conducted by SFWMD.

Table 3-3. Displays enzyme activity values (mean and standard error) at the four biomarkers measured (POX activity, EXOC activity, PPO activity and LYS activity) as a function of collection site within Florida Bay. The shade assigned to each site at a given parameter reflects the proportional value at that parameter, as compared to the entire data set, with white representing the lowest value of the set and dark pink (POX), blue (EXOC), red (PPO), green (LYS), and gray (standard error at all four biomarkers) representing the highest value of the set. Sample size n = 10 individuals per bay site. Samples collected in May 2015.

Bay Site	POX Activity (Δ Abs_{470} µg $protein^{-1}$)		EXOC Activity (nmol MU µg $protein^{-1}$)		PPO Activity (Δ Abs_{490} µg $protein^{-1}$)		LYS Activity (% inhibition µg $protein^{-1}$)	
	Mean	SE	Mean	SE	Mean	SE	Mean	SE
JON	0.6789	0.0986	1.4537	0.2382	3.5620	0.3368	5.2269	1.6655
RKB	1.0850	0.0956	0.6715	0.1440	3.8214	0.3268	4.1880	0.8796
GAR	0.4562	0.0840	0.6852	0.1352	1.5884	0.2586	1.0571	0.8210
RAN	0.3042	0.0782	0.3550	0.0586	1.3980	0.1990	2.0188	0.6075
WHP	0.4909	0.0541	0.5976	0.1267	3.0078	0.3869	2.5285	1.3117
TWN	0.9480	0.1184	1.6810	0.8137	4.5235	0.7682	5.1594	0.6734
TER	0.6659	0.0734	0.5801	0.0898	2.3747	0.2644	3.5852	1.4997
LIL	1.2581	0.2047	0.6153	0.1801	5.4260	0.9312	5.3958	1.1351
EAG	1.2451	0.1953	9.0829	5.9448	8.3865	1.4867	4.8705	2.4106
JOE	2.9585	0.2678	2.6956	0.3482	13.1048	1.5864	5.5811	3.0861
DUC	2.2005	0.5606	2.1477	0.5498	15.0220	2.1733	9.1730	6.3972
LON	1.7396	0.2274	3.7396	0.8045	18.3241	2.3159	11.8887	2.6628
BLK	1.6486	0.1135	5.2910	3.8904	13.4845	2.5808	4.0952	1.2592
MAN	2.2062	0.4861	1.1859	0.3749	9.3448	2.2658	8.5021	3.0408
CAR	2.5044	0.4432	3.7403	2.2240	12.4770	3.0820	12.8543	5.9424

the left-to-right direction) (figures 3-14 A, 3-15 A, 3-16 A, and 3-17 A). Sites significantly differed from one another, overall, at the POX and PPO biomarkers with a 99% confidence interval ($\alpha = 0.01$; $p < 0.00001$ for both metrics), but the differences between sites were not significant, overall, at the EXOC and LYS biomarkers ($\alpha = 0.05$; $p = 0.120$ and $p = 0.115$, respectively).

Furthermore, many of the westernmost sites (and some of those more centrally located; figure 3-3) had IQR which fell below the mean (dashed line with values in caption, in figures 3-14 A, 3-15 A, 3-16 A, and 3-17 A; "✱" superscript after site name, below) and/or median (dotted line with values in caption, in figures 3-14 A, 3-15 A, 3-16 A, and 3-17 A; "†" superscript after site name, below) across all sites [at POX: JON*†, GAR*†, RAN*†, WHP*†, TWN*, and TER*† (figure 3-14 A); at EXOC: JON*, RKB*, GAR*, RAN*†, WHP*†, TWN*, TER*†, LIL*, and EAG* (figure 3-15 A); at PPO: JON*†, RKB*, GAR*†, RAN*†, WHP*†, TWN*, TER*† and LIL* (figure 3-16 A); at LYS: GAR*, RAN*, and TER*† (and BLK*, which was in the NE region) (figure 3-17 A)]. Conversely, there was a clear trend in elevated immune levels in the (north)easternmost sites; many had IQR which fell above the mean (dashed line with values in caption, in figures 3-14 A, 3-15 A, 3-16 A, and 3-17 A; "✱" superscript after site name, below) and/or median (dotted line with values in caption, in figures 3-14 A, 3-15 A, 3-16 A, and 3-17 A; "†" superscript after site name, below) across all sites [at POX and PPO: JOE*†, DUC*†, LON*†, BLK*†, MAN†, and CAR† (figure 3-14 A and 3-16 A); at EXOC: JOE*†, DUC†, LON†, and CAR† (figure 3-15 A); at LYS: JOE*†, DUC†, and LON*† (and RKB*† and TWN† which were in the NE region) (figure 3-17 A)]. This disparity in immune status among western and eastern sites is also apparent in the visual color

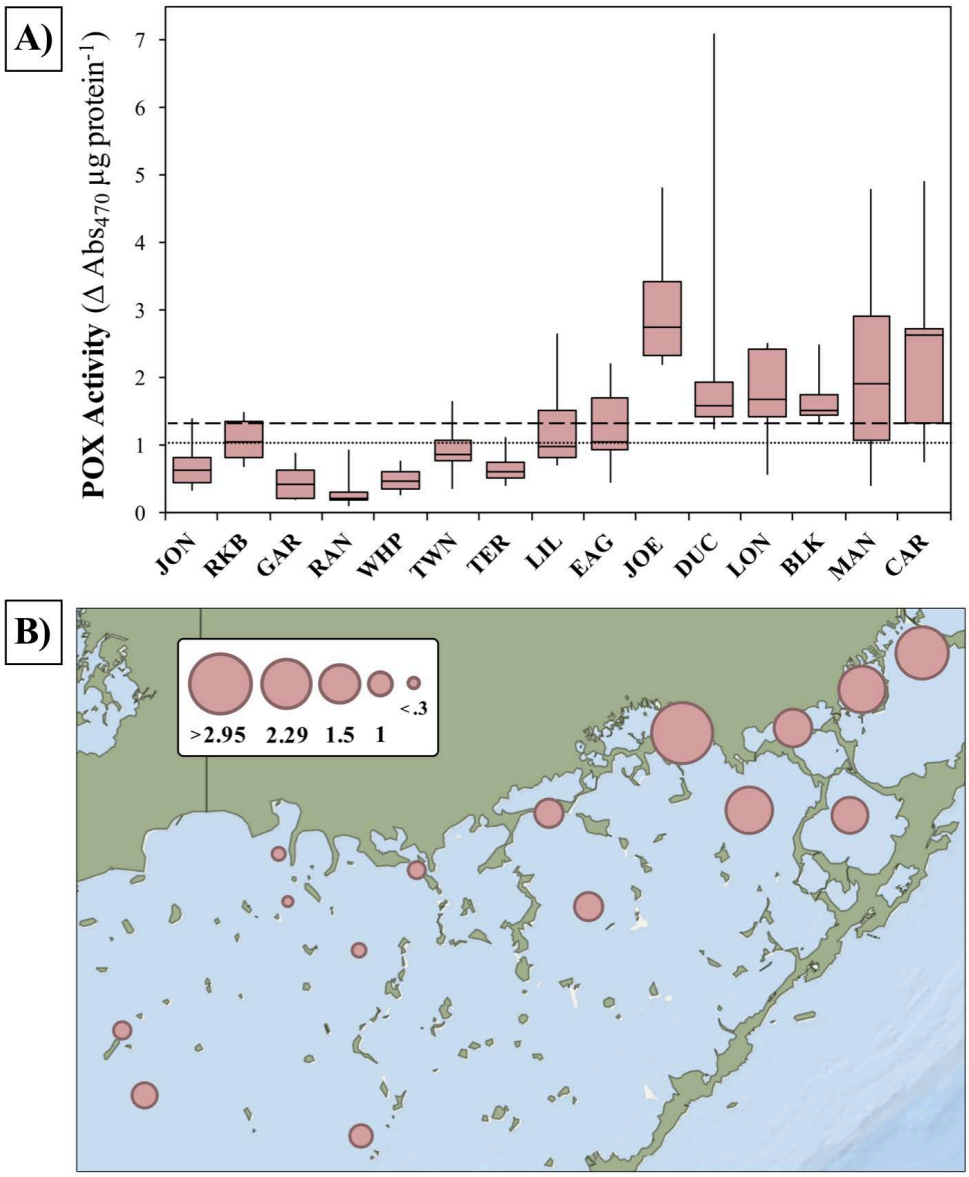

Figure 3-14. [A)] Box plot and [B)] map displaying POX activity (average ΔAbs_{470} µg protein^{-1} across 10 individuals collected at a given site) as a function of collection site in Florida Bay. In part A, the main box in each plot represents the interquartile range (IRQ) of the data, with a median line intersecting the box at the second quartile. The lower and upper lines (whiskers) extending from each box in either direction signify the minimum and maximum (respectively) spread of the data outside of the IRQ. The coarse dashed line represents the mean POX activity across all sites and the fine dotted line represents the median POX activity across all sites (mean = 1.352 ΔAbs_{470} µg protein^{-1}; median = 1.037 ΔAbs_{470} µg protein^{-1}). In part B, the magnitude of the circle represents the average POX activity value across 10 individuals collected at that site. Samples collected in May 2015. Base map obtained using ArcGIS software (ESRI, Version 10.5.1.).

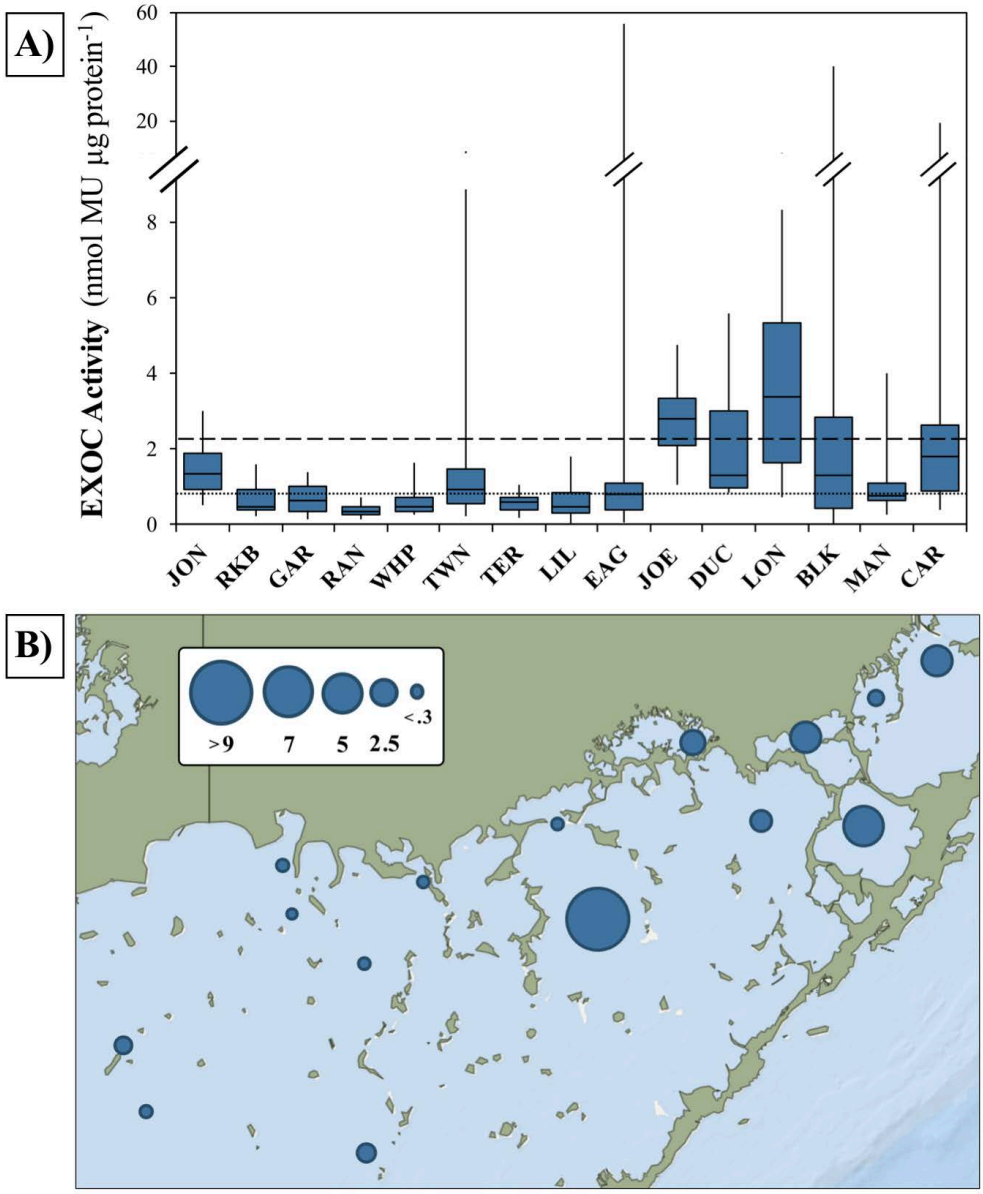

Figure 3-15. [A)] Box plot and [B)] map displaying EXOC activity (average nmol MU µg protein^{-1} across 10 individuals collected at a given site) as a function of collection site in Florida Bay. In part A, the main box in each plot represents the interquartile range (IRQ) of the data, with a median line intersecting the box at the second quartile. The lower and upper lines (whiskers) extending from each box in either direction signify the minimum and maximum (respectively) spread of the data outside of the IRQ. The coarse dashed line represents the mean EXOC activity across all sites and the fine dotted line represents the median EXOC activity across all sites (mean = 2.282 nmol MU µg protein^{-1}; median = 0.823 nmol MU µg protein^{-1}). In part B, the magnitude of the circle represents the average EXOC activity value across 10 individuals collected at that site. Samples collected in May 2015. Base map obtained using ArcGIS software (ESRI, Version 10.5.1.).

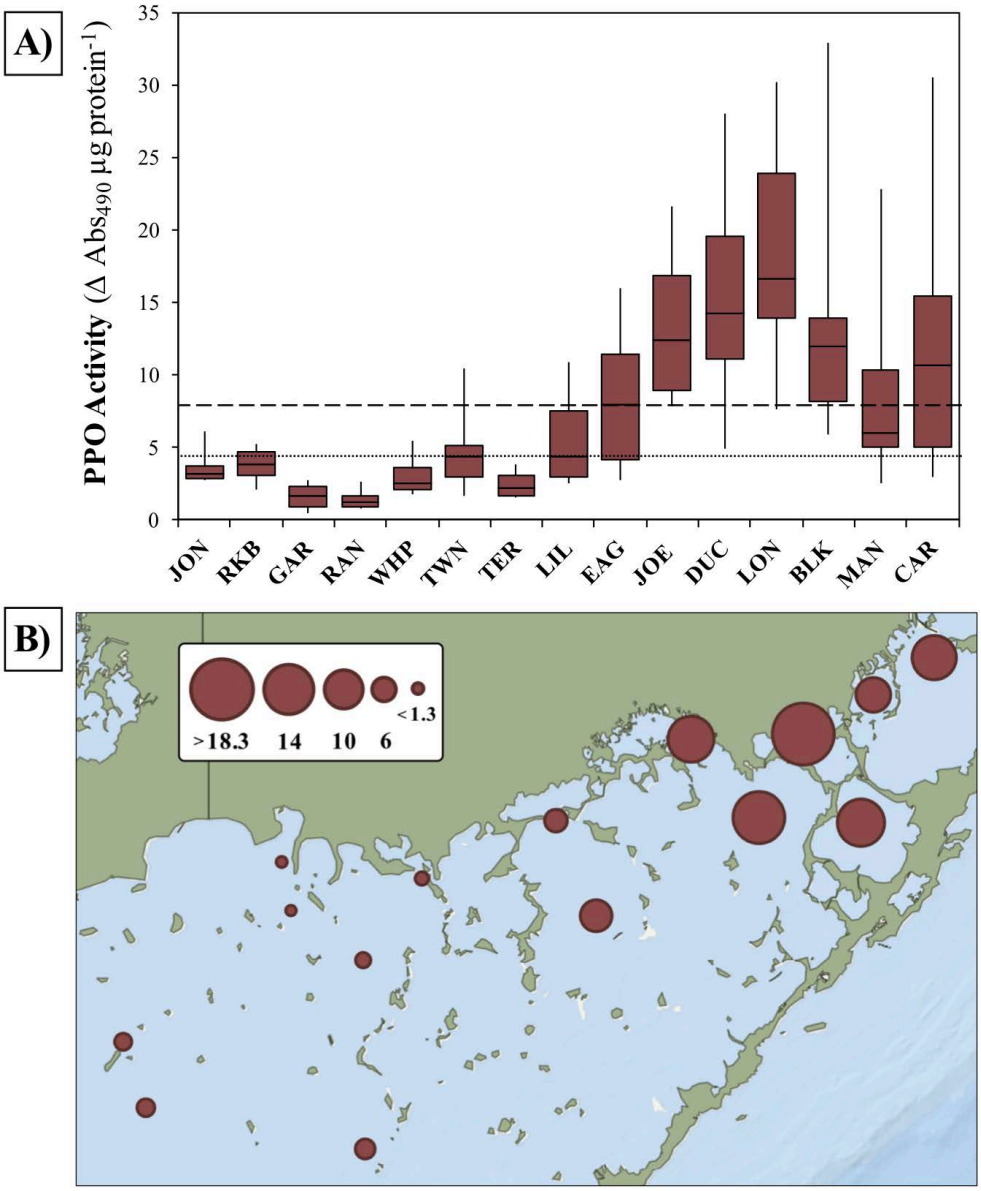

Figure 3-16. [A)] Box plot and [B)] map displaying PPO activity (average ΔAbs_{490} µg protein^{-1} across 10 individuals collected at a given site) as a function of collection site in Florida Bay. In part A, the main box in each plot represents the interquartile range (IRQ) of the data, with a median line intersecting the box at the second quartile. The lower and upper lines (whiskers) extending from each box in either direction signify the minimum and maximum (respectively) spread of the data outside of the IRQ. The coarse dashed line represents the mean PPO activity across all sites and the fine dotted line represents the median PPO activity across all sites (mean = 7.691 ΔAbs_{490} µg protein^{-1}; median = 4.536 ΔAbs_{490} µg protein^{-1}). In part B, the magnitude of the circle represents the average PPO activity value across 10 individuals collected at that site. Samples collected in May 2015. Base map obtained using ArcGIS software (ESRI, Version 10.5.1.).

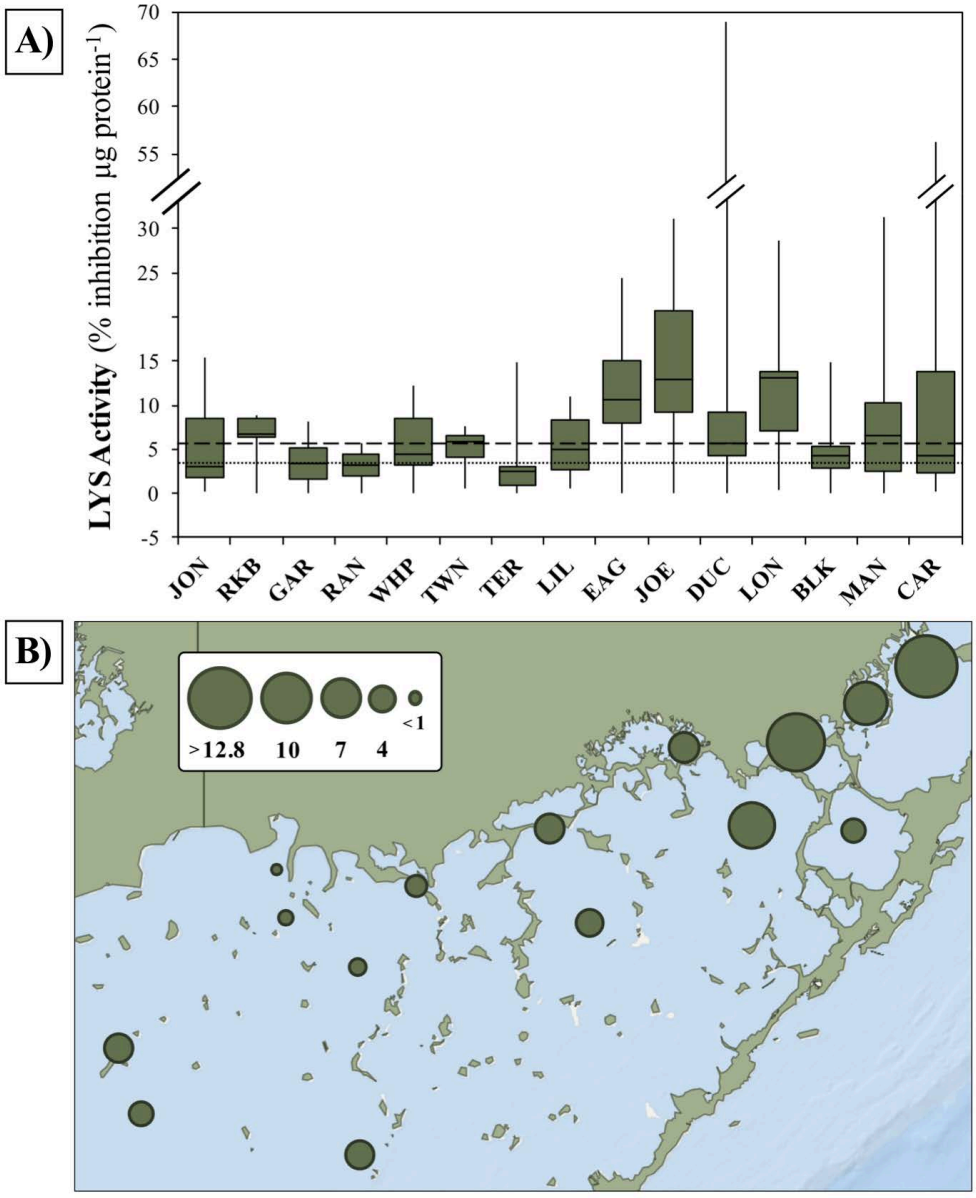

Figure 3-17. [A)] Box plot and [B)] map displaying LYS activity (average % inhibition µg protein^{-1} across 10 individuals collected at a given site) as a function of collection site in Florida Bay. In part A, the main box in each plot represents the interquartile range (IRQ) of the data, with a median line intersecting the box at the second quartile. The lower and upper lines (whiskers) extending from each box in either direction signify the minimum and maximum (respectively) spread of the data outside of the IRQ. The coarse dashed line represents the mean LYS activity across all sites and the fine dotted line represents the median LYS activity across all sites (mean = 5.694% inhibition µg protein^{-1}; median = 3.618% inhibition µg protein^{-1}). In part B, the magnitude of the circle represents the average LYS activity value across 10 individuals collected at that site. Samples collected in May 2015. Base map obtained using ArcGIS software (ESRI, Version 10.5.1.).

gradient appearing in table 3-3 from-west to-east (top-to-bottom, table 3-3) and in the maps generated (figures 3-14 B, 3-15 B, 3-16 B, and 3-17 B).

The immune class grouping, generated using multivariate analyses which considered all four immune biomarkers (figure 3-18, 3-19, 3-20), largely reinforced the trends seen at the individual level in terms of geography. The (south)westernmost sites were grouped together in "Immune Class A" (comprised of JON, RKB, TWN, and LIL), with the exception of LIL, a centrally located coastal basin (figures 3-3, 3-20). A group of four (northern) central sites (GAR, RAN, WHP, and TER) were classified together in "Immune Class B," and the remaining sites (EAG, JOE, DUC, LON, BLK, MAN, and CAR), all located in the (north)eastern portion of the bay, were clustered together based on their immune profile similarities (figures 3-3, 3-20). These groupings were reinforced when plotted as box plots for each biomarker as function of the newly established immune classes (figure 3-21).

Morphological Characteristics across Immune Status Classes

Box plots and bar graphs were generated to visually display the spread of data for *T. testudinum* morphological characteristics, grouped as a function of the immune status classes previously established (figures 3-22, 3-23). The IQRs of both spring and fall mean canopy height and mean leaf area in Immune Class C were lower than the mean values for these parameters across all immune classes/sampling sites (bay-wide mean canopy height in spring/fall = 15.693/19.249 cm; bay-wide mean total leaf area in spring/fall = 30.460/28.225 cm^2) (figure 3-22 B, C). Furthermore, the mean canopy height and mean leaf area of individuals in Immune Class C was significantly lower than those of the other two immune

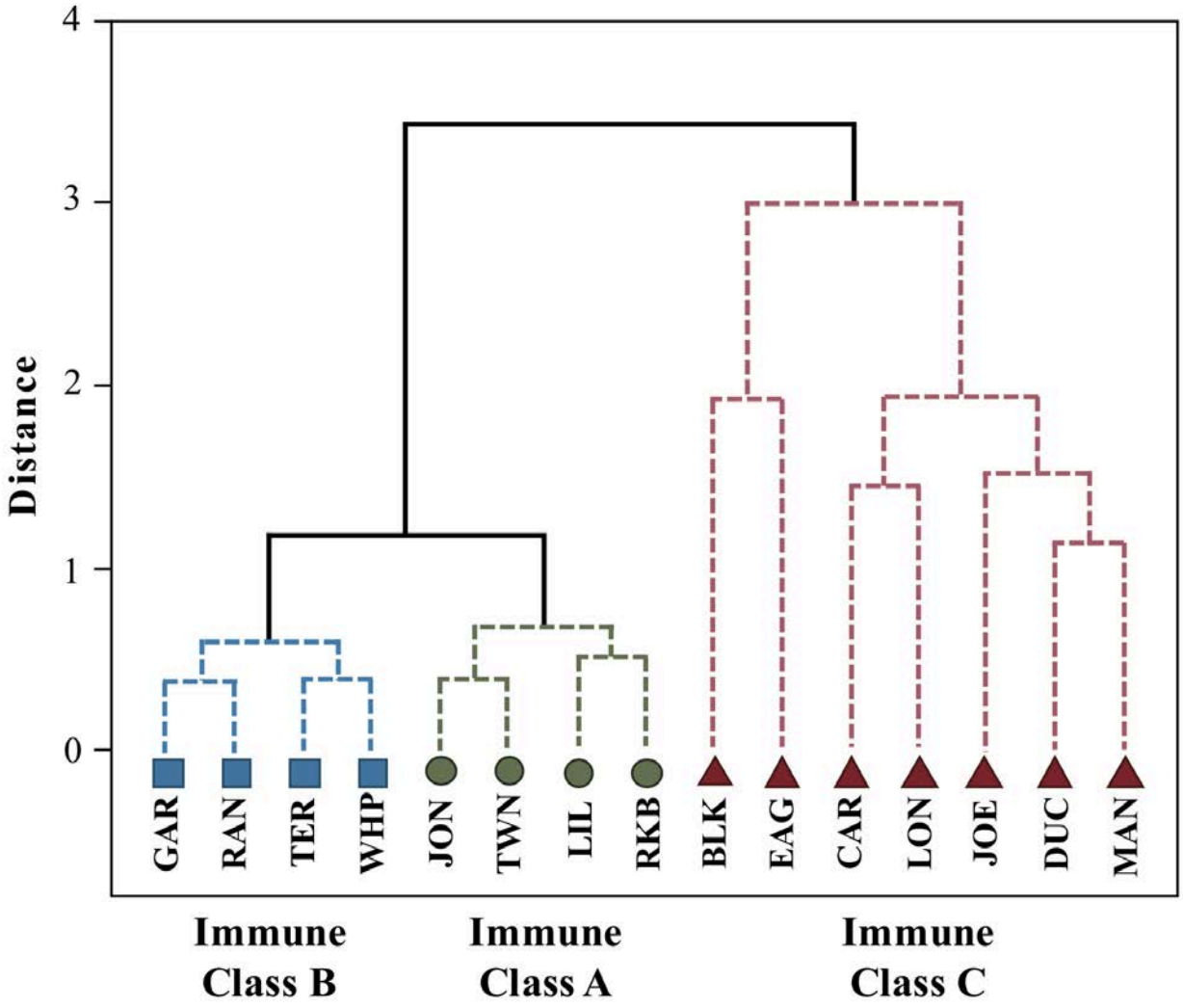

Figure 3-18. CLUSTER analysis grouping sites into immune classes based on average site activity levels at the four biomarkers measured (POX activity, EXOC activity, PPO activity and LYS activity). Dashed lines indicate groups not separated ($p<0.05$) by SIMPROF.

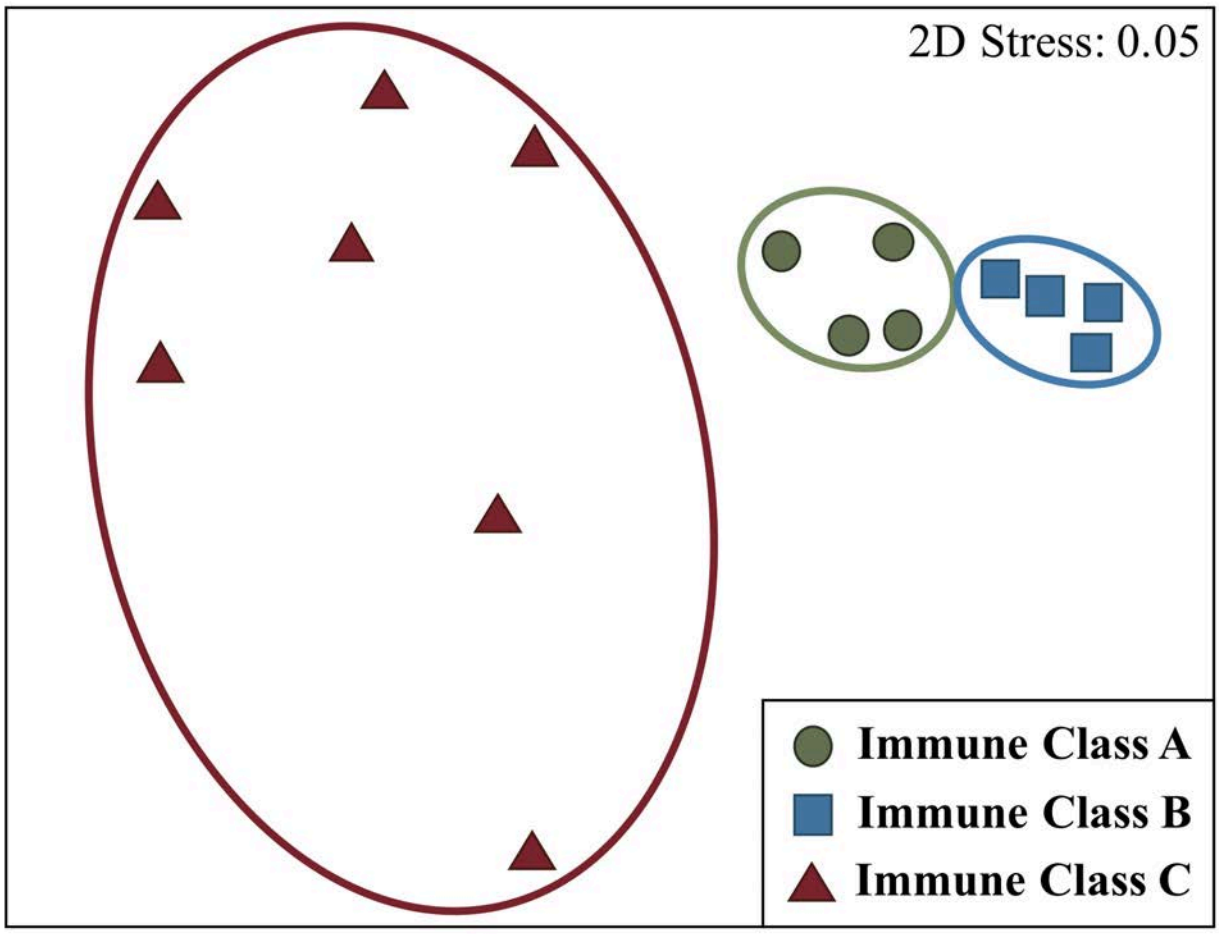

Figure 3-19. MDS plot grouping sites into immune classes based on average site activity levels at the four biomarkers measured (POX activity, EXOC activity, PPO activity and LYS activity).

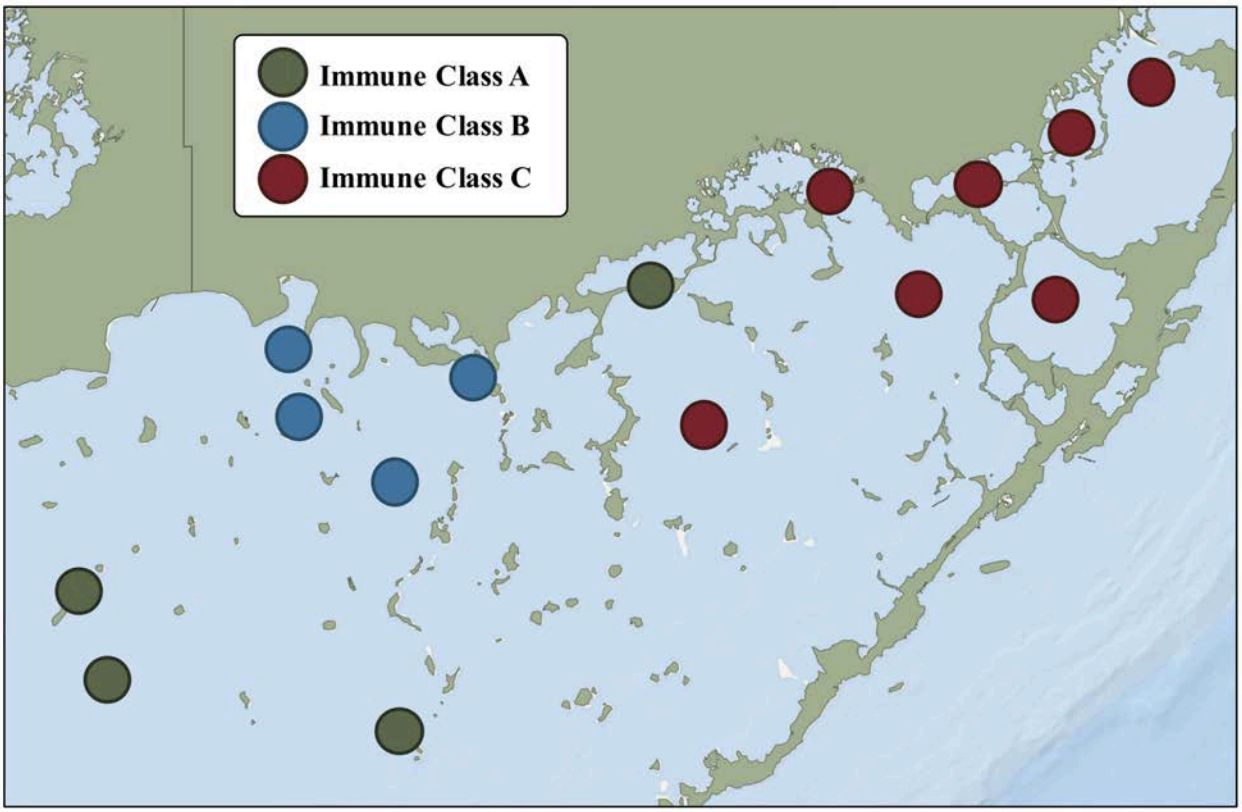

Figure 3-20. Map displaying the immune classes as a function of the geographic distribution in Florida Bay. Sites were grouped according to CLUSTER and MDS analyses based on average site activity levels at the four biomarkers measured (POX activity, EXOC activity, PPO activity and LYS activity). Samples collected in May 2015. Base map obtained using ArcGIS software (ESRI, Version 10.5.1.).

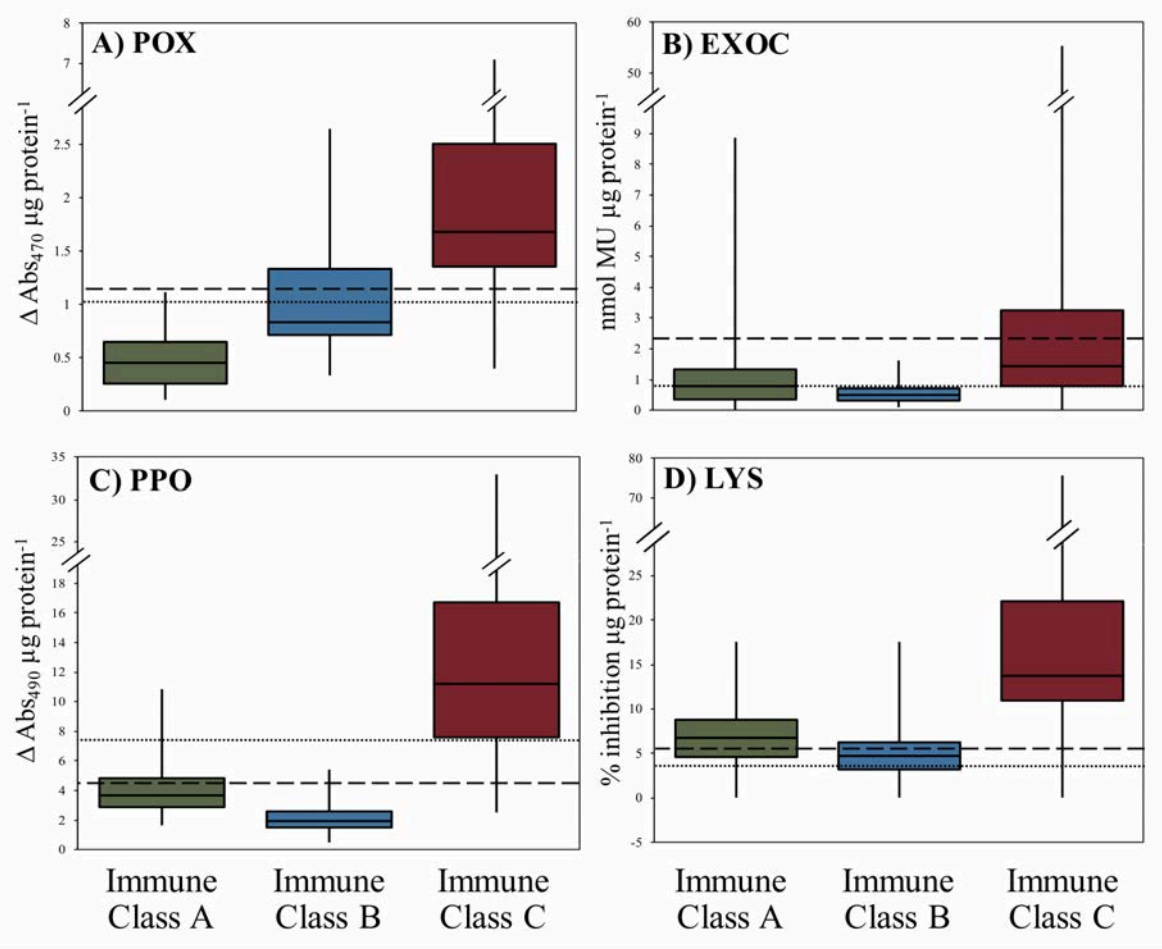

Figure 3-21. Box plots displaying immune enzyme activity (part A: POX activity; part B: EXOC activity; part C: PPO activity; part D: LYS activity) as a function of immune class. Sample sizes for each part as follows: "Immune Class A," n = 40; "Immune Class B," n = 40; "Immune Class C," n = 70. The main box in each plot represents the interquartile range (IRQ) of the data, with a median line intersecting the box at the second quartile. The lower and upper lines (whiskers) extending from each box in either direction signify the minimum and maximum (respectively) spread of the data outside of the IRQ. The coarse dashed line represents the average biomarker activity level across all sites and the fine dotted line represents the average biomarker activity level across all sites (see figures 3-13 through 3-16 for mean and median values).

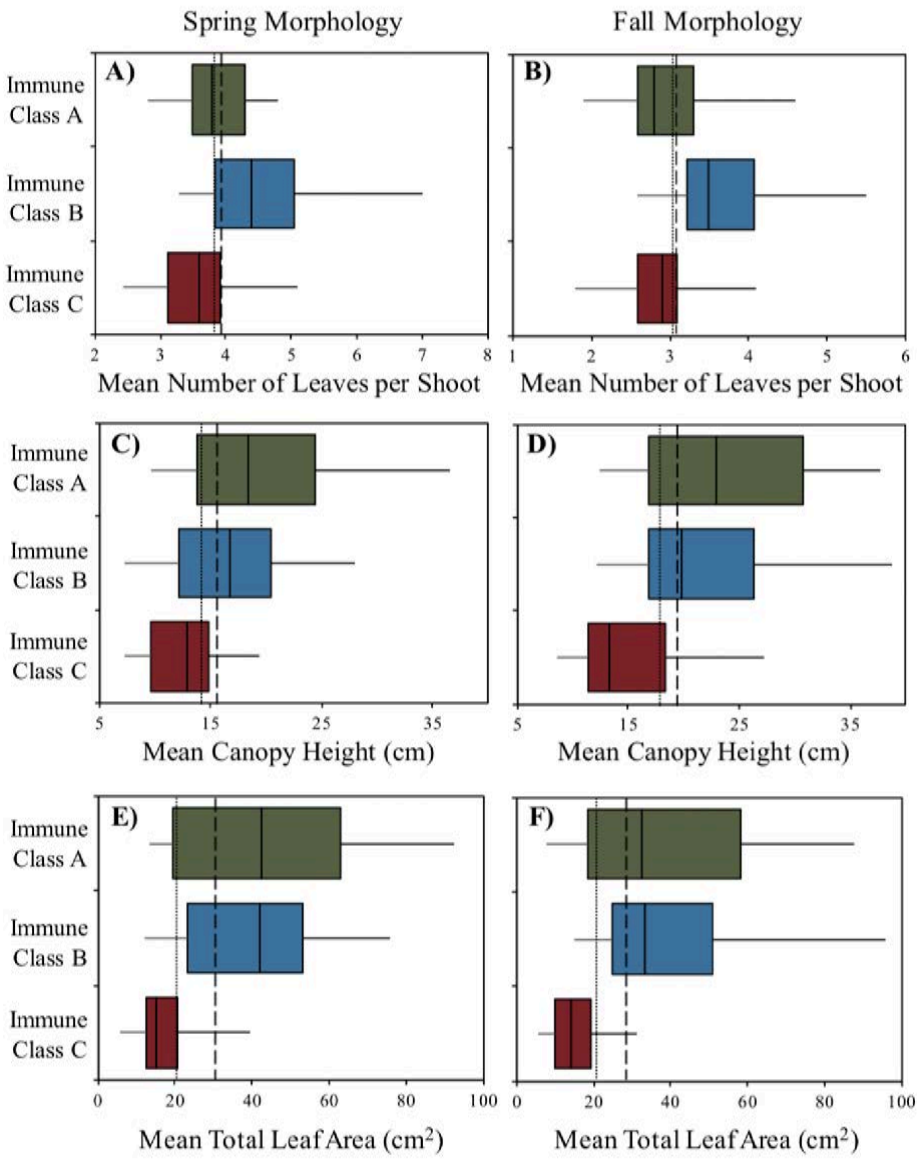

Figure 3-22. Box plots displaying *T. testudinum* leaf morphometrics data [parts A & B: number of leaves per shoot; parts C & D: mean canopy height (cm); parts E & F: mean leaf area per shoot (cm^2)] collected biannually during the spring (A, C, E) and fall (B, D, F) from January 2010 to May 2015 as a function of immune class. Sample sizes as follows: "Immune Class A," n = 24; "Immune Class B," n = 24; "Immune Class C," n = 42. The main box in each plot represents the interquartile range (IRQ) of the data, with a median line intersecting the box at the second quartile. The lower and upper lines (whiskers) extending from each box in either direction signify the minimum and maximum (respectively) spread of the data outside of the IRQ. The coarse dashed line represents the mean value at that parameter across all sites during that season and the fine dotted line represents the median value at that parameter across all sites during that season (see figure 3-11 for mean and median values). Data obtained through FHAP survey database (M. Durako, pers. comm.).

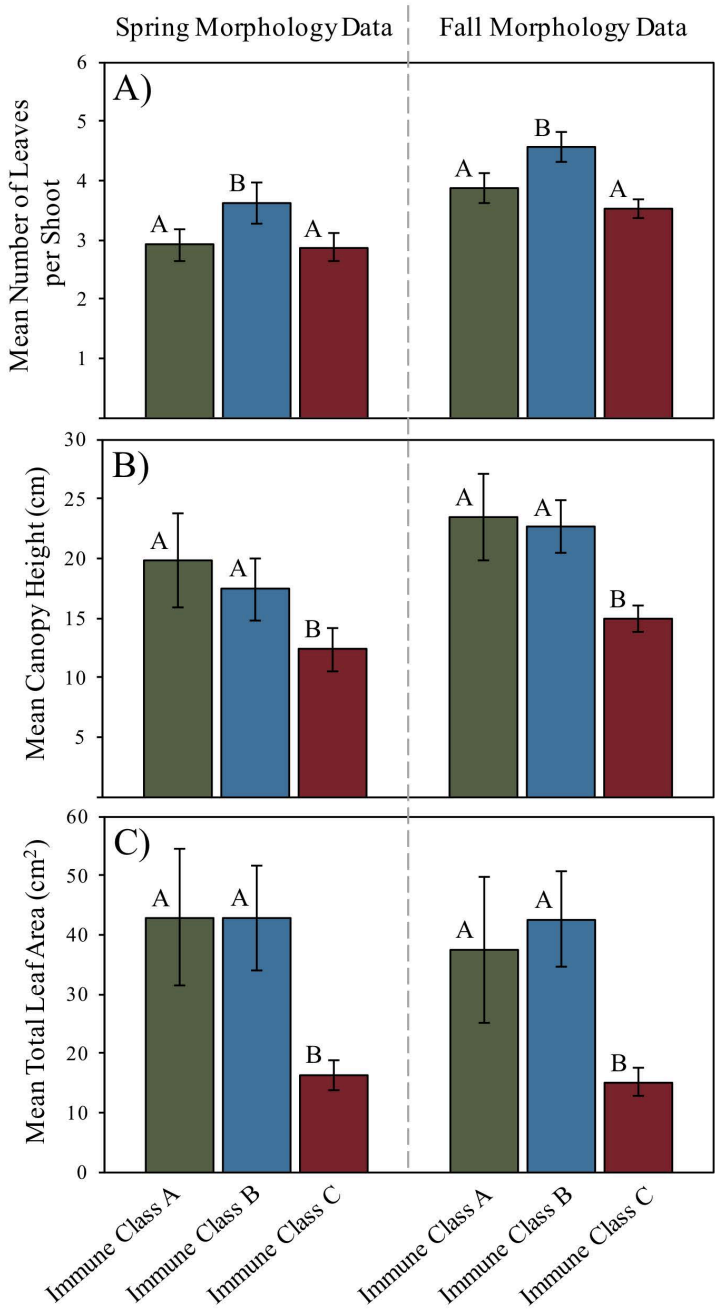

Figure 3-23. Bar graphs displaying *T. testudinum* leaf morphometrics data [part A: number of leaves per shoot; part B: mean canopy height (cm); part C: mean leaf area per shoot (cm^2)] collected biannually during the spring and fall from January 2010 to May 2015 as a function of immune class. Sample sizes as follows: "Immune Class A," n = 24; "Immune Class B," n = 24; "Immune Class C," n = 42. Error bars reflect ±1 SEM. Different letters (A & B) represents significant differences in mean morphometric data between two groups as determined by ANOVA analyses, followed by multiple comparisons LSD posthoc tests (two-tailed, $\alpha = 0.05$). Data obtained through FHAP survey database (M. Durako, pers. comm.).

classes (Immune Class A and B) across both seasons with a 99% confidence interval (α = 0.01; $p < 0.0001$) (figure 3-23 B, C).

Water Quality Characteristics across Immune Status Classes

Box plots were generated to visually display the spread of data at six water quality parameters [dissolved oxygen (mg/L), nitrate (mg/L), total phosphate (mg/L), pH (field units), conductivity (field μS/cm), temperature (°C) and turbidity (NTU)], grouped as a function of immune class (figure 3-24). Of these characteristics, mean temperature was the most similar among immune classes (figure 3-24 G) and was the only water quality parameter where the overall differences between groups was not significant ($\alpha = 0.05$; $p = 0.765$). All other water quality parameters varied significantly as a function of immune class according to global tests of significance with 99% confidence levels ($\alpha = 0.01$; $p < 0.0001$) (figure 3-24 A-F, H). Notable trends included a substantially larger spread and IQR region for nitrate levels in Immune Class C as compared to classes A and B (figure 3-24 B). Additionally, the spread of salinity and conductivity values extended much lower among Immune Class C individuals as compared to the other classes (figure 3-24 E, F). Overall, the box plots showed that the immune classes differed from one another at water quality parameters, and Immune Class C differed more profoundly from immune classes A and B across many of these metrics (figure 3-24).

Relating Immune and Pathogen Severity Classes to a Biogeographical Model of the FL Bay

Over the past several decades, many attempts have been made to partition the bay into discrete regions based on biogeochemical characteristics and ecological gradients (e.g. Wanless & Tagett

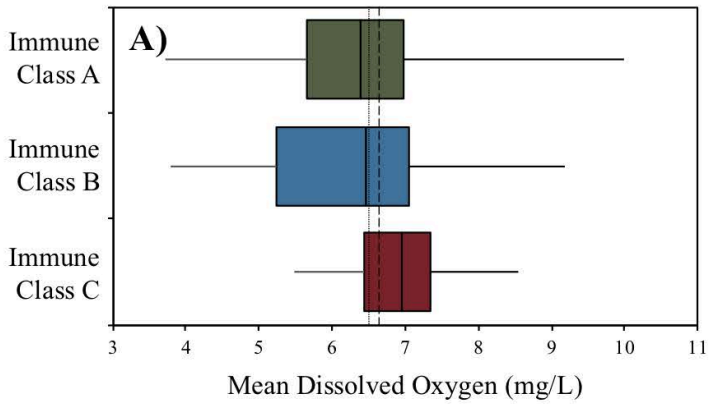
A)
Immune Class A
Immune Class B
Immune Class C
3
4
5
6
7
8
9
10
11
Mean Dissolved Oxygen (mg/L)

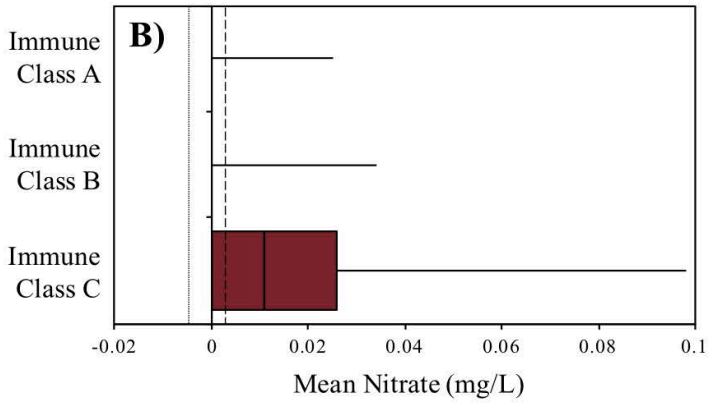
B)
Immune Class A
Immune Class B
Immune Class C
-0.02
0
0.02
0.04
0.06
0.08
0.1
Mean Nitrate (mg/L)

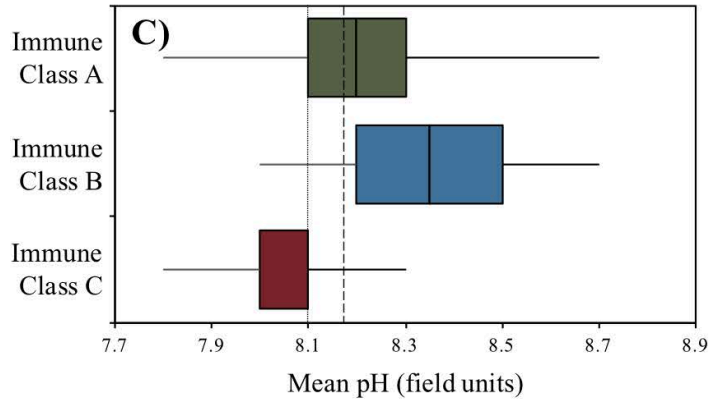
C)
Immune Class A
Immune Class B
Immune Class C
7.7
7.9
8.1
8.3
8.5
8.7
8.9
Mean pH (field units)

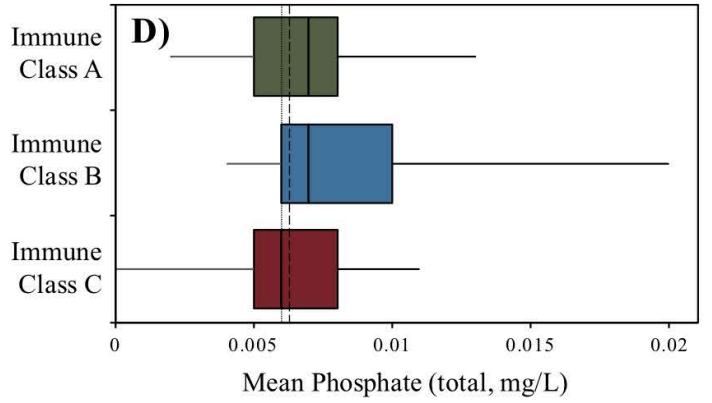
D)
Immune Class A
Immune Class B
Immune Class C
0
0.005
0.01
0.015
0.02
Mean Phosphate (total, mg/L)

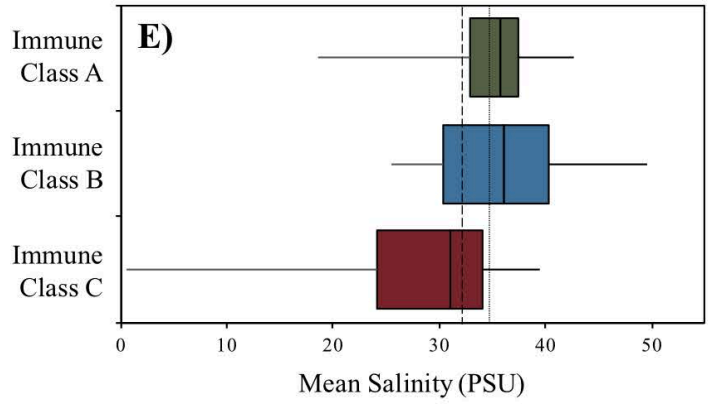
E)
Immune Class A
Immune Class B
Immune Class C
0
10
20
30
40
50
Mean Salinity (PSU)

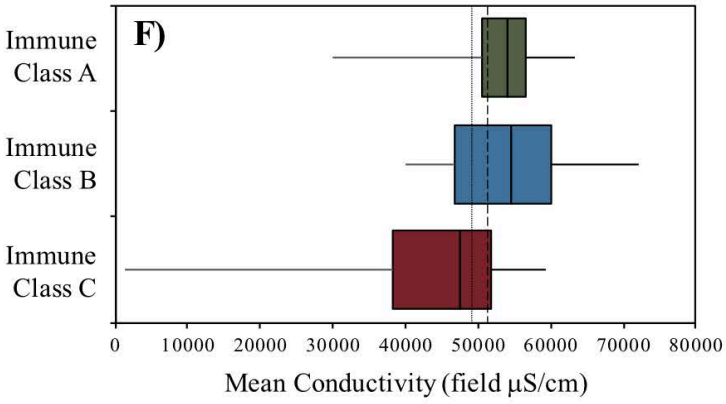
F)
Immune Class A
Immune Class B
Immune Class C
0
10000
20000
30000
40000
50000
60000
70000
80000
Mean Conductivity (field µS/cm)

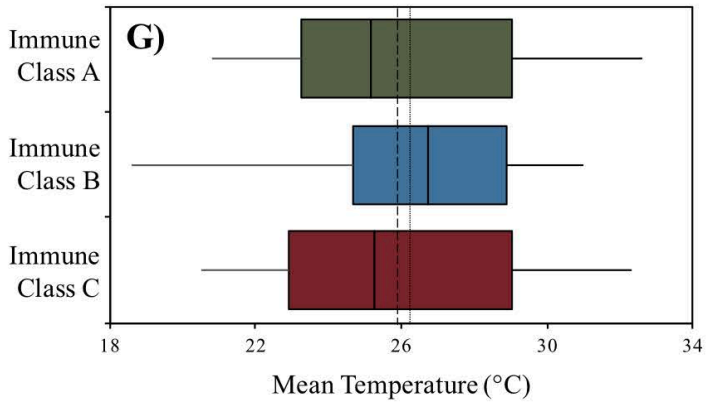
G)
Immune Class A
Immune Class B
Immune Class C
18
22
26
30
34
Mean Temperature (°C)

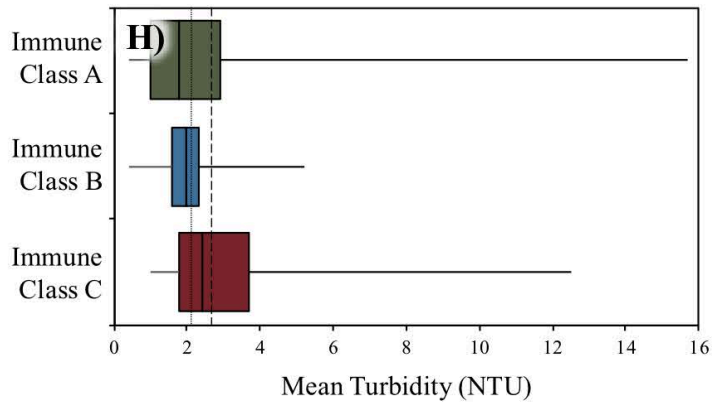
H)
Immune Class A
Immune Class B
Immune Class C
0
2
4
6
8
10
12
14
16
Mean Turbidity (NTU)

Figure 3-24 (*previous two pages*). Box plots displaying water quality parameter characteristics [part A: dissolved oxygen (mg/L); part B: nitrate (mg/L); part C: phosphate (total, mg/L); part D: pH (field units); part E: salinity (PSU); part F: conductivity (μS/cm); part G: temperature (°C); part H: turbidity (NTU)] collected monthly from January 2013 to May 2015 at the 15 Florida Bay sites analyzed in this study. Sample sizes (reflecting removal of CAR and MAN sites) as follows: "Immune Class A," n = 168; "Immune Class B," n = 172; "Immune Class C," n = 210. The main box in each plot represents the interquartile range (IRQ) of the data, with a median line intersecting the box at the second quartile. The lower and upper lines (whiskers) extending from each box in either direction signify the minimum and maximum (respectively) spread of the data outside of the IRQ. The coarse dashed line represents the mean value at that parameter across all sites and the fine dotted line represents the median value at that parameter across all sites (see figure 3-12 for mean and median values). Data obtained through the DBHYDRO tool (https://www.sfwmd.gov/science-data/dbhydro) funded and conducted by SFWMD.

1989, Boyer et al. 1999, Bricker et al. 2011, Briceño et al. 2013). We conducted a thorough literature search and compiled a set of biogeographical/ecological models, which were then compared to the spatial patterns observed in our data (figures 3-25, 3-26). One model, a projected reorganization of seagrass communities based on changes in freshwater inflow proposed by Herbert et al. (2011), coincided with the geographical distribution of the immune status classes we established in this study. These two data set layers were superimposed over a map of Florida Bay [with Herbert et al. (2011) zone delineations outlined in black; figure 3-25] and the biogeochemical zones were grouped based on the immune classes within the zone(s) (immune classes A, B, and C are shaded in green, blue, and red, respectfully; figure 3-25). These zones are hereafter referred to "Immune Zone A," through "Immune Zone C."

Patterns associated with Salinity Metrics

Detailed Immune Zone C Analysis

Once established, the immune zones were compared to the previously established pathogen level-based site classification ("Very High," "High," "Moderate," "Low," and "None") and the resulting map is depicted in figure 3-26. Immune Zone A (shaded green) contained one site with high pathogen loading (JON) and three sites with moderate pathogen loading (RKB, TWN, and LIL) (figure 3-26). Immune Zone B (shaded blue) held one site with very high pathogen loading (TER), two sites with high pathogen loading (GAR and RAN), and one site with low pathogen loading (WHP) (figure 3-26). Finally, Immune Zone C contained the remaining sites, which included three with very high pathogen loading (JOE, LON, and MAN) and four with no pathogen loading (EAG, DUC, BLK, and CAR) (figure 3-26). Immune Zone C stood out due to the striking contrast between sites; the pathogen severity

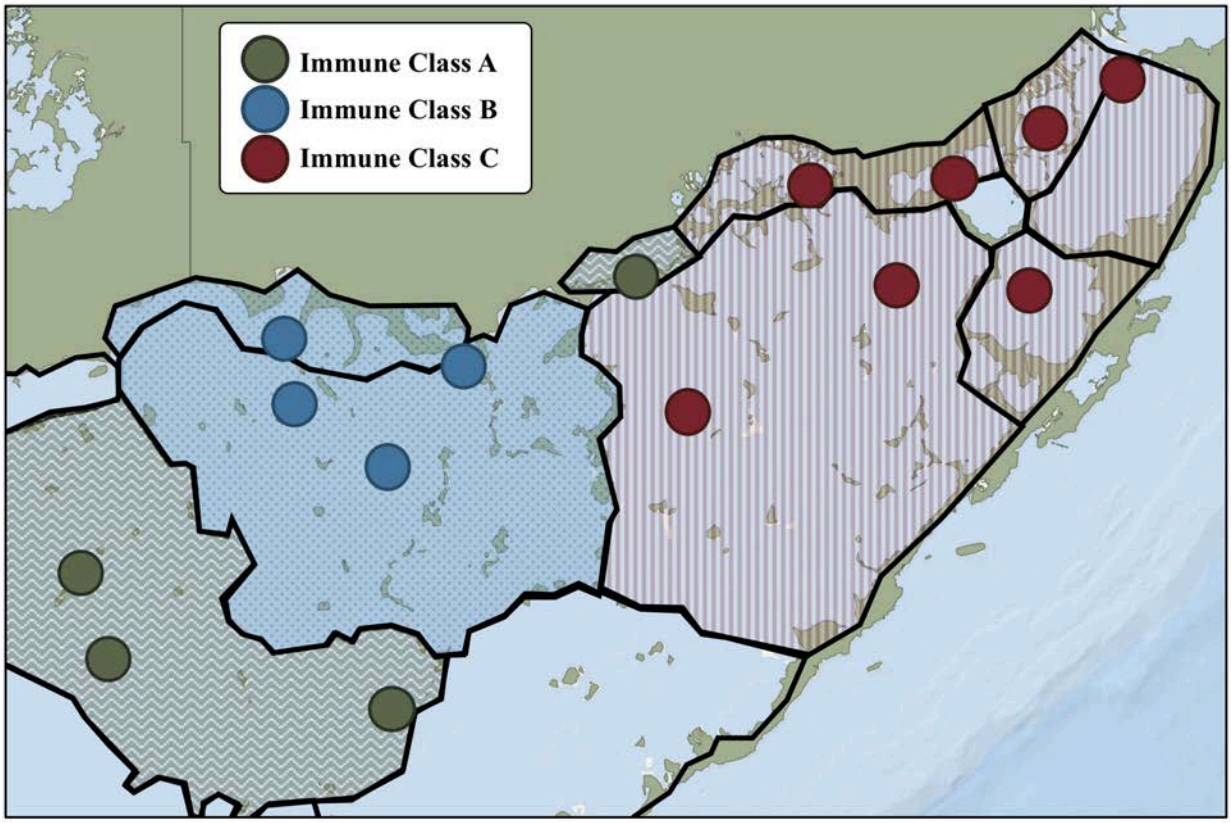

Figure 3-25. Map displaying immune classes as a function of the geographic distribution in Florida Bay layered over biogeochemical segmentation of the bay as defined in Herbert et al. (2011). Biogeochemical segments shaded according to associated immune class sites. Base map obtained using ArcGIS software (ESRI, Version 10.5.1.).

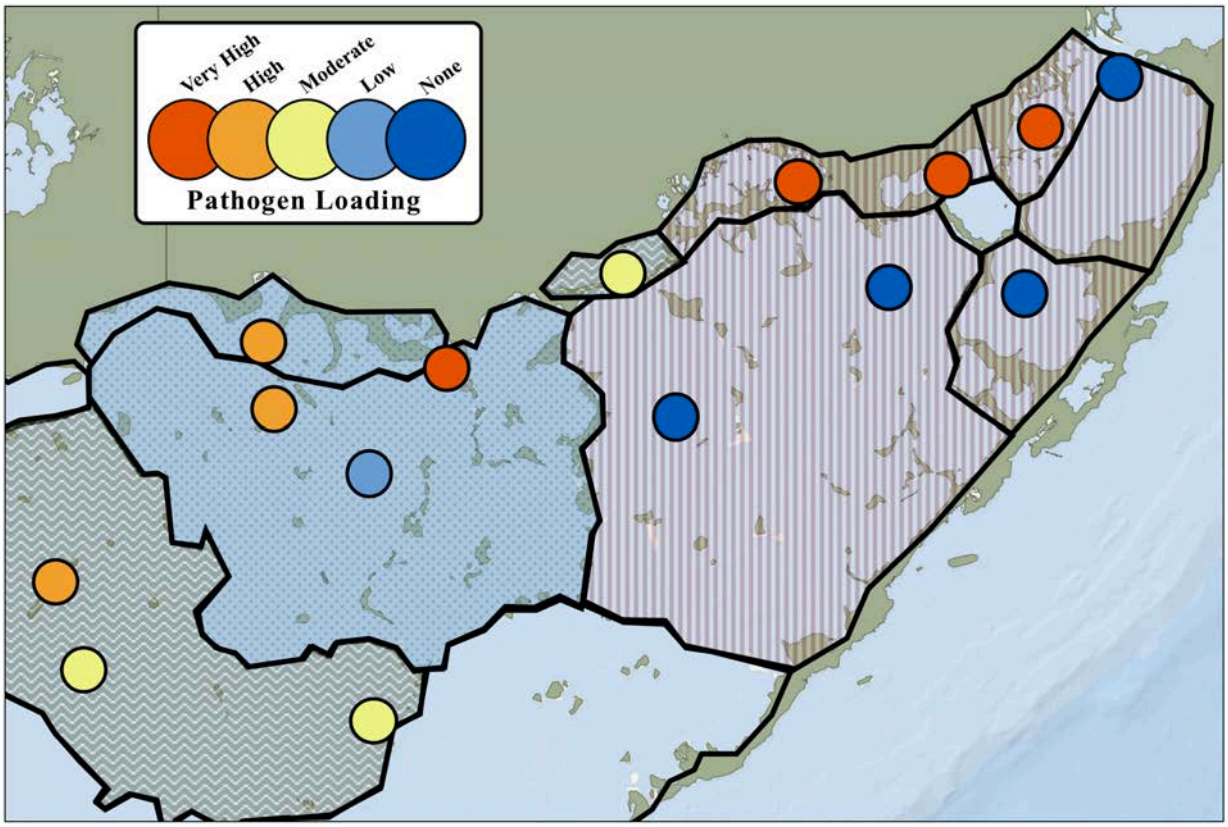

Figure 3-26. Map displaying pathogen severity classes as a function of the geographic distribution in Florida Bay layered over biogeochemical segmentation of the bay as defined in Herbert et al. (2011). Biogeochemical segments shaded according to associated immune class sites (see figure 3-24). Base map obtained using ArcGIS software (ESRI, Version 10.5.1.).

levels fell to either extreme in the range of possible classes at close to a 1:1 ratio (figure 3-26). For this reason, this immune zone and the sites within it became the focus of subsequent analyses.

It was observed that “Very High” pathogen severity-grouped sites in Immune Zone C were located within semi-enclosed coastal basins, and due to the proximity of recent Taylor Slough water diversions to these sites (figure 3-2), salinity was investigated further. A box plot comparing summary statistics of salinity measurements from 2013 to 2015 between Immune Zone C “None” and “Very High” pathogen loading classes revealed that the IRQ salinity range was much greater and extended much lower among “Very High” pathogen loading individuals as compared to those with no pathogen detected (“None,” figure 3-27 A). Additionally, the entire IRQ range for those sites with very high pathogen loading was below both the mean and median lines calculated across all sites in the bay (red dashed and dotted lines, respectively; mean salinity = 32.267; median salinity = 33.9) (figure 3-27 A). The bar graph illustrates the statistically validated difference between distributions of the two groups ($\alpha = 0.01$; $p < 0.0001$). Additionally, this graph revealed that the disparity between the two groups under comparison was due exclusively to low mean salinity values in the “Very High” pathogen loading class (orange), as the mean salinity across all sites (red dashed line) was almost identical to the mean salinity of the class where no pathogen was detected (“None,” in blue; figure 3-27).

The line graph plotting individual sites (in Immune Zone C) at monthly time points from 2010 to 2015 (color coded by pathogen severity classes; blue = “None,” red-orange = “Very High”) revealed important trends at a higher temporal resolution (figure 3-28). While

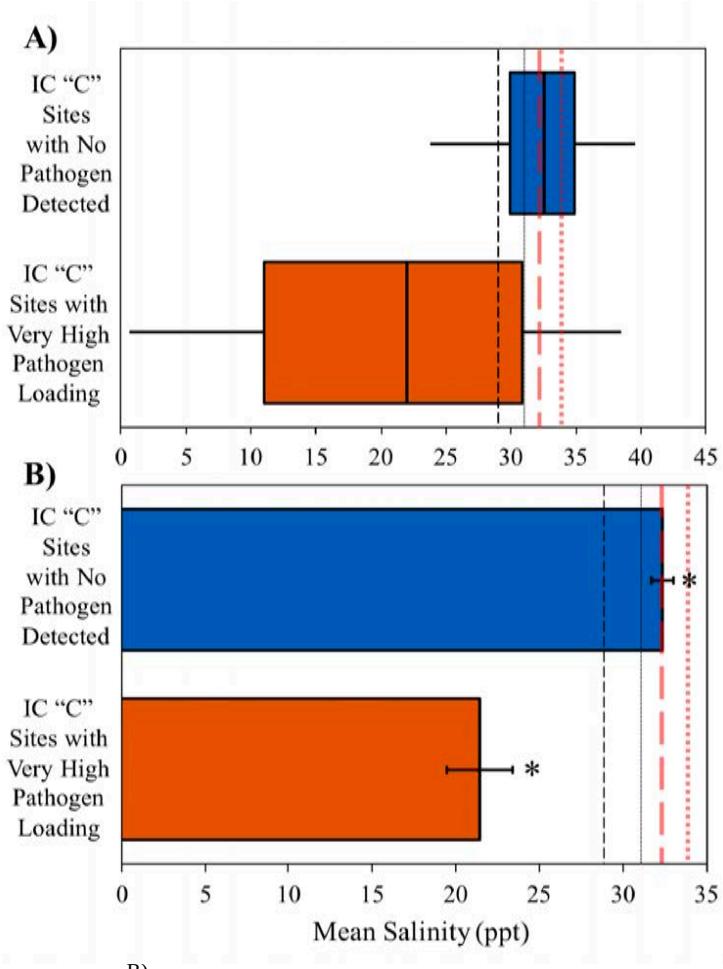

Figure 3-27. [A)] Box plots and [B)] bar graphs displaying mean salinity values (in ppt, equivalent to PSU) collected monthly from January 2013 to May 2015 as a function of pathogen severity classes falling within Immune Class C (see figure 3-25). IC "C" sites with "Very High" pathogen loading (in orange) include JOE and LON (MAN removed due to lack of WQ data) and IC "C" sites with no pathogen loading ("None," in blue) include EAG, DUC and BLK (CAR removed due to lack of WQ data). Sample sizes as follows: "No Pathogen Detected," n = 84; "Very High Pathogen Loading," n = 126. In part A, the main box in each plot represents the interquartile range (IRQ) of the data, with a median line intersecting the box at the second quartile. The lower and upper lines (whiskers) extending from each box in either direction signify the minimum and maximum (respectively) spread of the data outside of the IRQ. In part B, error bars reflect ±1 SEM. Asterisk (*) represents two-tailed significant difference at $\alpha = 0.01$. In parts A & B, the black coarse dashed line represents the mean value at that parameter across all Immune Class C sites and the fine black dotted line represents the median value at that parameter across all Immune Class C sites (mean = 32.267 ppt; median = 33.900 ppt). In parts A & B, the red coarse dashed line represents the mean value at that parameter across all sites and the fine red dotted line represents the median value at that parameter across all sites (see figure 3-12 E for mean and median values). Data obtained through the DBHYDRO tool (https://www.sfwmd.gov/science-data/dbhydro) funded and conducted by SFWMD.

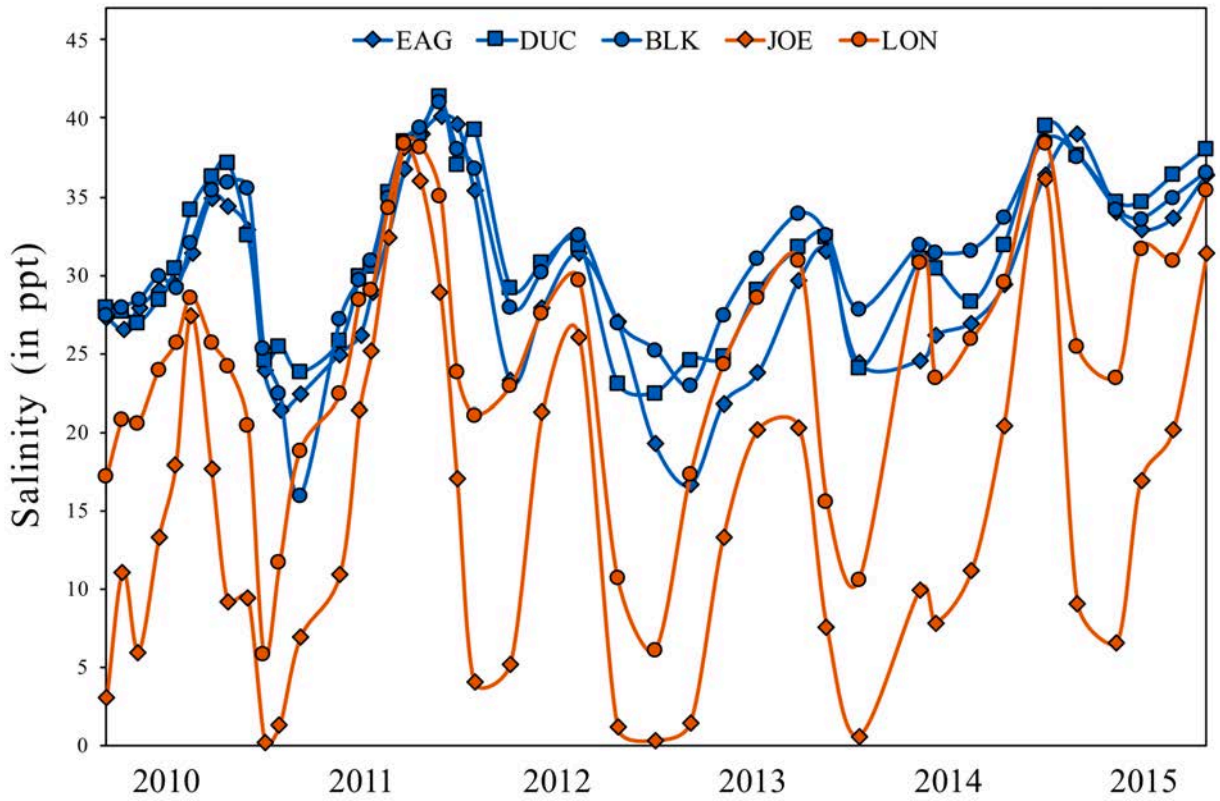

Figure 3-28. Line graphs displaying monthly salinity measurements (in ppt, equivalent to PSU) from January 2010 to May 2015 taken at five sites (EAG, DUC, BLK, JOE and LON) which were grouped under Immune Class C (see figure 3-25). EAG, DUC and BLK were further classified as having no pathogen loading ("None," in blue), while JOE and LON were classified under the "Very High" pathogen severity class (in orange). Sample size n = 42 per site.

fluctuations in EAG, DUC, and BLK salinity were generally confined between upper and lower margins within ~15 ppt of one another, changes occurring at LON, and especially JOE, were of extreme magnitude; while fluctuation "crest" points (i.e., maximum values) were comparable to those of the other three sites, the "troughs" (i.e., minimum values) regularly dipped into severely hyposaline conditions, causing fluctuation "amplitudes" ("crest" to "trough") to occur at anywhere between ~ 20 to ~38 ppt (figure 3-28).

Logistic Regression Model Relates Salinity Measures and Pathogen Loading

Following multivariate predictor selection techniques, we identified a relationship between pathogen loading and maximum seasonal change in salinity, at the site level. More specifically, a logistic regression curve was fit to paired pathogen loading and maximum seasonal salinity change values and the model explained a significant portion (88.6%) of the variation ($\alpha = 0.01$; $p < 0.01$) (figure 3-29).

3.5 Discussion

The purpose of this study was to identify ecologically significant trends that existed in patterns between: [1)] pathogen loading and immune status; [2)] pathogen loading and geographic site; [3)] pathogen loading and morphometric characteristics; [4)] pathogen loading and water quality data; [5)] immune status and geographic site; [6)] immune status and morphometric characteristics; and [7)] immune status and water quality data. Due to the sheer volume of comparisons which were generated, the aim of this discussion is not to exhaustively address every single feature of the data, but to draw attention to pronounced trends that fit together to form a cohesive argument on the underlying ecological interactions which, we propose, appear to govern this system.

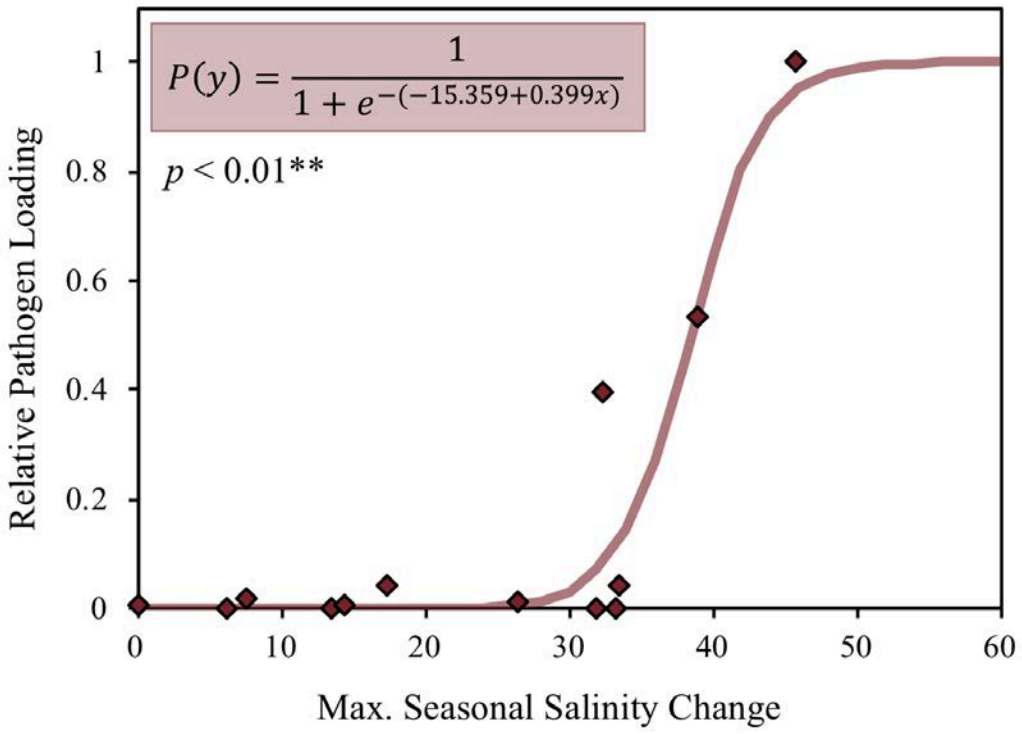

Figure 3-29. Logistic regression curve fit to x-y scatterplot of relative pathogen loading (proportional average *Labyrinthula* cell count across individuals) at a given site as a function of the maximum seasonal change in salinity (from 2010-2015) at that site. The chi-squared value analyzing goodness-of-fit is significant with 99% confidence ($\alpha = 0.01$).

Unlike the results of the lab-based experimental investigation, which revealed significant positive correlations between pathogen loading and two of the four immune biomarkers (POX and EXOC), the correlative analyses between pathogen loading and immune biomarkers in field-collected samples (pooled together, regardless of location in the bay) revealed no significant associations. The lack of a linear relationship between biomarker activity and *Labyrinthula* loading is not surprising, however. In the lab-controlled experiments, factors influencing biomarker activity were, to our best ability, minimized to only represent presence of the pathogen and one of the four abiotic stressor treatments; this luxury does not exist when studying a natural population. It is not only likely, but almost guaranteed, that the activity levels of POX, EXOC, PPO and LYS were responsive to a variety of factors (of biotic and abiotic origin) influencing the immune response of each and every *Thalassia testudinum* individual collected in Florida Bay. However, the downstream analyses (discussed below) took the inherent complexity of natural systems into consideration and, as a result, we were able to identify intriguing patterns that existed among our data.

Our survey of *Labyrinthula* prevalence and severity in Florida Bay was the first of its kind to employ a universal qPCR-based method to detect pathogen loading down to a specific cell count (see Chapter 2 for evidence that favors this approach over the historical Wasting Index method). Overall, *Labyrinthula* was present in one or more individuals (at ecologically significant quantities) in 10 of the 15 Florida Bay sites. Furthermore, it was noted that all individuals with very high pathogen loading (meaning, those grouped in the “Very High” pathogen severity class) were in close proximity to coastal basins (figure 3-10).

The next piece of significant information came from trends associated with the immune classes which grouped sites together based on similarities across the enzyme biomarkers (POX, EXOC, PPO and LYS). Notably, immune levels were substantially elevated in one immune class ("Immune Class C") which contained sites located in the northeastern region of Florida Bay. Furthermore, trends in leaf morphology revealed that immune class C was also distinguished from the other two in overall size; these individuals were much smaller than individuals within sites grouped into the other two immune classes (figure 3-23 C).

The coherence of the geographical distribution of our immune classes with the zone delineation patterns proposed in Herbert et al. (2011) further validated the notion that there was an association between plant immunity and the biogeochemistry of the bay and, more specifically, the biogeochemistry predicted to occur in response to CERP restoration efforts. It is not altogether surprising that this relationship was not readily apparent in our univariate analysis of water quality as a function of immune site, because we only considered three-year averages across six water quality parameters, whereas the zones proposed by Herbert et al. (2011) were the product of a complex analysis which predicted changes in 18 distinct ecophysiographic zones based pre-marinization trends and sophisticated set of hydrological modeling techniques. In addition to providing an external source of evidence that supported our immune classifications, these ecophysiological zones (or, as we refer to them as, "immune zones") revealed a significant trend in the northeastern sites. Sites in this zone had either very high pathogen loading or none whatsoever (immune zone C, figure 3-26). Further analysis revealed that there were pronounced differences in spatiotemporal trends of salinity between these site groupings, suggesting that the sites with very high pathogen loading were distinguished from those with no pathogen loading in

that they exhibited significantly lower salinity values, on average, as well as extreme periods of hyposalinity.

Based on these observations, we propose the following argument: pathogen severity in Florida Bay is dictated, at least in part, by a complex association between variations in plant morphology, immune status, and hyposalinity events across sites in the bay. More specifically, our evidence suggests that, as a result of a complex amalgam of environmental pressures, there is a pronounced difference in phenotype between the western and northeastern sites surveyed in the bay. These differences are most likely a product of plasticity, and not genetic diversity (Bricker et al. 2011), though this hypothesis will be tested explicitly using microsatellite genotyping techniques, an aspect of the project which was excluded from the scope of this thesis.

Furthermore, the association between small-bodied individuals and elevated immune status among northeast sites, and between larger-bodied plants and relatively low immune status among western sites, suggests that the immune systems of smaller individuals must work harder to protect their tissues from a wide variety of abiotic and biotic stressors, many of which were not likely assessed explicitly in this study. It is possible that immune levels are upregulated in these individuals due to their small size; proportionally speaking, a relatively small microbial invasion event would affect a larger extent of the total plant tissue if the plant had less tissue, overall. From the other perspective, larger-bodied individuals may not be required to maintain a high level of immune protection, because microbial invasions over a small portion of their tissue may be inconsequential to the overall health of the individual. This assertion introduces the concept of host resistance verses tolerance to pathogens. An excellent review of these concepts in plant pathosystems was conducted by Pagan and Garcia-Arenal (2018). They define resistance

as the active contribution made by a host to prevent or limit pathogen multiplication, whereas tolerance involves the ability of a host to minimize the deleterious effects of the pathogen on overall fitness, regardless of the degree of infection inflicted by the pathogen (Pagan & Garcia-Arenal 2018). They further assert that the two strategies generally coexist and are not mutually exclusive (Pagan & Garcia-Arenal 2018), indicating that it is, indeed, plausible to suggest that different *T. testudinum* individuals might employ different strategies to deal with *Labyrinthula* (and/or other foreign invaders) depending on the unique, location-dependent factors which they are subjected to.

This idea that northeastern and western turtlegrass individuals have adopted differential strategies somewhere along a continuum (punctuated on either end by complete resistance and complete tolerance) is further supported by the observation that, in general, western sites appeared to sustain moderate levels of pathogen loading that did not appear to significantly upregulate their overall immune status, at the chosen biomarkers (figure 3-21). Conversely, the observation that northeastern sites appeared to contain the pathogen in an all-or-none manner suggests that they actively fought off any degree of infection. This strategy appears to have been useful at sites where hyposalinity stress was minimal, but individuals which were small-bodied, had high immune activity, and were routinely experienced hyposaline stress in the coastal basins succumbed to seagrass wasting disease (figure 3-26). The overall mechanism by which we propose plant morphology, immune status and hyposalinity events across sites in the bay interact to drive differences in the host species' susceptibility in pathogen loading is depicted in figure 3-30.

Finally, the idea that wide fluctuations in salinity play a role in the prevalence and severity of seagrass wasting disease in *T. testudinum* tissue is reinforced by a logistic regression model fit to data which plotted maximum seasonal change verses pathogen loading as a function of site. This relationship suggests that, in general, individuals can tolerate low-to-moderate salinity fluctuations, but after reaching a threshold magnitude of change around 36-38 (figure 3-29), they succumb to the pathogen and harbor large quantities of the disease-causing agent in their tissues.

These results suggest that the restoration projects implemented by management initiatives like Comprehensive Everglades Restoration Program (CERP) may not only result in the competitive exclusion of *T. testudinum* by other seagrass species (Fourqurean et al. 2003, Lirman & Cropper 2003), but the hydrological changes which result in increased freshwater flow into Florida Bay (and especially coastal basins) have implications for turtlegrass in disease epidemiology, as well. The overwhelming likelihood for substantial shifts in marine systems in the coming decades due to local, regional, and global changes emphases the need for refined management strategies that effectively assess the capacity of important species, like seagrasses, to persevere amid periods of unpredictable fluctuation. The absence of a strong foundation rooted in knowledge often translates to misinformed policy, misdirected resources, and a failure to preserve the integrity of the system under management. Because effective management strategies rely so heavily on scientific input, understanding the dynamics surrounding an ecosystem's most integral parts is of dire importance; therefore, studies which integrate the data obtained through long-term management initiatives like FHAP delivers an invaluable tool in our

efforts to understand the local biotic and abiotic factors which dictate the abundance and distribution of species over time.

REFERENCE MATERIALS

Adams, J. & Bate, G. (1994). The ecological implications of tolerance to salinity by *Ruppia cirrhosa* (Petagna) Grande and *Zostera capensis* Setchell. *Botanica Marina*, *37*(5), pp. 449- 456.

Adl, S.M., Simpson, A.G., Lane, C.E., Lukeš, J., Bass, D. , Bowser, S.S., … & Spiegel, F.W. (2012). The revised classification of eukaryotes. *Journal of Eukaryotic Microbiology*, *59*(5), pp. 429-514.

Almagro, L., Gómez Ros, L., Belchi-Navarro, S., Bru, R., Ros Barceló, A., & Pedreño, M. (2008). Class III peroxidases in plant defense reactions. *Journal of Experimental Botany*, *60*(2), pp. 377-390.

Andrews, J. & Rouse, D. (1982). Plant pathogens and the theory of r- and K-selection. *The American Naturalist*, *120*(3), pp. 283.

Armitage, S., Thompson, J., Rolff, J., & Siva-Jothy, M. (2003). Examining costs of induced and constitutive immune investment in *Tenebrio molitor*. *Journal of Evolutionary Biology*, *16*(5), pp. 1038-1044.

Bergmann, N., Fricke, B., Schmidt, M., Tams, V., Beining, K., Schwitte, H., et al. (2011). A quantitative real-time polymerase chain reaction assay for the seagrass pathogen *Labyrinthula zosterae*. *Molecular Ecology Resources*, *11*(6), pp. 1076-1081.

Billingham M., Reusch T., Alberto F., & Serrao E. (2003). Is asexual reproduction more important at geographical limits? A genetic study of the seagrass *Zostera marina* in the Ria Formosa, Portugal. *Marine Ecology Progress Series*, *265*, pp. 77–83.

Bishop, N. (2013). *Effects of Multiple Abiotic Stressors on the Susceptibility of the Seagrass* Thalassia testudinum *to* Labyrinthula *sp., the Causative Agent of Wasting Disease.* (Master's Thesis, University of N. Florida). http://digitalcommons.unf.edu/etd/471

Bishop, N., Martin, D., & Ross, C. (2017). Effects of multi-stress exposure on the infection dynamics of a *Labyrinthula* sp.-turtle grass pathosystem. *Marine Ecology Progress Series*, *581*, pp. 119-133.

Blakesley, B., Berns, D., Merello, M., Hall, M., & Hyniova, J. (2002). The dynamics and distribution of the slime mold *Labyrinthula* sp. and its potential impacts on *Thalassia testudinum* populations in Florida. www.tbeptech.org (December 2002).

Blanca, M., Alarcon, R., Arnau, J., Bono, R., & Bendayan, R. (2017). Non-normal data: Is ANOVA still a valid option? *Psicothema*, *29*(4), pp. 552-557.

Bockelmann, A., Tams, V., Ploog, J., Schubert, P., & Reusch, T. (2013). Quantitative PCR reveals strong spatial and temporal variation of the wasting disease pathogen, *Labyrinthula zosterae* in northern European eelgrass (*Zostera marina*) Beds. *PLoS ONE*, *8*(5), p. e62169.

Borum, J., Sand-Jensen, K., Binzer, T., Pedersen, O., & Greve, T.M. (2006). Oxygen movement in seagrasses. In: Larkum, A., Orth, R., & Duarte, C. (Eds.). *Seagrasses: Biology, Ecology, and Conservation*, Springer, pp. 303-321.

Boström, C., Jackson, E., & Simenstad, C. (2006). Seagrass landscapes and their effects on associated fauna: A review. *Estuarine, Coastal, and Shelf Science*, *68*, pp. 383-403.

Boyer, J., Fourqurean, J., & Jones, R. (1999). Seasonal and long-term trends in the water quality of Florida Bay (1989-1997). *Estuaries*, *22*(2), pp. 417.

Briceño, H., Boyer, J., Castro, J., & Harlem, P. (2013). Biogeochemical classification of South Florida's estuarine and coastal waters. *Marine Pollution Bulletin*, *75*(1-2), pp.187-204.

Bricker, E., Waycott, M., Calladine, A., & Zieman, J. (2011). High connectivity across environmental gradients and implications for phenotypic plasticity in a marine plant. *Marine Ecology Progress Series*, *423*, pp. 57-67.

Bull, J., Kenyon, E., & Cook, K. (2011). Wasting disease regulates long-term population dynamics in a threatened seagrass. *Oecologia*, *169*(1), pp. 135-142.

Burdick, D., Short, F., & Wolf, J. (1993). An index to assess and monitor the progression of wasting disease in eelgrass *Zostera marina*. *Marine Ecology Progress Series*, *94*, pp. 83-90.

Burdon, J. & Chilvers, G. (1982). Host density as a factor in plant disease ecology. *Annual Review of Phytopathology*, *20*(1), pp. 143-166.

Burge, C., Mark Eakin, C., Friedman, C., Froelich, B., Hershberger, P., Hofmann, E., Petes, L., Prager, K., Weil, E., Willis, B., Ford, S., & Harvell, C. (2014). Climate change influences on marine infectious diseases: Implications for management and society. *Annual Review of Marine Science*, *6*(1), pp. 249-277.

Butcher, R. (1934). *Zostera*. Report on the present condition of eelgrass on the coasts of England, based on a survey during August to October, 1933. *ICES Journal of Marine Science*, *9*(1), pp. 49-65.

Carlton, J., Vermeij, G., Lindberg, D., Carlton, D., & Dudley, E. (1991). The first historical extinction of a marine invertebrate in an ocean basin: The demise of the eelgrass limpet, *Lottia alveus. Biological Bulletin*, *180*, pp. 72–80.

Chitrampalam, P., Goldberg, N., & Olsen, M. (2015). *Labyrinthula* species associated with turfgrasses in Arizona and New Mexico. *European Journal of Plant Pathology*, *143*(3), pp. 485-493.

Clarke, K., Somerfield, P., & Gorley, R. (2008). Testing of null hypotheses in exploratory community analyses: similarity profiles and biota-environment linkage. *Journal of Experimental Marine Biology and Ecology*, *366*(1-2), pp. 56-69.

Cole, A. (2017) *Relationships Between Water Quality Variables and Benthic Macrophyte Communities in Florida Bay*. (Master's Thesis, University of North Carolina at Wilmington).

Cole, A., Durako, M., & Hall, M. (2018). Multivariate Analysis of Water Quality and Benthic Macrophyte Communities in Florida Bay, USA Reveals Hurricane Effects and Susceptibility to Seagrass Die-Off. *Frontiers in Plant Science*, *9*(630).

Costanza, R., et al. (1997). The value of the world's ecosystem services and natural capital. *Nature*, *387*, pp. 253-260.

Cotton, A. (1933). Disappearance of *Zostera marina. Nature*, *132*(3329), pp. 277-277.

Couch, C., Mydlarz, L., Harvell, C., & Douglas, N. (2008). Variation in measures of immunocompetence of sea fan coral, *Gorgonia ventalina*, in the Florida Keys. *Marine Biology*, *155*(3), pp. 281-292.

Cróquer, A. & Weil, E. (2009). Changes in Caribbean coral disease prevalence after the 2005 bleaching event. *Diseases of Aquatic Organisms*, *87*(1-2), pp. 33-43.

Dawes, C. J., Phillips, R. C., Morrison, G., & Dawes, C. J. (2004). *Seagrass Communities of the Gulf Coast of Florida: Status and Ecology*. Florida Fish and Wildlife Conservation Commission Fish and Wildlife Research Institute.

den Hartog, C. & Kuo, J. (2006). Taxonomy and biogeography of seagrasses. In: Larkum, A., Orth, R. and Duarte, C. (Eds.). *Seagrasses: Biology, Ecology, and Conservation.* Springer, pp. 1-23.

Dennison, W., Orth, R., Moore, K., Stevenson, J., Carter, V., Kollar, S., Bergstrom, P., & Batiuk, R. (1993). Assessing water quality with submersed aquatic vegetation. *BioScience, 43*(2), pp. 86-94.

Douglas, N., Mullen, K., Talmage, S. and Harvell, C. (2006). Exploring the role of chitinolytic enzymes in the sea fan coral, Gorgonia ventalina. *Marine Biology, 150*(6), pp. 1137-1144.

Duarte, C. M. (2002). The future of seagrass meadows. *Environmental Conservation, 29*(2), pp. 192-206.

Duarte, C., Fourqurean, J., Krause-Jensen, D., & Olesen, B. (2006). Dynamics of seagrass stability and change. In: Larkum, A., Orth, R. and Duarte, C. (Eds.). *Seagrasses: Biology, Ecology, and Conservation.* Springer, pp. 271-294

Durako, M. & Kuss, K. (1994). Effects of *Labyrinthula* infection on the photosynthetic capacity of *Thalassia testudinum*. *Bulletin of Marine Science, 54*(3), pp. 727-732.

Engel, S., Puglisi, M., Jensen, P., & Fenical, W. (2006). Antimicrobial activities of extracts from tropical Atlantic marine plants against marine pathogens and saprophytes. *Marine Biology, 149*(5), pp. 991-1002.

Fischer-Piette, E., Heim R., & Lami, R. (1932). Note preliminaire sur une maladie bacterienne des *Zosteres*. *Comptes renudues des seances de l'Academie des Sciences, 195,* pp. 1420-1422.

Fourqurean, J., Boyer, J., Durako, M., Hefty, L., & Peterson, B. (2003). Forecasting responses of seagrass distributions to changing water quality using monitoring data. *Ecological Applications, 13*(2), pp. 474-489.

Fourqurean, J.W. & Robblee, M.B. (1999). Florida Bay: a history of recent ecological changes. *Estuaries*, *22*(2B), pp. 345-357.

Garcias-Bonet, N., Sherman, T., Duarte, C., & Marbà, N. (2011). Distribution and pathogenicity of the protist *Labyrinthula* sp. in western Mediterranean seagrass meadows. *Estuaries and Coasts*, *34*(6), pp. 1161-1168.

Gertzen, R. & Escobar, M. (2014). Assays of polyphenol oxidase activity in walnut leaf tissue. *BIO-PROTOCOL,* [online] *4*(16). Available at: https://bio-protocol.org/e1213

Ghosh, M. (2006). Antifungal properties of haem peroxidase from *Acorus calamus*. *Annals of Botany*, *98*(6), pp. 1145-1153.

Greenberg, J., Guo, A., Klessig, D., & Ausubel, F. (1994). Programmed cell death in plants: A pathogen-triggered response activated coordinately with multiple defense functions. *Cell, 77*(4), pp. 551-563.

Greenwood, W., Kruse, S., & Swarzenski, P. (2006). Extending electromagnetic methods to map coastal pore water salinities. *Ground Water, 44*(2), pp. 292-299.

Grover, A. (2012). Plant chitinases: Genetic diversity and physiological roles. *Critical Reviews in Plant Sciences, 31*(1), pp.57-73.

Hackney, J., & Durako, M. (2004). Size–frequency patterns in morphometric characteristics of the seagrass *Thalassia testudinum* reflect environmental variability. *Ecological Indicators, 4*(1), pp. 55-71.

Hall, M.O., Durako, M.J., Fourqurean, J.W., & Zieman, J.C. (1999). Decadal changes in seagrass distribution and abundance in Florida Bay. *Estuaries, 22*, pp. 445–459.

Hall, M.O, Madley, K., Durako, M.J., Zieman, J.C., & Robblee, M.B. (2007). Florida Bay. In: Handley, L., Altsman, D., & DeMay, R. *Seagrass status and trends in the northern Gulf of Mexico: 1940-2002, U.S. Geological Survey Scientific Investigations Report 2006–5287*, pp. 243-254.

Hammerstrom, K.K., Kenworthy, W.J., Whitfield, P.E., & Merello, M. F. (2007). Response and recovery dynamics of seagrasses *Thalassia testudinum* and *Syringodium filiforme* and macroalgae in experimental motor vessel disturbances. *Marine Ecology Progress Series, 345*, pp. 83-92.

Heck, K., Carruthers, T., Duarte, C., Hughes, A., Kendrick, G., Orth, R., & Williams, S. (2008). Trophic transfers from seagrass meadows subsidize diverse marine and terrestrial consumers. *Ecosystems, 11*(7), pp. 1198-1210.

Hemminga, M. & Duarte, C. (2008). *Seagrass Ecology*. Cambridge: Cambridge University Press.

Herbert, D., Perry, W., Cosby, B., & Fourqurean, J. (2011). Projected reorganization of Florida Bay seagrass communities in response to the increased freshwater inflow of Everglades restoration. *Estuaries and Coasts, 34*(5), pp. 973-992.

Hiraga, S., Sasaki, K., Ito, H., Ohashi, Y., & Matsui, H. (2001). A large family of Class III plant peroxidases. *Plant and Cell Physiology, 42*(5), pp. 462-468.

Hoegh-Guldberg, O. & Bruno, J. F. (2010). The impact of climate change on the world's marine ecosystems. *Science, 328*(1523), pp. 1523-1528.

Janssen, T. & Bremer, K. (2004). The age of major monocot groups inferred from 800+ rbcL sequences. *Botanical Journal of the Linnean Society, 146*(4), pp. 385-398.

Kenworthy, W.J., Wyllie-Echeverria, S., Coles, R.G., Pergent, G., & Pergent-Martini, C. (2006). Seagrass conservation biology: An interdisciplinary science for protection of the seagrass biome. In: Larkum, A., Orth, R., & Duarte, C. (Eds.). *Seagrasses: Biology, Ecology, and Conservation.* Springer, pp. 303-321.

Kuo, J. & den Hartog, C. (2006). Seagrass morphology, anatomy, and ultrastructure. In: Larkum, A., Orth, R. and Duarte, C. (Eds.). *Seagrasses: Biology, Ecology, and Conservation.* Springer, pp. 51-87.

Lee, T.N., Johns, E., Melo, N., Smith, R., Ortner, P., & Smith, D. (2006). On Florida Bay hypersalinity and water exchange. *Bulletin of Marine Science, 79*(2), pp. 301-327.

Les, D., Cleland, M., & Waycott, M. (1997). Phylogenetic studies in Alismatidae, II: Evolution of marine angiosperms (seagrasses) and hydrophily. *Systematic Botany, 22*(3), pp. 443-463.

Li, L. & Steffens, J. (2002). Overexpression of polyphenol oxidase in transgenic tomato plants results in enhanced bacterial disease resistance. *Planta, 215*(2), pp. 239-247.

Lirman, D. & Cropper, W. (2003). The influence of salinity on seagrass growth, survivorship, and distribution within Biscayne Bay, Florida: Field, experimental, and modeling studies. *Estuaries, 26*(1), pp. 131-141.

Lovrekovich, L. & Farkas, G. (1965). Induced protection against wildfire disease in tobacco leaves treated with heat-killed bacteria. *Nature, 205*(4973), pp. 823-824.

Ma, Y. & Berkowitz, G. (2011). Danger at your door: pathogen signals and programmed cell death in plants. *New Phytologist, 192*(1), pp.1-3.

Madden, C., Rudnick, D., McDonald, A., Cunniff, K., & Fourqurean, J. (2009). Ecological indicators for assessing and communicating seagrass status and trends in Florida Bay. *Ecological Indicators, 9*(6), pp. 68-82.

Marbà, N. & Duarte, C.M. (1998). Rhizome elongation and seagrass clonal growth. *Marine Ecology Progress Series*, *174*, pp. 269-280.

Martin, A.C. (1954). A clue to the eelgrass mystery. *Transactions of the N. American Wildlife and Natural Resources Conference, 19*, pp. 441-449.

Martin, D., Chiari, Y., Boone, E., Sherman, T., Ross, C., Wyllie-Echeverria, S., Gaydos, J., & Boettcher, A. (2016). Functional, phylogenetic and host-geographic signatures of *Labyrinthula* spp. provide for putative species delimitation and a global-scale view of seagrass wasting disease. *Estuaries and Coasts*, *39*(5), pp. 1403-1421.

Mayer, A. (2007). Polyphenol oxidases in plants and fungi: going places? A review. *ChemInform*, *38*(5), pp. 2318-2331.

McKone, K. & Tanner, C. (2009). Role of salinity in the susceptibility of eelgrass *Zostera marina* to the wasting disease pathogen *Labyrinthula zosterae*. *Marine Ecology Progress Series*, *377*, pp. 123-130.

Moffitt, J. & Cottam, C. (1941). Eelgrass depletion on the Pacific coast and its effect upon the black brant. *Wildlife Restoration Management Leaflet*, *204*, 26 pages.

Muehlstein, L. (1992). The host-pathogen interaction in the wasting disease of eelgrass, *Zostera marina*. *Canadian Journal of Botany*, *70*(10), pp. 2081-2088.

Muehlstein, L., Porter, D., & Short, F. (1988). *Labyrinthula* sp., a marine slime mold producing the symptoms of wasting disease in eelgrass, *Zostera marina*. *Marine Biology*, *99*(4), pp. 465-472.

Muehlstein, L., Porter, D., & Short, F. (1991). *Labyrinthula zosterae* sp. nov., the causative agent of wasting disease of eelgrass, *Zostera marina*. *Mycologia*, *83*(2), pp. 180.

Mydlarz, L. & Harvell, C. (2007). Peroxidase activity and inducibility in the sea fan coral exposed to a fungal pathogen. *Comparative Biochemistry and Physiology, Part A, 146*(1), pp. 54-62.

Neumann, B., Vafeidis, A., Zimmermann, J., & Nicholls, R. (2015). Future coastal population growth and exposure to sea-level rise and coastal flooding - a global assessment. *PLoS ONE*, *10*(3), p.e0118571.

Nuttle, W., Fourqurean, J., Cosby, B., Zieman, J. & Robblee, M. (2000). Influence of net freshwater supply on salinity in Florida Bay. *Water Resources Research*, *36*(7), pp. 1805-1822.

Orth, R. J., Carruthers, T. J., Dennison, W. C., Duarte, C. M., Fourqurean, J. W., Heck Jr, K. L., …Williams, S. L. (2006). A global crisis for seagrass ecosystems. *Bioscience*, *56*(12), pp. 987-996.

Orth, R.J., Heck, K.L. Jr., & van Montfrans, J. (1984). Faunal communities in seagrass beds: A review of the influence of plant structure and prey characteristics on predator–prey relationships. *Estuaries, 7*, pp. 339-350.

Osbourn, A. (1996). Preformed Antimicrobial Compounds and Plant Defense against Fungal Attack. *The Plant Cell*, *8*(10), p. 1821.

Pagan, I. & Garcia-Arenal, F. (2018). Tolerance to plant pathogens: Theory and experimental evidence. *International Journal of Molecular Sciences*, *19*(3), p. 810.

Papenbrock, J. (2012). Highlights in seagrasses' phylogeny, physiology, and metabolism: What makes them special? *ISRN Botany*, *2012*, pp. 1-15.

Pérez M., Duarte C.M., Romero J., Sand-Jensen K., & Alcoverro T. (1994) Growth plasticity in *Cymodocea nodosa* stands: The importance of nutrient supply. *Aquatic Botany, 47*(3-4), pp. 249-264.

Petersen, H. E. (1934). Wasting disease of eelgrass (*Zostera marina*). *Nature, 134*, pp. 143-144.

Punja, Z.K. & Zhang, Y.Y. (1993). Plant chitinases and their roles in resistance to fungal diseases. *Journal of Nematology*, *25*(4), pp. 526-540.

Raghukumar, S. (2002). Ecology of the marine protists, the *Labyrinthulomycetes* (*Thraustochytrids* and *Labyrinthulids*). *European Journal of Protistology*, *38*(2), pp. 127-145.

Ralph, P., Durako, M., Enríquez, S., Collier, C., & Doblin, M. (2007). Impact of light limitation on seagrasses. *Journal of Experimental Marine Biology and Ecology*, *350*(1-2), pp. 176-193.

Ralph, P. & Short, F. (2002). Impact of the wasting disease pathogen, *Labyrinthula zosterae*, on the photobiology of eelgrass Zostera marina. *Marine Ecology Progress Series*, *226*, pp. 265-271.

Ralph, P., Tomasko, D., Seddon, S., Moore, K., & Macinnis-Ng, C. (2006). Human impact on seagrasses: eutrophication, sedimentation and contamination. In: Larkum, A., Orth, R., & Duarte, C. (Eds.). *Seagrasses: Biology, Ecology, and Conservation.* Springer, pp. 303-321.

Ray, B., Johnson, M., Cammarata, K., & Smee, D. (2014). Changes in seagrass species composition in northwestern Gulf of Mexico estuaries: Effects on associated seagrass fauna. *PLoS ONE*, *9*(9), p.e 107751.

Renn, C. (1934). Wasting disease of *Zostera* in American waters. *Nature*, *134*, pp. 416.

Renn, C. (1935). A mycetozoan parasite of *Zostera marina*. *Nature*, *135*, pp. 544-545.

Robblee, M., Barber, T., Carlson, P., Durako, M., Fourqurean, J., & Muehlstein, L. et al. (1991). Mass mortality of the tropical seagrass *Thalassia testudinum* in Florida Bay (USA). *Marine Ecology Progress Series*, *71*, pp. 297-299.

Robinson, R.A. (1976). Plant pathosystems. *Advanced Series in Agricultural Sciences, vol. 3. Springer-Verlag, Berlin*, *3*, pp. 15-31.

Rudnick, D., Ortner, P., Browder, J., & Davis, S. (2005). A conceptual ecological model of Florida Bay. *Wetlands*, *25*(4), pp. 870-883.

Schneider, C.A., Rasband, W.S., & Eliceiri, K.W. (2012). NIH Image to ImageJ: 25 years of image analysis. *Nature Methods*, *9*(7), pp. 671-675

Schomer, N.S. & Drew, R.D. (1982). An ecological characterization of the lower Everglades, Florida Bay, and the Florida Keys. *US Fish & Wildlife Service Report, #14-16-009-80-999*

Simons, T. & Ross, A. (1970). Enhanced peroxidase activity associated with induction of resistance to tobacco mosaic virus in hypersensitive tobacco. *Phytopathology*, *60*(2), pp. 383.

Sheridan, P. (1997). Benthos of adjacent mangrove, seagrass and non-vegetated habitats in Rookery Bay, Florida, USA. *Estuarine, Coastal, and Shelf Science. 44*(4), pp. 455-469.

Short, F.T. & Burdick, D.M. (1996). Quantifying eelgrass habitat loss in relation to housing development and nitrogen loading in Waquoit Bay, Massachusetts. *Estuaries, 19*(3), pp. 730-739.

Short, F.T., Burdick, D.M., Short, C.A., Davis, R.C., & Morgan, P.A. (2000). Developing success criteria for restored eelgrass, salt marsh and mud flat habitats. *Ecological Engineering*, *15*(3), pp. 239-252.

Short, F.T., Muelstein, L., & Porter, D. (1987). Eelgrass wasting disease: Cause and recurrence of a marine epidemic. *Biological Bulletin, 173*(3), pp. 557-562.

Short, F.T. & Wyllie-Echeverria, S. (1996). Natural and human-induced disturbance of seagrasses. *Environmental Conservation, 23*(1), pp. 17-27.

Steele, L., Caldwell, M., Boettcher, A., & Arnold, T. (2005). Seagrass-pathogen interactions: 'Pseudo-induction' of turtlegrass phenolics near wasting disease lesions. *Marine Ecology Progress Series, 303*, pp. 123-131.

Strickland, J. (1958). Solar radiation penetrating the ocean. A review of requirements, data and methods of measurement, with particular reference to photosynthetic productivity. *Journal of the Fisheries Research Board of Canada, 15*(3), pp. 453-493.

Sullivan, B. (2011). *Correlating Multiple Players in the Mass-wasting of Seagrass* (Master's Thesis, University of Washington).

Sullivan, B., Robinson, K., Trevathan-Tackett, S., Lilje, E., Gleason, F. & Lilje, O. (2017). The first isolation and characterization of the protist *Labyrinthula* sp. in southeastern Australia. *Journal of Eukaryotic Microbiology, 64*(4), pp. 504-513.

Sullivan, B., Sherman, T., Damare, V., Lilje, O., & Gleason, F. (2013). Potential roles of *Labyrinthula* spp. in global seagrass population declines. *Fungal Ecology, 6*(5), pp. 328-338.

Thipyapong, P., Hunt, M., & Steffens, J. (2004). Antisense downregulation of polyphenol oxidase results in enhanced disease susceptibility. *Planta, 220*(1), pp. 105-117.

Trevathan-Tackett, S. (2011). *Physiology and Biochemistry of the Tropical Seagrass* Thalassia testudinum *in Response to Hypersalinity Stress and* Labyrinthula *sp. Infection.* (Master's Thesis, University of N. Florida). http://digitalcommons.unf.edu/etd/391

Trevathan-Tackett, S., Lane, A., Bishop, N., & Ross, C. (2015). Metabolites derived from the tropical seagrass *Thalassia testudinum* are bioactive against pathogenic *Labyrinthula* spp.. *Aquatic Botany*, *122*(2015), pp. 1-8.

Trevathan-Tackett, S., Lauer, N., Loucks, K., Rossi, A. & Ross, C. (2013). Assessing the relationship between seagrass health and habitat quality with wasting disease prevalence in the Florida Keys. *Journal of Experimental Marine Biology and Ecology, 449*, pp. 221-229.

Trevathan-Tackett, S., Sullivan, B., Robinson, K., Lilje, O., Macreadie, P., & Gleason, F. (2018). Pathogenic *Labyrinthula* associated with Australian seagrasses: Considerations for seagrass wasting disease in the southern hemisphere. *Microbiological Research, 206*(2018), pp. 74-81.

Tsui, C.K.M., Marshall, W., Yokoyama, R., Honda, D., Lippmeier, J.C., Craven, K.D., Peterson, P.D., & Berbee, M.L. (2009). Labyrinthulomycetes phylogeny and its implications for the evolutionary loss of chloroplasts and gain of ectoplasmic gliding. *Molecular Phylogenetics and Evolution, 50*, pp. 129-140.

Tutin, T.G. (1938). The autoecology of *Zostera marina* in relation to its wasting disease. *New Phytology, 37*(1), pp. 50-71.

van Diggelen, J., Rozema, J., & Broekman, R. (1987). Mineral composition of and proline accumulation by *Zostera marina* L. in response to environmental salinity. *Aquatic Botany, 27*(2), pp. 169–176.

van Tussenbroek, B.I., Vonk, J.A., Stapel, J., Erftemeijer, P.L.A., Middelburg, J.J., & Zieman, J.C. (2006). The biology of *Thalassia*: paradigms and recent advances in research. In: Larkum, A., Orth, R., & Duarte, C. (Eds.). *Seagrasses: Biology, Ecology, and Conservation.* Springer, pp. 303-321.

Vitousek, P. M., Aber, J. D., Howarth, R. W., Likens, G. E., Matson, P. A., Schindler, D. W., ... & Tilman, D. G. (1997). Human alteration of the global nitrogen cycle: sources and consequences. *Ecological applications*, *7*(3), 737-750.

Walker, D., Kendrick, G., & McComb, A. (2006). Decline and recovery of seagrass ecosystems—the dynamics of change. In: Larkum, A., Orth, R., & Duarte, C. (Eds.). *Seagrasses: Biology, Ecology, and Conservation.* Springer, pp. 551-565

Wang, S., Ng, T., Chen, T., Lin, D., Wu, J., Rao, P., & Ye, X. (2005). First report of a novel plant lysozyme with both antifungal and antibacterial activities. *Biochemical and Biophysical Research Communications, 327*(3), pp. 820-827.

Wanless, H. & Tagett, M. (1989). Origin, growth, and evolution of carbonate mudbanks in Florida Bay. *Bulletin of Marine Science, 44*(1), pp. 454-489.

Waycott, M., Duarte, C., Carruthers, T., Orth, R., Dennison, W., & Olyarnik, S., et al. (2009). Accelerating loss of seagrasses across the globe threatens coastal ecosystems. *Proceedings of The National Academy of Sciences, 106*(30), pp. 12377-12381.

Waycott, M., Procaccini, G., Les, D.H., & Reusch, T.B.H. (2006). Seagrass evolution, ecology and conservation: a genetic perspective. In: Larkum, A., Orth, R., & Duarte, C. (Eds.). *Seagrasses: Biology, Ecology, and Conservation.* Springer, pp. 303-321.

Zapata, O. & McMillan, C. (1979). Phenolic acids in seagrasses. *Aquatic Botany, 7*, pp. 307-317.

Zieman, J., Fourqurean, J., & Frankovich, T. (1999). Seagrass die-off in Florida Bay: long-term trends in abundance and growth of turtle grass, *Thalassia testudinum*. *Estuaries, 22*(2), pp. 460.

Zieman, J., Fourqurean, J., & Iverson, R. (1989). Distribution, abundance and productivity of seagrasses and macroalgae in Florida Bay. *Bulletin of Marine Sciences, 44*(1), pp. 292-311.

Zimmerman, R. (2006). Light and photosynthesis in seagrass meadows. In: Larkum, A., Orth, R., & Duarte, C. (Eds.). *Seagrasses: Biology, Ecology, and Conservation.* Springer, pp. 303-321.

Zimmerman, R. & Dekker, A. (2006). Aquatic optics: Basic concepts for understanding how light affects seagrasses and makes them measurable from space. In: Larkum, A., Orth, R. and Duarte, C. (Eds.). *Seagrasses: Biology, Ecology, and Conservation.* Springer, pp. 295-301.

PAIGE J. DUFFIN VITAE

EDUCATION

Master of Science, Biology **Fall 2015 – Present**
College of Arts and Sciences; University of North Florida; Jacksonville, FL
Area of Concentration: Ecology/Environmental Biology
Graduating GPA: 3.90
Graduation: Summer 2018

Bachelor of Science, Biology (Honors Program) **Fall 2011 – Spring 2015**
College of Arts and Sciences; University of North Florida; Jacksonville, FL
Area of Concentration: Coastal Biology
Upper Level Coursework GPA: 3.92; Overall GPA: 3.66
Graduated with *Magna Cum Laude* Institutional Honors

RESEARCH EXPERIENCE

Graduate Research Assistantship *(Paid Position)* **Fall 2016 – Spring 2017**
Biology Department; University of North Florida; Jacksonville, FL
One Year Paid Assistantship Awarded and Funded by the UNF Biology Dept.

Graduate Research **Summer 2015 – Present**
Biology Department; University of North Florida; Jacksonville, FL
Principal Investigator: Dr. Cliff Ross
Masters Thesis Project: "*Investigating the relationship between local environmental stressors and individual host genotype on the immune status and wasting disease susceptibility in a dominant seagrass species*"

Undergraduate Research
Biology Department; University of North Florida; Jacksonville, FL
Research Assistant in Dr. Cliff Ross's Lab **Summers of 2012 & 2014**
Area of Research: Factors affecting Caribbean coral larvae recruitment
Research Assistant in Dr. David Waddell's Lab **Spring 2012 – Spring 2015**
Area of Research: Skeletal muscle atrophy/Molecular Genetics
Undergraduate Research Thesis *(with publication):* "*Characterization of RING Finger/SPRY Domain Containing 1 (Rspry1) and NEFA-interacting Nuclear Protein 30 (Nip30) transcriptional regulation*"

TEACHING EXPERIENCE

Graduate Teaching Assistant
Biology Department; University of North Florida; Jacksonville, FL
General Biology I Lab (BSC 1010 C) **2015 – 2016, Spring 2018**
Principles of Biology Lab (BSC 1105 C) **Fall 2017**

BIO-FLITE Laboratory Instructor **August 2016**
General Biology I Lab (BSC 1010 C) Instructor for the Biology Intensive Orientation for Freshman Learning Improvement and Transition Enhancement (BIO-FLITE) Program offered by the UNF Biology Dept.

Supplemental Instructor for Genetics Undergraduate Course (PCB 3063C)
Biology Department; University of North Florida; Jacksonville, FL
Primary Instructor: Dr. David Waddell **Fall 2014 - Spring 2015**
Primary Instructor: Dr. Matt Gilg **Spring 2016**

PRESENTATIONS

"Assessing prevalence and severity of seagrass wasting disease in Florida Bay as a function of immune status in the host species, Thalassia testudinum"
Oral Presentation at the Annual Benthic Ecology Meeting; Corpus Christi, TX March 2018

"Seagrass Wasting Disease: The Infection Dynamics of a Labyrinthula sp. – Turtlegrass Pathosystem"
Oral Presentation at the SE Estuarine Research Society Spring Meeting; St. Augustine, FL March 2018

"Roles of host genotype and environmental stressors in the susceptibility of turtlegrass to wasting disease"
Oral Presentation at the Coastal & Estuarine Research Fed. Meeting; Providence, RI November 2017

"The role of environmental stressors and host immunocompetence in wasting disease prevalence and severity in the seagrass Thalassia testudinum"
Oral Presentation at the Annual Plant Biology Conference; Honolulu, HI June 2017

"The role of environmental stressors and host immunocompetence in wasting disease prevalence and severity in the seagrass Thalassia testudinum"
Poster Presentation at the Annual Benthic Ecology Meeting; Myrtle Beach, SC April 2017

"Investigating the relationship between local environmental stressors and individual host genotype on the immune status and wasting disease susceptibility in a seagrass species"
Poster Presentation at the SE Phycological Colloquy Annual Meeting; Valdosta, GA November 2016

"Investigating the relationship between local environmental stressors and individual host genotype on the immune status and wasting disease susceptibility in a seagrass species"
Poster Presentation at the UNF Natural Sciences Poster Session; Jacksonville, FL November 2016

"Characterization of RING Finger/SPRY Domain Containing 1 (Rspry1) and NEFA-interacting Nuclear Protein 30 (Nip30) Transcriptional Regulation"
Poster Presentation at the UNF SOARS Poster Session; Jacksonville, FL April 2015

"Characterization of RING Finger/SPRY Domain Containing 1 (Rspry1) and NEFA-interacting Nuclear Protein 30 (Nip30) Transcriptional Regulation"
Poster Presentation at the Annual Experimental Biology Conference; Boston, MA March 2015

"Activation of RING Finger/SPRY Domain Containing 1 (Rspry1) and NEFA-interacting Nuclear Protein 30 (Nip30) During Skeletal Muscle Atrophy"
Poster Presentation at the Annual SICB Conference; West Palm Beach, FL January 2015

"*Transcriptional Repression of RING Finger/SPRY Domain Containing 1 (Rspry1) by Muscle-specific RING Finger 1 (MuRF1)"*
Poster Presentation at the UNF SOARS Poster Session; Jacksonville, FL April 2014

PUBLICATIONS

Waddell, D., **Duffin, P.**, Haddock, A., Triplett, V., Saredy, J., Kakareka, K., & Eldredge, J. (2016). Isolation, expression analysis and characterization of NEFA-interacting nuclear protein 30 and RING finger and SPRY domain containing 1 in skeletal muscle. *Gene, 576*(1), 319-332.

AWARDS AND SCHOLARSHIPS

Biology Graduate Research Enhancement Scholarship **Spring 2017**
Graduate Summer Research Grant **Summer 2016**
UNF Biology Dept. Excellence Award: Researcher of the Year **Spring 2015**
Graduated with *Magna Cum Laude* Latin Honors **Spring 2015**
ASBMB Travel Award Recipient
Spring 2015

Academic Dean's List
Four-Year Presidential Scholarship Award **Fall 2011- Spring 2015**
Four-Year Full Bright Futures Scholarship **Fall 2011- Spring 2015**
Supplemental Funding to Presidential Scholarship **2011-2014**
Awarded based on academic merit
Transformational Learning Opportunity (TLO) Presidential Scholarship **Spring 2014**
COAS (TLO) Skeletal Muscle Research Scholarship **Spring 2014**
FIO Field Studies Trip Travel Award Grant **Summer 2013**
COAS (TLO) Coral Reef Research Scholarship **Summer 2012**

OTHER RELEVANT EXPERIENCE

Research Experience for Undergraduates (REU) Mentor **Summer 2016**
Mentored an undergraduate research intern for 10 weeks through the REU program, a research training experience hosted by the UNF coastal biology program and funded by the National Science Foundation.

Intern at Environmental Services, Inc. **Spring 2014**
Working as an intern at this environmental consulting firm, combining knowledge of regional policies, county regulations, and ecology to consult companies as their activities affect the local environment.